LAMINAR BOUNDARY LAYER PROBLEMS ASSOCIATED WITH FLOW THROUGH TURBOMACHINES

Thesis by

Artur Mager

In Partial Fulfillment of the Requirements

for the Degree of

Doctor of Philosophy

California Institute of Technology

Pasadena, California

1953

ACKNOWLEDGMENTS

I wish to express my sincere thanks and gratitude to Dr. Frank E. Marble for his valuable advice, sound constructive criticism, many important ideas and above all, his very warm personal interest, friendly attitude and continuous encouragement which made this investigation most stimulating and enjoyable.

I am also very grateful to Dr. Hsue-Shen Tsien, who not only has given me his valuable time in a number of thought provoking discussions, but also suggested the general approach of small perturbations which bore such fruitful results.

A great help in crystallizing some of my ideas were the discussions with Dr. H. G. Loos and with Mr. G. J. Adams.

The investigation of the flow over sharply laterally curved surfaces was sponsored by the Air Research and Development Command under Contract No. AF 18(600)-178.

I wish to express my appreciation to Miss G. Pauwels for help with numerical calculations and to Miss Ruth Winkel for typing the thesis.

SUMMARY

This analysis deals with three-dimensional boundary layer flows which are of particular interest in the design of turbomachinery. By assuming only small lateral pressure gradients and applying perturbation procedure to the steady, laminar boundary layer equations of motion a set of zeroth and first order equations is found. While the zeroth order equations are just the two-dimensional ones for flow over flat plate, the first order equations retain the characteristic Blasius similarity for a family of external flows expressible by $U^* = Bx^m z^i$, $W^* = Ax^n z^k$ (where U^* & W^* are the perturbation velocities, x & z are the coordinates and A & B are arbitrary constants). For various types of such external flows (which may or may not be rotational) boundary layer velocity distributions were found by a numerical solution.

The investigation is divided into two parts, the first one dealing with boundary layer flows over plane surfaces and the second one considering such flows over surfaces with very sharply varying lateral curvature. In order to obtain solutions in the second part it was necessary to expand the appropriate equations in terms of the product of the local surface curvature and the boundary layer thickness. In addition, the effects of compressibility and rotation (of the surface) on the flows over a plane surface were quantitatively evaluated.

Comparison of the present results with the more exact solutions of other investigators in certain special cases, and with the visual studies of three-dimensional boundary layer flow in cascades, indicates a fair qualitative agreement.

TABLE OF CONTENTS

SYMBOLS

A, B, D constants describing external flow and rotation

$\bar{b}$ vector position of fluid element

c curvature of the external flow streamline, also curvature of the $\bar{z}$ axis

d function connected with u° flow when curvature is infinite

$\mathfrak{D}$ quantity determining the nature of the momentum-integral equations

E energy

f function connected with u^* flow

F function connected with u° flow

g, G functions connected with w^* flow

h_1, h_2, h_3 length stretching factors

H_1, H_2 expressions appearing in momentum-integral equations

$\bar{i}, \bar{j}, \bar{k}$ unit vectors in Cartesian system

k function connected with u° flow over curved wall

l function connected with u^* flow over curved wall

M Mach number based on standard conditions

M arbitrary function of x, z or $\bar{x}$, $\bar{z}$.

p pressure

P_1, P_2 parameters used in momentum-integral equations

$\bar{q}$ vector velocity $\bar{i}u + \bar{j}v + \bar{k}w$

$\bar{q}_{12}$ vector velocity $\bar{q}_1 + \bar{q}_2 = \bar{i}u + \bar{k}v$

$\bar{q}_1$ vector velocity along s_1 coordinate

$\bar{q}_2$ vector velocity along s_2 coordinate

$\bar{Q}$ $\bar{q}_{12}$ for $\eta \to \infty$ $= \bar{i}U + \bar{k}W$

} without the bar these designate the corresponding magnitudes

r perpendicular distance of fluid element from axis of rotation

R gas constant

Re Reynolds number $\frac{U^\circ x}{\nu}$

s_1 coordinate along the streamline of the external flow

s_2 coordinate normal to the streamline of the external flow

t function connected with w^* flow over curved wall

T temperature

$u v w$ velocities in the boundary layer

$U V W$ velocities of the external flow

$x y z$ Cartesian coordinates

$\bar{x} \bar{y} \bar{z}$ curvilinear coordinates

$X Y Z$ coordinates in compressible flow

y coordinate used for very large curvature $= \frac{1}{c} + \bar{y}$

α limiting deflection - deflection of boundary layer flow from direction of external flow at $y = 0$

β angle betwee tangent to $\bar{z}$ axis and z axis

γ ratio of specific heats

δ boundary layer thickness

δ_i^+ $(i = 1,2)$ displacement thickness in s_1 s_2 coordinate system

δ_{ij}^{++} $(i=1,2 \quad j = 1,2)$ momentum thickness in s_1 s_2 coordinate system

$\Xi \lambda \zeta$ magnitude of components of vorticity

ξ curvature parameter $= c\sqrt{\frac{\nu \bar{x}}{U^\circ}}$

η similarity variable $= y\sqrt{\frac{U^\circ}{\nu x}}$ ALSO $\bar{y}\sqrt{\frac{U^\circ}{\nu \bar{x}}}$

ϑ direction of $\bar{q}_{12}$ vector

Θ direction of $\bar{Q}$ vector

κ thermal conductivity

μ absolute viscosity

ν kinematic viscosity

ρ density

σ, χ hyperbolic coordinates

$\tau_{0,i}$ shear at $y=0$ $(i=1,2)$

$\psi\ \varphi$ magnitude of vector potential components

$\bar{\omega}$ vector angular velocity

$\omega_1 \omega_2 \omega_3$ components of angular velocity along $x\ y\ z$ axes respectively

Ω stream function

∇ differential operator

Superscripts

$^\circ$ basic flow quantities, also standard quantities in compressible flow

* perturbation quantities

$'$ differentiation with respect to

$^-$ bar above quantity indicates compressible flow (vectors excepted)

n, m, i, k exponents of $x\ \xi\ z$ respectively in description of external flow

Subscripts

n, m, i, k functions correspond to the specific exponents n, m, i, k

partial differentiation may be indicated by subscripts.

I. INTRODUCTION

A. Fluid Mechanical Problems of Turbomachinery

Due to the demands of supersonic flight, the designer of modern compressors and turbines used in flight propulsion is faced today with an ever more acute problem of increase in power requirements. The conventional solution as represented by almost any turbomachine in present usage and development, consists of sufficiently increasing the size of the machinery until the power requirements are met. In practice, inasmuch as the cross-sectional area of the machine is usually limited, this amounts to the addition of extra stages and thus an increase in axial length of the machine. Because the stages of these machines are designed to operate at very moderate pressure ratios, far below those obtainable in cascades and single stage experiments, the important engineering problem,of increase in power output per unit weight of the machinery, remains unsolved. This impasse is primarily due to the fact, that whenever turbomachinery of high pressure ratio per stage is designed, real fluid effects become very important and must be accounted for in the design.

These real fluid effects demonstrate themselves primarily in the so called secondary flow and in three-dimensional boundary layer flow. The term secondary flow is usually used to designate flows arising from nonuniform total pressure or enthalpy, in regions not bordering on physical boundaries where the effects of viscosity may be neglected. On the other hand, by the term three-dimensional boundary layer flow, we understand similar flows in the relatively thin regions next to solid

walls, where viscosity plays a dominant part. The intimate understanding of secondary flow, as well as three-dimensional boundary layer behavior, is a necessary prerequisite to a successful design of the high pressure ratio per stage turbomachinery.

When the external flow (that is flow immediately adjacent to the region designated as boundary layer) is curved, the development of the boundary layer is strongly influenced by the corresponding normal pressure gradient toward the center of curvature, giving rise to a "crosswise" flow. In a corner between the blades and the hub, or the blades and the casing of a turbomachine, this problem is even more complicated, due to the interaction effects of the boundary layer flowing over this very sharply curved surface, and due to the sharp curvature itself. The lack of theories explaining the behavior of boundary layer when a lateral curvature of the external flow exists, or when the boundary layer flow takes place in a corner, has been especially apparent in connection with the problem of turbomachinery design.

B. Review of Three-Dimensional Boundary Layer Flow Investigations

A critical review of the hitherto carried investigations reveals a definite division of these into three separate groups. The first group consists of the investigations of the forms of the boundary layer equations, and discussion of boundary layer behavior as inferred from these forms, without an actual solution of the equations. The second group of investigations concerns itself with solutions of some specialized cases

of three-dimensional boundary layer flow. Finally, the third group consists of general, but approximate treatment of three dimensional boundary layer flow by momentum-integral method. In accordance with this division, but not in order of their chronological appearance, the various investigations will now be discussed.

Howarth[1] establishes the form of three-dimensional, incompressible boundary layer equations in a general orthogonal curvilinear coordinate system (s_1, y, s_2). Since these equations make use of the length elements, defined with respect to the Cartesian coordinate system by: $(dx)^2 + (dy)^2 + (dz)^2 \equiv (h_1)^2(ds_1)^2 + (dy)^2 + (h_3)^2(ds_2)^2$, they are applicable to many configurations. The only important restriction limiting their use lies in the fact that neither of the stretching factors $h_1(s_1, s_2)$ & $h_3(s_1, s_2)$ is a function of the coordinate y perpendicular to the wall over which the boundary layer is flowing. Howarth's equations are therefore restricted to the cases where the lateral curvature of the wall, over which the flow takes place, is not very large, and cannot be applied to corner boundary layer flows. Nevertheless, by considering this form of the equations, Howarth is able to point out the significance of the remaining two curvatures, and in particular, he points out that for boundary layers flowing over cylinders, the curvature effects vanish from the equations of motion. Consequently, for these cases the boundary layer equations may be written in the Cartesian form.

Hayes[2] also considers a coordinate system similar to that of Howarth (and therefore subject to the same limitations), but gives

his equations in the differential, as well as integral form. Furthermore, he makes no restriction of incompressibility, and gives the appropriate forms of the energy equation as well. By assigning specific values to the stretching factors Hayes is able to discuss the form of those equations in cylindrical flow, conical flow, over a body of revolution, and in a coordinate system fitting the streamlines of the external flow (often called intrinsic coordinate system). One important result so obtained is the conclusion, that the action of the external stream curvature is needed for the production of cross flow. Hayes notes a number of simplifications which could be made when the actual solution of the equations is attempted. One of these is linearization based on the small size of cross flow. Another is the possibility of correlation of the compressible boundary layer flow (with no heat transfer and Prandtl number equal to unity) with that of constant density. Hayes found that this correlation, which in two-dimensional boundary layer flow is obtained by stretching of the y coordinate (and is designated sometimes as the Howarth's transformation), in three-dimensional boundary layer flow may cause the appearance of fictitious curvature terms.

The work of Moore[3] concerns itself with the compressible form of the boundary layer equations in a Cartesian system and also in a system suitable for application to conical flows. By defining the components of a vector potential in terms of the velocities, he is able to satisfy the continuity condition identically, and thus, reduce by one

the number of equations entering the problem. The application of the so called Howarth's transformation, and (in the case of conical flows) modified Mangler's transformation, gives to these equations a form which is somewhat similar to that for incompressible, two-dimensional boundary layer. In discussion of these equations, Moore shows that, when the external flow streamlines are straight and parallel, the shape of the leading edge has no effect on the three-dimensional boundary layer flow, as long as the curvature of the leading edge varies in a continuous manner. He notes also that in compressible flows having conical symmetry, the Blasius similarity variable may be applied, thus reducing the number of independent variables to two, and implying a parabolic boundary layer development along rays from the apex.

Of interest to turbomachinery applications is the work of Burgers,[4] who considers the equations and problems which arise in the study of boundary layers formed in just such machines. In particular, he concentrates on the effect of angular velocity, and establishes the form of boundary layer equations applicable to a Cartesian coordinate system rotating with a constant angular velocity about an axis fixed in space.

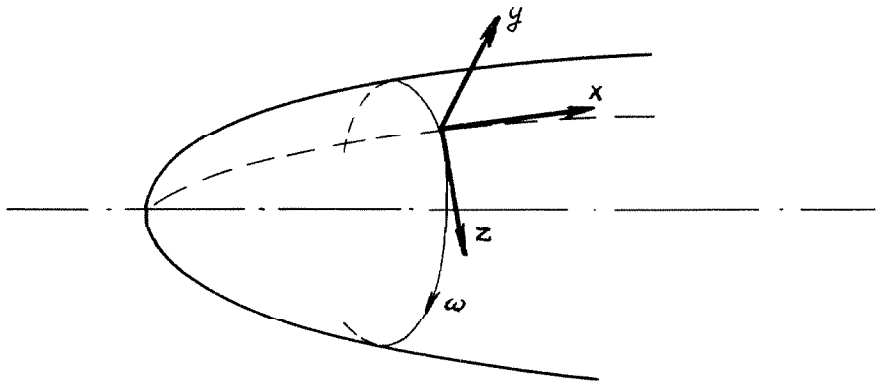

By considering successively the cases involving the tangential velocity (in the z direction) and the angular velocity $\bar{\omega}$, Burgers is able to demonstrate qualitatively the presence of the additional forces caused by the rotation which (depending on the shape of the surface over which the boundary layer is developing) may, or may not, offset the effect of pressure gradients in the x direction. In addition to these considerations, Burgers attempts also to discuss the effect of the blades, but inasmuch as he neglects to establish the equations governing such flow, (axial symmetry considerations cannot apply here) this part of his paper is necessarily approximate and sketchy. In general therefore, Burgers investigation is limited mainly to axially symmetric cases, and also to cases when the external flow (considered with respect to an inertial system) is irrotational. These two conditions are certainly not true in the more realistic approach to the turbomachinery problem.

The work of Tetrevin,[5] who gives the momentum-integral equations for fluid of variable density and viscosity is essentially superseded by the more general equations given by Hayes.

The investigations falling into the second group of this classification, in the main consist of cases where:

a) the changes with respect to one of the independent coordinate are zero,

b) where there is some sort of symmetry, and

c) where there is some characteristic parameter which is small.

For instance, Prandtl[6] and Sears[7] are able to treat the cases of infinitely long yawed cylinder, where if x and z coordinates are taken in the chordwise and spanwise directions respectively, none of the physical quantities involved in the flow can be functions of z .

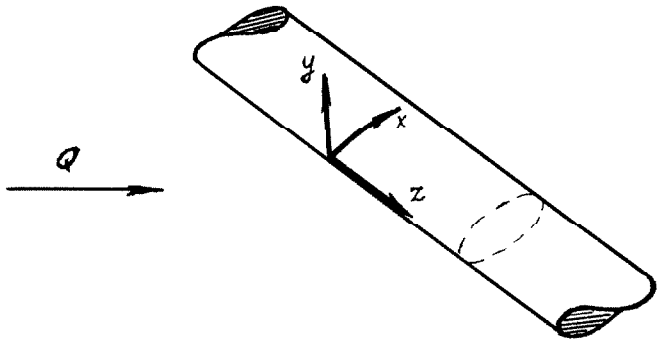

This results in the separation of momentum equations, and in fact, the equations in the chordwise direction remain the same as in the two-dimensional case. This property of the equations is also utilized by Wild,[8] who computes the boundary layer over a yawed infinite wing using the momentum-integral method, and by Young and Booth,[9] who apply the same method to turbulent boundary layer. Since the equations in the chordwise direction remain identical to those for two-dimensional flow, the phenomenon of chordwise flow reversal occurs exactly at the position of separation in two-dimensional boundary layer flow. Consequently all the above solutions have the drawback of not being able to indicate the position of chordwise flow reversal in real wings, where undoubtedly the boundary layer quantities are not independent of the spanwise coordinate. Nevertheless it is interesting to note that experiments of Altman and Hayter[10] seem to show that

even in the case of small localized spanwise pressure gradients, the chordwise boundary layer appears to be independent of the spanwise boundary layer, and thus the above mentioned (and often called "simple sweep") theories should give reasonably good results as far as the general development of boundary layer thickness and computations of drag (in absence of flow reversal) are concerned.

Another case where the boundary layer quantities are independent of one of the coordinates, occurs in the investigation of Bödewart,[11] who considered axially symmetric rotary flow over solid ground, a case which may be important in meteorology. No separation of the

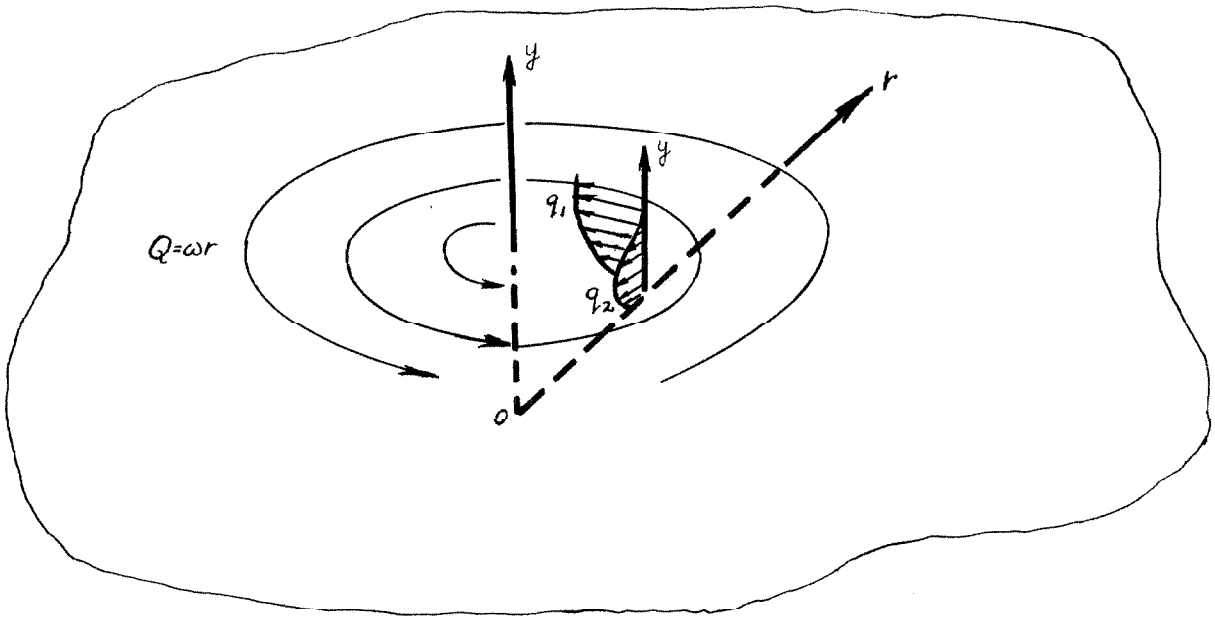

equations occurs, but nevertheless the equations may be converted into ordinary differential equations if a similarity parameter based on the square root of the product of curvature and local external flow velocity is used. Bödewart obtained the solution of these equations, and one of his most interesting results is that; the deflection α , of the boundary layer flow at the ground from the direction of the external flow, equals about 50.6° inwards, and is independent of the radius. This then points to the effect of the rotation of the surface, for when such occurs in an otherwise stationary fluid (as computed by von Kármán in Reference 12), the boundary layer due to the action of the centrifugal force is displaced outwards.

When the restriction of axial symmetry in Bödewart's case is removed, and thus the plate, over which the boundary layer flow takes place, posses a definite leading edge, solutions for rotary flows may be obtained if an expansion in terms of total turning of the external flow is considered. For small turning, considering only first order terms,

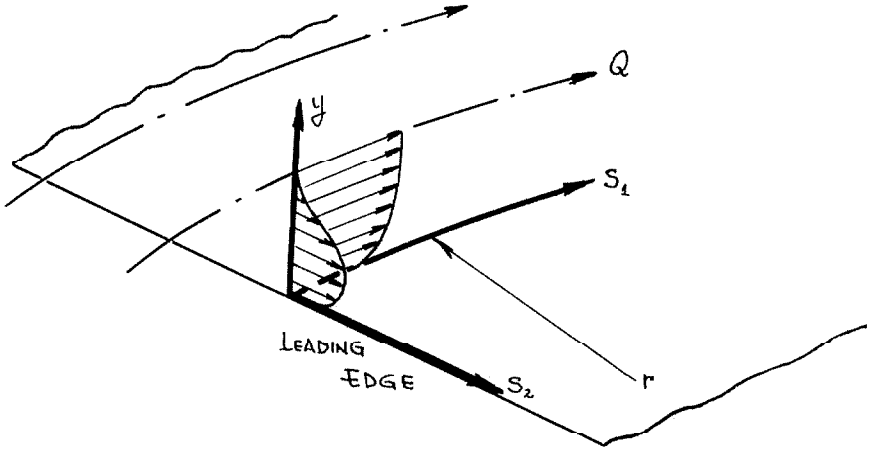

Mager and Hansen[13] found such a solution for compressible and incompressible cases. In this solution the limiting deflection is also independent of the radius, but is shown to depend directly on the turning of the external flow. Compressibility, besides the characteristic "stretching" of the y coordinate, is shown to exercise a scale effect on the crosswise flow (that is in the S_2 direction) in the boundary layer.

Of somewhat more direct application to turbomachinery and helicopter blading design may be the results of Fogarty,[14] who considers laminar boundary layer flow on a slowly rotating blade at large distances from the axis of rotation. These two assumptions are

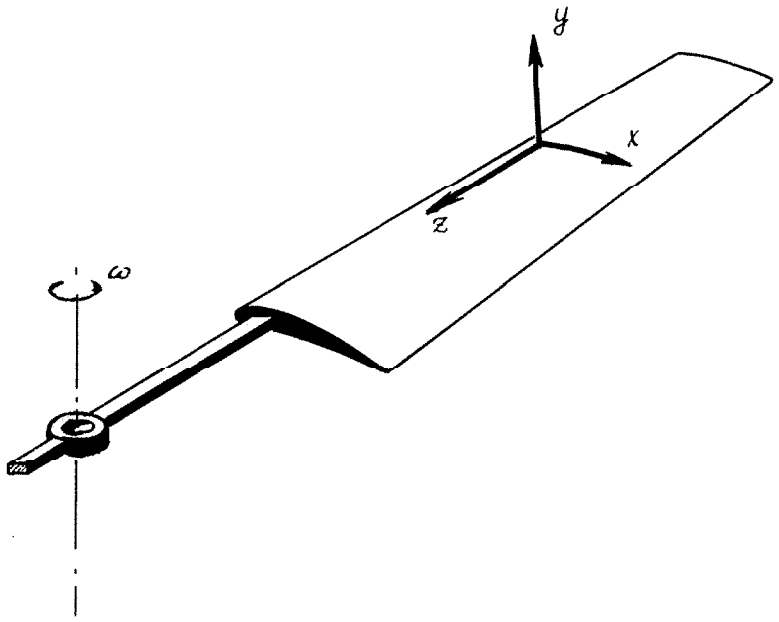

sufficient to achieve a separation of the momentum equations, so that the velocity in the chordwise direction (just like in the yawed wing case) becomes completely independent of the spanwise velocity, and of the angular velocity, while the second momentum equation becomes linear.

Actually, as it will become apparent later, the assumption of small angular velocity, provided it is interpreted properly, is not as critical as may seem at first in application to axial type of turbomachinery, and the results of Fogarty, which show rather small effects of the rotation, should be applicable there if an additional limitation that the external flow be potential is also satisfied.

Another investigation treating rotation of the surface, over which the boundary layer is flowing, is that by Howarth,[15] who by expanding in terms of polar angle, establishes the form of equations describing the boundary layer on a sphere rotating in a stationary fluid. Because the convergence is expected to be slow, the solution may be considered practical only for small values of this parameter; that is, near the poles. Howarth actually neglects to solve the so obtained equations, and considers, instead, an approximate solution by the momentum-integral method.

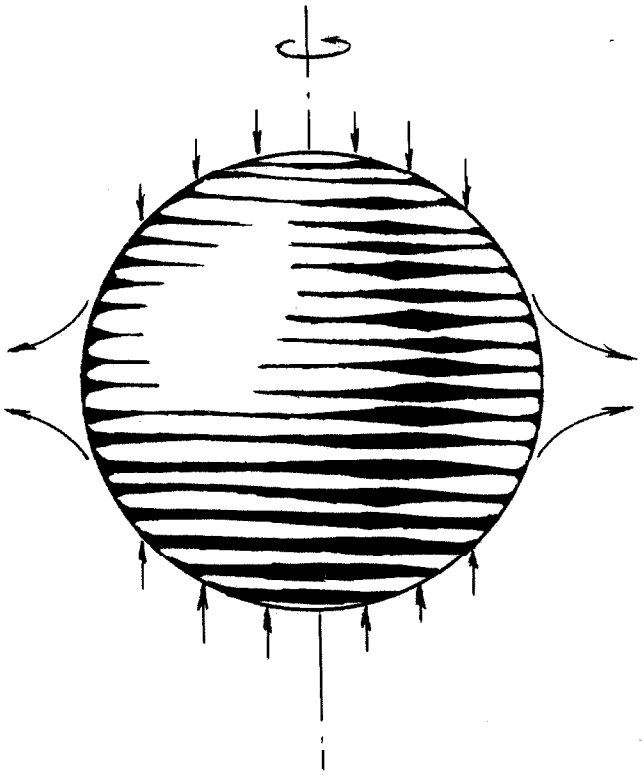

Thus calculated results indicate that inflow into the boundary layer occurs over large part of the surface, while the outflow is confined to the vicinity of the equatorial plane. At the equatorial plane there is then an interesting region of interaction between the boundary layers from the two hemispheres, but unfortunately, the boundary layer equations fail to represent this region adequately. In addition to the rotating sphere, Howarth discusses in the same paper also the case of a thin, hollow, semi-infinite cylinder rotating about an axis parallel to the external flow velocity Q . The boundary layer velocities for this

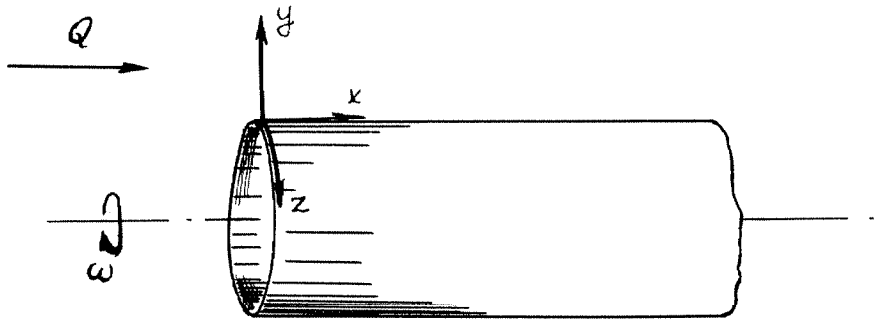

case (in all three directions) are shown to be identical to those obtained by Blasius for flow over a flat plate.

In another investigation,[16] Howarth also treats the flow near a stagnation point; that is, when the external flow velocities are representable by $U = Bx$, $W = Az$, and the external flow streamlines are given by $z = \text{CONST.}\ (x)^{A/B}$. Howarth shows that in this case the equations are reducible to two simultaneous, third order, total differential equations

containing the single parameter (A/B). The shape of the streamlines indicates clearly that when $(A/B) = 0$, the equations must correspond to two-dimensional flow, and when $(A/B) = 1.0$, the equations describe a flow about a body of revolution located symmetrically in the stream. These are the two limiting cases, and therefore the solutions of the equations for $0 \leqslant (A/B) \leqslant 1.0$ are of interest.

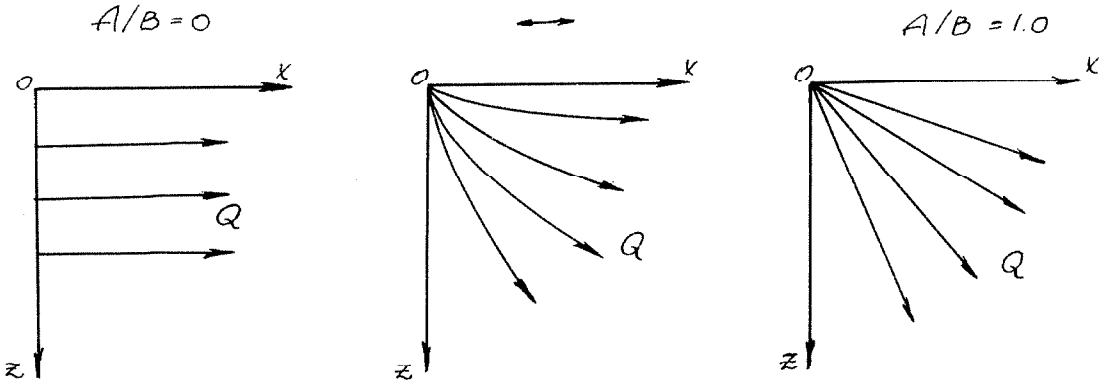

By expanding in powers of (A/B), Howarth obtains such solutions when (A/B) is small. For large values of (A/B), Adams numerical method was used. The deflection α, of boundary layer flow at the surface from the direction of the external flow, is greatest for $(A/B) \rightarrow 0$, and equals 21°, when the external flow has turned through 55.8°. For $(A/B) = 1.0, \alpha = 0$, and there is no crosswise flow in the boundary layer.

Of considerably greater practical interest than the cases treated by Howarth, are the results of Moore,[17, 18, 19] who obtained solution for boundary layer flow over a cone at angle of attack to a supersonic stream. These solutions show, that when angle of attack is assumed small (solution obtained by method of perturbations), although the

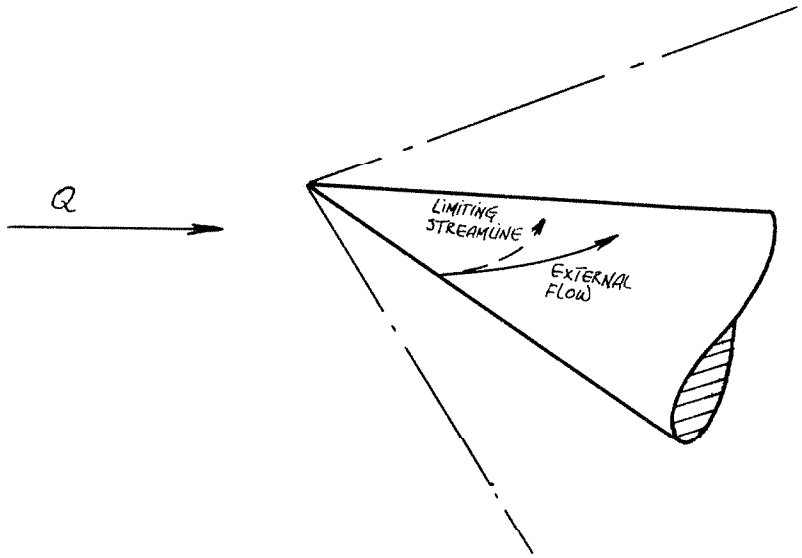

boundary layer thickens on the downstream side of the cone, no separation of the circumferential flow occurs. On the other hand, when the considerations are restricted to the planes of symmetry of the flow, regardless of the angle of attack, on the downstream side of the cone solutions exist for only very limited values of the angle of attack. This is in line with the remarks of Hayes,[2] and Moore suspects this fact to be connected with laminar separation of the circumferential flow. The validity of these results is still in question. It is possible that Moore's inability to find solutions, for certain angles of attack, is due to the improper assumption about the character of the external flow. It is thus implied that if for large angles of attack the external flow is considered rotational, and if the velocity of the external flow normal to the wall is not neglected - the boundary layer type of solution may be recovered.

The advantages of symmetry are used in the two investigations dealing with boundary layer flow in a corner between two intersecting

walls. Carrier[20] considers such a flow when the angle between the two walls is $\pi/2$, with no pressure gradients in the external flow, and obtains a solution by numerical relaxation of the appropriate equations of motion. This solution shows that Blasius type of similarity holds, and constant velocity lines deviate only slightly from hyperbolic shape, this deviation being greatest close to the line of symmetry. Loitzianskii

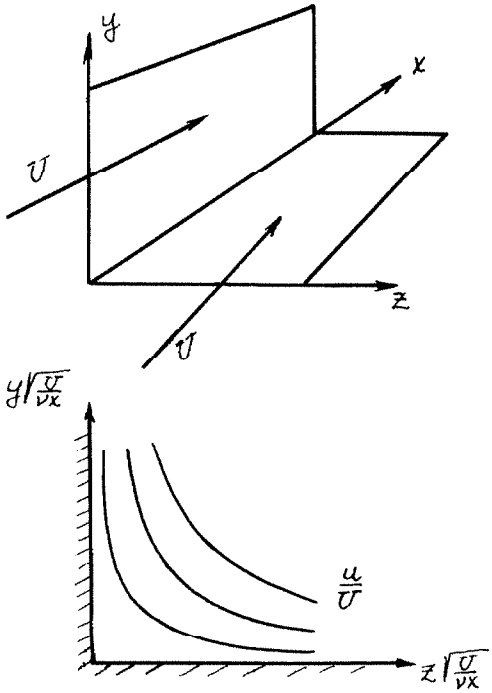

and Bolshakow[21] treated the boundary layer flow between two walls intersecting at an arbitrary angle. No pressure gradient of the external flow was considered, but because the momentum-integral method was used, the results apply to laminar, as well as to turbulent boundary layers.

These results indicate that, except for the cases where the included angle between the two walls is small (of the order of 10^{o} or less), the effect of the interference of the two boundary layers on the drag is insignificant.

As may be seen from this review, the investigations falling into the second class treat only very specialized cases of three-dimensional boundary layer flow, and furnish a comparatively small amount of information as far as the general behavior of the three-dimensional boundary layer is concerned.

Of greatest practical interest to turbomachinery designers are the general, but approximate, treatments of three-dimensional boundary layer flow by use of momentum-integral method as given by Timman[22] and by Mager.[23] Both of these references use an intrinsic coordinate system, and show that when written in such system, the equations reduce

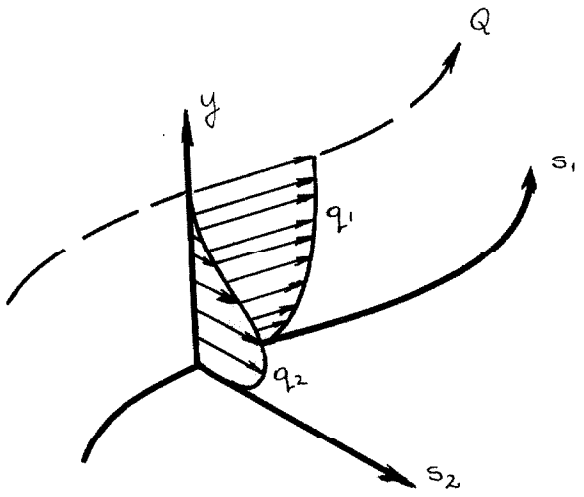

to two quasi-linear, partial differential equations, which may be parabolic, hyperbolic, or elliptic, depending on the relations between the assumed velocity distributions and the parameters describing these distributions. In Reference (22), laminar boundary layer is considered, and hyperbolic nature of the equations is assumed, so that a solution by method of characteristics is suggested. In Reference (23), on the other hand, for turbulent boundary layer, the examination of the experimental data of Gruschwitz[24] indicated a parabolic nature of the equations, and consequently, solutions were obtained by integration along a streamline of the external flow. Inasmuch as the data of Reference (24) pertain to only one special case of turbulent boundary layer (in a curving duct), the important question, which remained unanswered, is whether a solution of three-dimensional momentum-integral equations by method of characteristics is feasible.

Another important question which remained unanswered is that of the velocity distributions to be used in the momentum-integral method. Timman made his choice of velocity distributions from purely qualitative argument, and there is no assurance whether these velocities correspond to real flows. Mager, on the other hand, used Gruschwitz data to establish velocity distributions, but he assumed his profiles to be fixed in shape, a condition which certainly is not satisfied in presence of pressure gradients. Since experimental data are lacking, it appears that much knowledge about velocity distributions could be gained from analytical solutions of three-dimensional boundary layer equations.

C. Statement of the Problem

The object of this investigation is a solution of the three-dimensional, steady, laminar boundary layer flow equations for a number of general external flows with small lateral pressure gradients, which may be of particular interest in turbomachinery, so that a proper choice of velocity distributions can be made when applying the integral methods. Also, on the basis of the results so obtained, the question of the nature of the momentum-integral equations will be reexamined in an effort to determine the proper procedure which should be used in their solution.

In addition, the boundary layer flow over very sharply curved surfaces in the transverse direction (but not too sharply, to cause interaction of the boundary layer), and in the presence of small lateral pressure gradients, will be investigated, so as to give the designers some insight into the phenomena that takes place in the corners. The investigation is limited to steady, laminar boundary layer flow because a) of our inability to treat the equations of unsteady and turbulent viscous motion of fluids, and b) it has been shown in two-dimensional boundary layer flow that the effect of the parameters important in laminar boundary layers has been qualitatively the same in turbulent boundary layer flow.

II. ANALYSIS OF THREE-DIMENSIONAL BOUNDARY LAYER FLOW OVER A PLANE

A. Preliminary Remarks

One useful approximation in the study of turbomachinery is to consider such a machine as developed at a particular radius into a series of infinite cascades. When boundary layer flow on the casing or hub of turbomachinery is studied, such development will prove of value, because as long as the ratio of boundary layer thickness to the radius of the developed cylinder is small, the effect of lateral curvature is negligible, and the basic equations remain essentially unchanged.[1]

An example of such a development at the casing radius of an axial flow compressor is illustrated in Figure 1. Consider now the so-called absolute flow, that is, the flow relative to the stationary casing (streamline "A"). As may be seen from Figure 1, this flow undergoes a series of small periodic deflections from the so-called mean flow, due to the action of the consecutive rotor and stator blade rows of a compressor. If desired, the physical blades could be considered infinitely thin and their action on the flow could be represented by an equivalent force field. In constructing a model for study of boundary layer flow on compressor casing, one could, therefore, consider the external flow caused by such a force field, and compute the boundary layer development corresponding to it. The small deviations of the external flow from the mean velocity suggest the use of small perturbation procedure in the solution of boundary layer equations. Since,

however, the mean velocity, which is the obvious invariant in such a procedure, is at a definite angle to the cascade axes, the perturbation quantities must be functions of both; the coordinate directed along the mean velocity (say x) and the one perpendicular to it (say z). A moments consideration will reveal that a completely analogous picture is obtained if the development of boundary layer on the hub of the compressor is desired (streamline "B"). Here, however, since the hub is rotating, it is necessary to use as the invariant quantity the so-called relative velocity, and in addition, in the boundary layer equations, the centrifugal and Coriolis forces must be included.

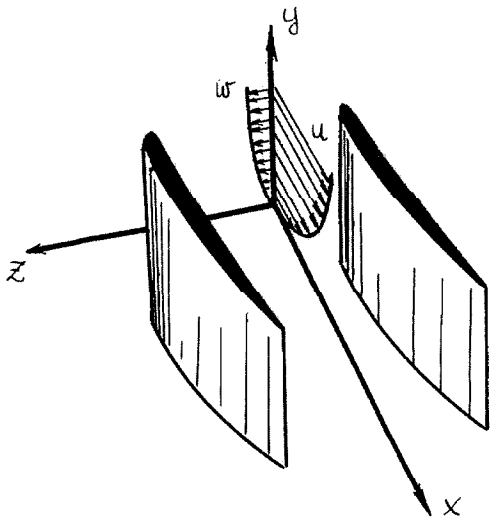

Now let us consider boundary layer development on the actual blades, away from either the hub or the casing. In general, the compressor blades are designed so that the external flow deflects only little in the radial direction from a cylindrical surface parallel to the axis of the compressor. Therefore, the perturbation procedure with

respect to some conveniently chosen relative (to the blade) velocity may again be used to advantage, and since the system is non-inertial, the Coriolis and centrifugal acceleration terms must be included in the equations. The blade surface as such is generally only slightly curved (with the exception of high impulse turbines), and therefore effects of this curvature may be neglected, just as is done in two-dimensional airfoil considerations.

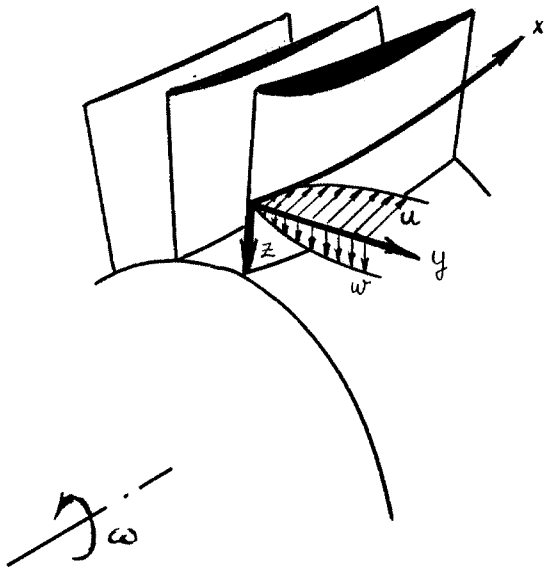

It appears, therefore, that a useful model for study of boundary layer behavior in turbomachinery may be constructed from the considerations of boundary layer flow over a plane surface, and affected by arbitrary, but small, pressure gradients. To illustrate the effect of Coriolis and centrifugal forces, the surface may be set in rotation with constant angular velocity about an axis; so located, that the component of the angular velocity perpendicular to the surface be small.

This restriction on the relative location of the axis of rotation should present no objections when axial type of turbomachinery is considered. This, then, is the model which will be subsequently investigated.

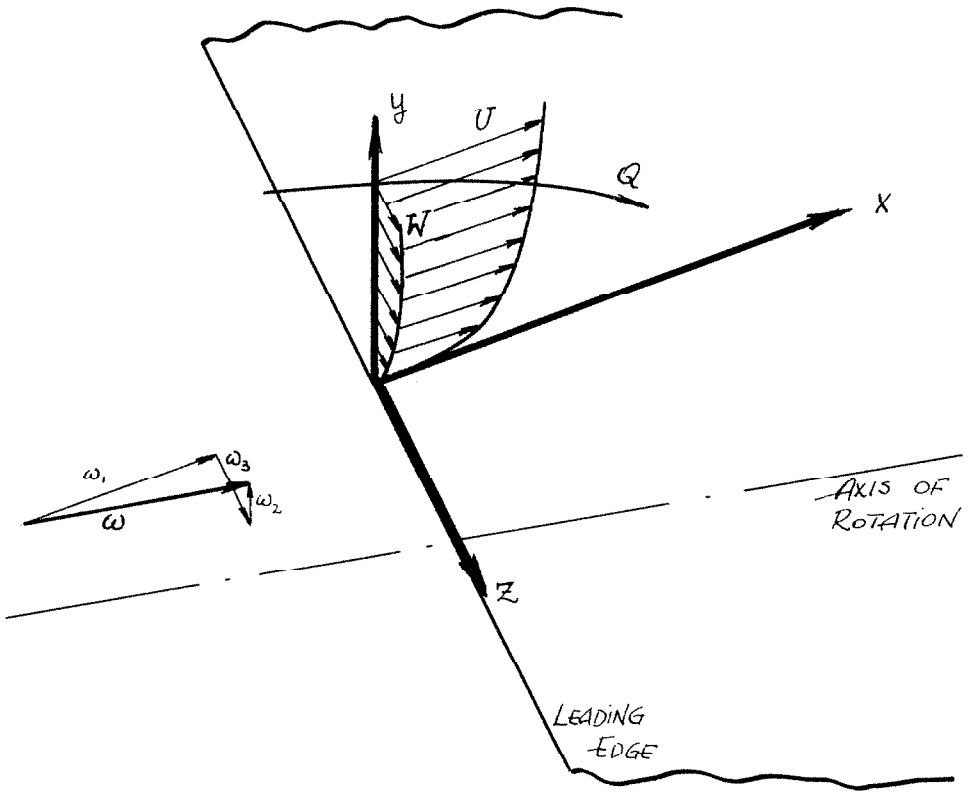

B. Boundary Layer Equations

The motion of an incompressible, steady, viscous fluid, flowing relative to a coordinate system rotating with a uniform angular velocity, is described by the momentum equations:

$$-\bar{q}\times(\nabla\times\bar{q}) + \bar{\omega}\times(\bar{\omega}\times\bar{b}) + 2\bar{\omega}\times\bar{q} = -\nabla\left(\frac{p}{\rho}+\frac{1}{2}\bar{q}^2\right) + \nu\left[\nabla(\nabla\cdot\bar{q}) - \nabla\times(\nabla\times\bar{q})\right] \qquad (1)$$

and the equation of continuity:

$$\nabla \cdot \bar{q} = 0 \tag{2}$$

Assuming that the velocity v is of $O(\delta)$, and restricting our considerations to a thin layer, so that y is of $O(\delta)$, but the velocities $u, \bar{\omega}$, w and the lengths x, z are of $O(1)$ as compared to some characteristic length and velocity, the order of magnitude of the various terms involved in Equations (1) and (2) may be evaluated. Neglecting all terms of $O(\delta)$, or smaller, as compared to those of $O(1)$, one obtains the boundary layer equations. For Cartesian system these are written as:

$$u u_x + v u_y + w u_z + 2\omega_2 w - \omega^2 r r_x = -\frac{1}{\rho} p_x + \nu u_{yy} \tag{3a}$$

$$2(\omega_3 u - \omega_1 w) - \omega^2 r r_y = -\frac{1}{\rho} p_y \tag{3b}$$

$$u w_x + v w_y + w w_z - 2\omega_2 u - \omega^2 r r_z = -\frac{1}{\rho} p_z + \nu w_{yy} \tag{3c}$$

and

$$u_x + v_y + w_z = 0 \tag{4}$$

Since as previously mentioned ωr and the velocities u and w are of $O(1)$, Equation (3b) indicates that p_y is of $O(1)$. This occurs because a pressure gradient is necessary to balance the effect of the centripetal and Coriolis forces. But the total change of pressure throughout the

boundary layer along a normal to the wall is still of $O(\delta)$, and although this is larger than on a nonrotating flat plate (where it is of $O(\delta^2)$), it may still be neglected. A reasonable assumption, therefore, is to consider p as a function of x and z only.

C. External Flow

The external flow is defined as the flow where the effects of viscosity may be neglected, regardless whether it is rotational or irrotational. This definition is different from that used in conventional mechanics of the boundary layer flow, and implies a division of the total flow field into a region where effects of viscosity are neglected, and a (still thiner) region where such effects are considered. If the external flow is rotational, then it must satisfy the Eulerian equations for the variation of pressure:

$$U U_x + V U_y + W U_z + 2(\omega_2 W - \omega_3 V) - \omega^2 r r_x = -\frac{1}{\rho} p_x \tag{5a}$$

$$U V_x + V V_y + W V_z + 2(\omega_3 U - \omega_1 W) - \omega^2 r r_y = -\frac{1}{\rho} p_y \tag{5b}$$

$$U W_x + V W_y + W W_z + 2(\omega_1 V - \omega_2 U) - \omega^2 r r_z = -\frac{1}{\rho} p_z \tag{5c}$$

and the equation of continuity:

$$U_x + V_y + W_z = 0 \tag{5d}$$

If this flow is irrotational then in addition to Equations (5), it must also satisfy:

$$\begin{aligned} \Pi &= W_y - V_z = 0 \\ \lambda &= U_z - W_x = 0 \\ \zeta &= V_x - U_y = 0 \end{aligned} \tag{6}$$

When the surface over which the flow takes place is rotating and the irrotationality of the external flow with respect to an inertial (non-rotating) system is maintained, then with reference to the non-inertial system the vorticity components are:

$$\begin{aligned} \Pi &= -2\omega_1 \\ \lambda &= -2\omega_2 \\ \zeta &= -2\omega_3 \end{aligned} \tag{7}$$

In the present analysis it will be assumed that Equations (6) and (7) are not necessarily satisfied, however, if the flow is rotational, the vorticity components Π and ζ, and in particular the derivatives U_y and W_y are small as compared to U_x. Furthermore since we are interested only in the thin boundary layer solution, the velocity V will be assumed of $O(\delta)$, so that terms like VU_y and VW_y will still be considered small as compared to UU_x. Thus retaining only terms of $O(UU_x)$, so as to be consistent with the boundary layer equations, we obtain from Equations (5):

$$U U_x + W U_z + 2\omega_2 W - \omega^2 r r_x = -\frac{1}{\rho} p_x \tag{8a}$$

$$U W_x + W W_z - 2\omega_2 U - \omega^2 r r_z = -\frac{1}{\rho} p_z \tag{8b}$$

The external flow components U, W and the angular velocity $\bar{\omega}$ are assumed known. In particular we take:

$$\begin{aligned} p &= p^\circ + p^*(x,z) && p^* \ll p^\circ \\ U &= U^\circ + U^*(x,z) && U^* \ll U^\circ \\ W &= W^*(x,z) && W^* \ll U^\circ \\ \bar{\omega} &= \bar{i}\omega_1 + \bar{j}\omega_2 + \bar{k}\omega_3 && \omega_2 \ll \omega_1, \omega_3 \end{aligned} \tag{9}$$

as describing the external flow and the angular velocity. In Equation (9) velocity U°, pressure p° and angular velocity $\bar{\omega}$ are assumed constant. The component ω_2 is taken of the same order when compared to ω_1 as U^* when compared to U°. The third external flow component V may be assumed as given by the $\lim_{y \to \delta} v$. Use of this assumption will be made when treating the boundary layer flow over sharply curved surface.

D. Derivation of the Perturbed Flow Equations

Corresponding to Equations (9), the flow in the boundary layer is expressed by:

$$\begin{aligned} u &= u^\circ + u^* \\ v &= v^\circ + v^* \\ w &= w^* \end{aligned} \tag{10}$$

Making use of Equations (8), (9), and (10) in Equations (3) and (4) one obtains the zeroth order equations:

$$u^\circ u^\circ_x + v^\circ u^\circ_y = \nu u^\circ_{yy}$$

$$u^\circ_x + v^\circ_y = 0 \tag{11}$$

and the first order equations:

$$u^\circ u^*_x + u^* u^\circ_x + v^\circ u^*_y + v^* u^\circ_y = U^\circ U^*_x + \nu u^*_{yy} \tag{12a}$$

$$u^\circ W^*_x + v^\circ W^*_y + 2\omega_2 (U^\circ - u^\circ) = U^\circ W^*_x + \nu W^*_{yy} \tag{12b}$$

$$u^*_x + v^*_y + W^*_z = 0 \tag{12c}$$

Equations (11) are just the Blasius equations and their solution is:

$$u^\circ = U^\circ F'(\eta)$$

$$v^\circ = \frac{1}{2}\sqrt{\frac{\nu U^\circ}{x}}(\eta F' - F)$$

$$\eta = y\sqrt{\frac{U^\circ}{\nu x}}$$

with F satisfying:

$$FF'' + 2F''' = 0$$

and boundary conditions:

$$F(0) = F'(0) = 0$$

$$F'(\infty) = 1.0$$

These values may then be used in the solution of the system of Equations (12). Introducing the vector potential components in the manner of Reference (3):

$$u^* = \psi_y$$
$$w^* = \varphi_y$$
$$v^* = -(\psi_x + \varphi_z)$$

Equation (12c) is identically satisfied, while Equations (12a) and (12b) become:

$$u^\circ \psi_{yx} + \psi_y u^\circ_x + v^\circ \psi_{yy} - (\psi_x + \varphi_z) u^\circ_y = U^\circ U^*_x + \nu \psi_{yyy}$$
$$u^\circ \varphi_{yx} + v^\circ \varphi_{yy} + 2\omega_z (U^\circ - u^\circ) = U^\circ W^*_x + \nu \varphi_{yyy} \qquad (13)$$

Now taking for:

$$\psi(x, \eta, z) = \frac{U^*}{U^\circ} \sqrt{\nu x U^\circ}\ f(\eta)$$
$$\varphi(x, \eta, z) = \frac{W^*}{U^\circ} \sqrt{\nu x U^\circ}\ g(\eta) \qquad (14)$$

so that the velocities in the boundary layer are given by:

$$u = U^\circ F' + U^* f'$$
$$w = W^* g'$$
$$v = -\frac{1}{2} \sqrt{\frac{\nu}{U^\circ x}} \left[U^\circ (F - F'\eta) + U^* (f - f'\eta) + 2x (U^*_x f + W^*_z g) \right] \qquad (15)$$

and Equations (13) become:

$$f''' + \frac{F}{2} f'' - \left(x \frac{U_x^*}{U^*} F'\right) f' + \left[F''\left(\frac{1}{2} + x \frac{U_x^*}{U^*}\right)\right] f + x \frac{W_z^*}{U^*} F'' g + x \frac{U_x^*}{U^*} = 0 \qquad (16a)$$

$$g''' + \frac{F}{2} g'' - \left(x \frac{W_x^*}{W^*} F'\right) g' + x \frac{W_x^*}{W^*} - 2\omega_2 x \frac{1}{W^*}(1 - F') = 0 \qquad (16b)$$

The appropriate boundary conditions are:

$$f(0) = f'(0) = g(0) = g'(0) = 0$$

$$f'(\infty) = g'(\infty) = 1.0 \qquad (17)$$

E. Discussion of Equations(16)

It is clear from the form of Equations (16), that in order to insure complete similarity, that is, in order to convert Equations (16) to two total differential equations in one independent variable η, the external flow U^*, W^* must be expressible in the form: $U^* = B x^m z^i$, $W^* = A x^n z^k$. A number of such cases for a given choice of i, k, m, and n will be discussed below. For the time being, suppose that an appropriate choice for the external flow has been made, and that Equations (16) are thus total differential equations. The inspection of the system reveals that Equation (16b) is completely independent of Equation (16a), and may be solved first for $g(\eta)$. This separation of equations indicates, that physically, to the first order of approximation,

the transverse flow w^* (or w) is completely independent of the u^* flow, and depends only on the gradients of the external lateral flow W^* and possibly the angular rotation term ω_z. Furthermore, it should be noted that only the gradients of W^* in the x direction enter Equation (16b). This means that the distribution of the w flow with η will not be affected by the W_z^* gradients, even if such exist.

The effect of the external flow gradients on the velocity distribution g' may be investigated by taking account of the boundary conditions at $\eta = 0$. In this way one obtains:

$$g'''(0) = \frac{x}{W^*}(2\omega_z - W_x^*) \tag{18}$$

It should be remembered that x will not enter this equation if proper substitution of W^* is made. In Equation (18), however, the old form is retained, so as to indicate more clearly the nature of the changes in $g'''(0)$ corresponding to changes in W_x^* and ω_z. The quantity $g'''(0)$ indicates the curvature of the profile of the w velocity distribution at $y = 0$. It may be seen from Equation (18) that the effect of angular velocity ω_z counteracts, in general, the effect of W_x^*. If ω_z is zero, (the plate is either stationary or the x axis is parallel to the axis of rotation) the sign of W_x^* will determine the sign of the curvature $g'''(0)$. This behavior of the w^* velocity profile is then completely analogous to the behavior of the two-dimensional velocity profile. There is, however, an important difference between the interpretation of this result in a two-dimensional boundary layer and a three-dimensional

boundary layer. From the sketch it may be seen that

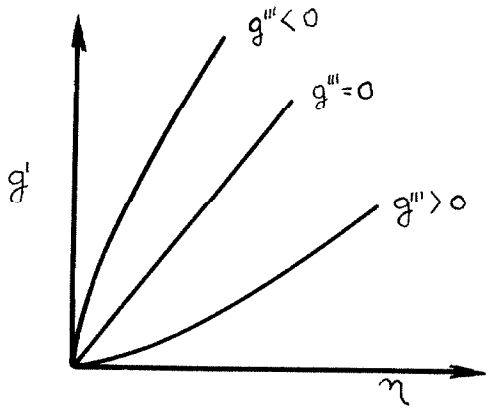

$g'''(0) > 0$ corresponding to $W^*_x < 0$ results in lower values of w close to the surface. If W^*_x is made sufficiently large negative, reversals of the w velocity may be expected. In two-dimensional flow such behavior of velocity profile leads to the separation of the boundary layer. In three-dimensional flow however, the decrease and possible reversal of the w velocity mean that only one component of the flow $\bar{q}_{12}$ ($\bar{q}_{12} = \bar{i}u + \bar{k}w$) has a tendency to change direction. The boundary layer, in general, will still adhere to the surface. Experimental evidence of this fact was obtained in Reference (25), where it is noted that on a yawed wing with turbulent boundary layer, the reversal of the u flow alone did not cause the large pressure fluctuations usually observed in separated two-dimensional boundary layers.

Equation (16a) is coupled with Equation (16b) through the term $x\frac{W^*_z}{U^*}F''g$. Clearly then, if W^* is not a function of z, the two equations are completely separated. This result is more general than the one derived for yawed infinite bodies, since U^* may remain an arbitrary

function of z . The curvature of the u^* velocity profile at $y=0$

$$f'''(0) = -x\frac{U_x^*}{U^*} \tag{19}$$

is given again by the velocity gradient in the x direction. Therefore, if the equations are uncoupled and U^* is not a function of z , the reversal of the u profile will occur exactly at the same position where separation occurs in two-dimensional flow. If U^* is a function of z, then the position of flow reversal will also be a function of z .

Since the fluid in the boundary layer is affected by the same pressure gradient as the external flow, but must follow it more closely having less inertia, an angular deflection exists between the streamlines of the external flow and those of the boundary layer flow. This deflection, which may be considered as a measure of "secondary flow" in the boundary layer (hereafter designated as crosswise flow), is greatest when the limiting streamline at $y = 0$ is considered. Designating the direction of the external flow by:

$$\theta = \text{Arctan}\frac{W^*}{U^\circ+U^*} \approx \frac{W^*}{U^\circ}$$

and that in the boundary layer by:

$$\vartheta(\eta) = \text{Arctan}\frac{W^*g'}{U^\circ F'+U^*f'} \approx \theta\frac{g'}{F'}$$

one obtains for the deflection to the first order of approximation:

$$\vartheta - \theta \approx \frac{W^*}{U^\circ}\left(\frac{g'}{F'} - 1\right)$$

and the limiting deflection:

$$\alpha \approx \frac{W^*}{U^\circ}\left(\frac{g''(0)}{F''(0)} - 1.0\right) \tag{20}$$

by L'Hospital's rule. Equation (20) shows that the existence of crosswise flow to our order of approximation is determined solely by Equation (16b), and is completely independent of the possible changes in the u velocity profile. One may thus state that the factors affecting crosswise flow in the boundary layer are the $x \frac{W_x^*}{W^*}$ gradient and the rotational velocity term $x \frac{\omega_z}{W^*}$.

In regard to rotation it should be noted, that since no derivatives of ω_z have occurred, this quantity could have been a function of x and z without affecting in any way Equations (16). This would actually take place if the plane $x z$ were slightly curved.

Equations (16) were obtained by use of the perturbation procedure. Inasmuch as all velocity components vanish at $y = 0$, one may properly question the validity of the perturbation procedure in the region $y \approx 0$. To clarify this objection an argument will be given which is similar to that advanced by Moore.[17]

Consider for example term $u u_x$ which appears in Equations (3a). Making use of Equations (15) and dividing by $(U^\circ)^2$

$$\frac{u}{U^{\circ 2}} u_x = \frac{1}{(U^\circ)^2}(u^\circ + u^*)(u^\circ + u^*)_x$$

$$= -\frac{\eta}{2x} FF' + \frac{U^*}{U^\circ}\left[\frac{U_x^*}{U^*} Ff - \frac{\eta}{2x}(f'F + fF')\right] + \left(\frac{U^*}{U^\circ}\right)^2\left(\frac{U_x^*}{U^*} f^2 - \frac{\eta}{2x} ff'\right)$$

Following the perturbation procedure, terms of $O\left(\frac{U^*}{U^\circ}\right)^2$ are neglected when compared to terms of $O\left(\frac{U^*}{U^\circ}\right)$. The question which needs to be answered is, whether this is proper, since both terms vanish as $\eta \to 0$. Writing the last two terms as:

$$-\frac{U^*}{U^\circ}\left[\left(\frac{\eta}{2x}F' - \frac{U_x^*}{U^*}F\right)f + \frac{\eta}{2x}Ff'\right]\left\{1.0 - \frac{\frac{U^*}{U^\circ}\left(\frac{U_x^*}{U^\circ}f - \frac{\eta}{2x}f'\right)f}{f\left(\frac{\eta}{2x}F' - \frac{U_x^*}{U^*}F\right) + \frac{\eta}{2x}f'F}\right\}$$

one asks whether under all conditions

$$\frac{U^*}{U^\circ}\,\frac{\left(\frac{U_x^*}{U^*}f - \frac{\eta}{2x}f'\right)f}{f\left(\frac{\eta}{2x}F' - \frac{U_x^*}{U^*}F\right) + \frac{\eta}{2x}f'F} \ll 1.0$$

or in other words, whether

$$\frac{\left(\frac{U_x^*}{U^*}f - \frac{\eta}{2x}f'\right)f}{\left(\frac{\eta}{2x}F' - \frac{U_x^*}{U^*}F\right)f + \frac{\eta}{2x}f'F}$$

is always of $O(1)$ or smaller. Expanding the functions f and F about $\eta = 0$ and making use of boundary conditions (17):

$$F(\eta) = \frac{F''(0)}{2!}\eta^2 + \frac{F'''(0)}{3!}\eta^3 + \cdots$$

$$f(\eta) = \frac{f''(0)}{2!}\eta^2 + \frac{f'''(0)}{3!}\eta^3 + \cdots$$

Substituting these expressions and taking the limit as $\eta \to 0$

$$\lim_{\eta \to 0} \frac{\left(\frac{U_x^*}{U^*} f - \frac{\eta}{2x} f'\right) f}{\left(\frac{\eta}{2x} F' - \frac{U_x^*}{U^*} F\right) f + \frac{\eta}{2x} f' F} = \text{CONST.} \frac{f''(0)}{F''(0)}$$

where the constant depends on the external flow. Since $F''(0)$ is not zero, the limit is at most of $0(1)$. Thus, the neglections due to the perturbation procedure are justifiable. It should be noted that if the flow ω^o were not Blasius flow, but some other flow in which $F''(0)$ could become zero (the flow would be separating), then the omissions due to the perturbation procedure could not be justified and one may expect it to fail.

F. Special Cases of Three-Dimensional Boundary Layer Flow

Since the external flow may be rotational, a large variety of choices can be made for the external flow, all of which will give total differential equations out of Equations(16). Cases illustrating the three-dimensional boundary layer behavior for some such choices are discussed below. It should be noted that, similarily to the corresponding two-dimensional situation in choosing expressions for U^* and W^*, it is assumed that these satisfy the equation of continuity only after due account is taken of the outflow from the boundary layer.

1) $W^* = A \; ; U^* = \bar{\omega} = 0$

This assumption presupposes that the external flow is potential with straight streamlines which are inclined at some definite angle to the x axis, and thus, also to the leading edge of the plate. For this case

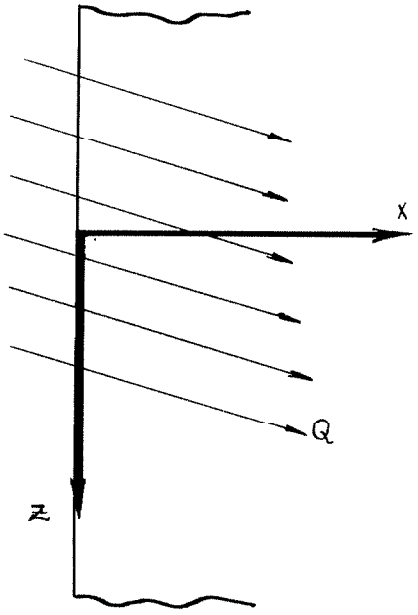

Equation (16a) need not be considered and Equation (16b) becomes:

$$g''' + \frac{F}{2} g'' = 0 \tag{23}$$

The solution which satisfied both Equation (23) and the boundary conditions (17) is obviously:

$$g = F \tag{24}$$

The limiting deflection becomes

$$\alpha = \frac{W^+}{U^\circ}\left(\frac{g''(0)}{F''(0)} - 1\right) = 0$$

showing that there is no crosswise flow in the boundary layer and all the flow takes place in the direction of the external flow. This result, then, is in agreement with a similar result obtained in Reference (3), and shows that the inclination of the leading edge has no effect whatsoever on the three-dimensional character of boundary layer flow, as long as the external flow has constant velocity and straight streamlines.

In applying momentum integral methods to three-dimensional boundary layer flow, it is usually convenient to consider the various displacement and momentum thicknesses, along, and normal to the direction of the external flow. In order to facilitate interpretation of the present results in this different coordinate system (δ_1, y, δ_2), the expressions for the various quantities involved in such analysis are derived in Appendix A, and will be evaluated for each case under discussion. In the present case, of course, the values of these expressions are known, and one has:

$$\frac{\delta_1^+}{x} = \frac{1.72}{Re^{1/2}}$$

$$\frac{\delta_{11}^{++}}{x} = \frac{0.664}{Re^{1/2}}$$

$$\delta_{12}^{++} = \delta_{21}^{++} = \delta_2^+ = 0$$

2) $W^* = Az \; ; \; U^* = Bx \; ; \; \bar{\omega} = 0$

This again is an example of an irrotational flow. The magnitude and direction of the external flow velocity are given by:

$$\frac{Q}{U^\circ} = 1 + \frac{U^*}{U^\circ} = 1 + \frac{B}{U^\circ}x$$

$$\theta = \frac{W^*}{U^\circ} = \frac{A}{U^\circ}z$$

The shape of the external flow streamlines is obtained from

$$\frac{dx}{U} = \frac{dz}{W} = \frac{dx}{U^\circ + Bx} = \frac{dz}{Az}$$

or

$$z = \text{CONST.}\left(U^\circ + Bx\right)^{A/B} \approx \text{CONST.}\left(1 + \frac{A}{U^\circ}x\right)$$

We thus have external flow with straight streamlines, but diverging

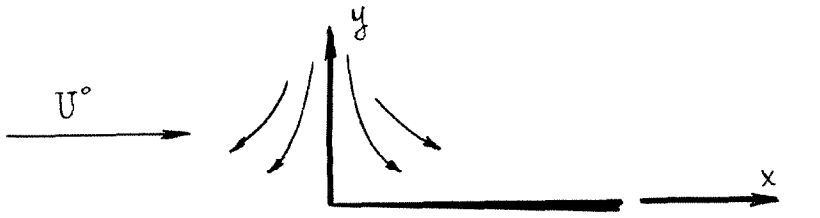

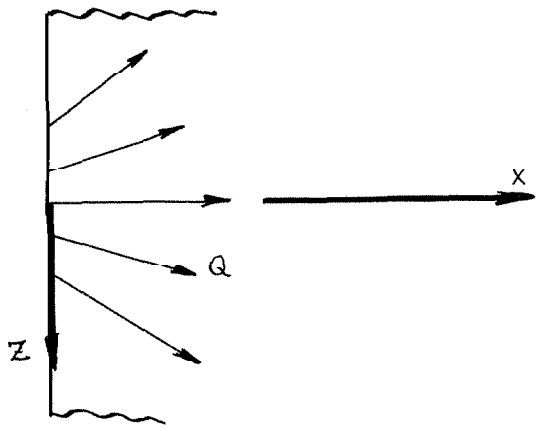

in the xz plane. This flow is similar to that studied by Howarth,[16] the difference lies in the location of the stagnation point which is here removed from the origin to a point $x = -\frac{U^\circ}{B}$.

Equations (16) become now:

$$f''' + \frac{F}{2} f'' - F' f' + \frac{3}{2} F'' f + \frac{A}{B} F'' g + 1 = 0 \tag{25a}$$

$$g''' + \frac{F}{2} g'' = 0 \tag{25b}$$

Clearly, again, the solution of Equation (25b) is

$$g = F$$

and thus, there is no crosswise flow in the boundary layer in spite of the divergence of the streamlines.

One seeks solutions of Equations (25a) involving the ratio A/B explicitly. These may be obtained setting

$$f = f_o + \frac{A}{B} f_1 \tag{26}$$

where f_o satisfies:

$$f_o''' + \frac{F}{2} f'' - F' f_o' + \frac{3}{2} F'' f_o + 1 = 0 \tag{27}$$

with boundary conditions:

$$f_o(0) = f_o'(0) = 0 \quad ; \quad f_o'(\infty) = 1.0$$

and f_1 satisfies:

$$f_1''' + \frac{F}{2} f_1'' - F' f_1' + \frac{3}{2} F'' f_1 + F'' F = 0 \qquad (28)$$

with boundary conditions:

$$f_1(0) = f_1'(0) = 0 \quad ; \quad f_1'(\infty) = 0$$

The solution of Equations (27) and (28) for f_0' and f_1', satisfying the appropriate boundary conditions, has been obtained by the numerical method described in Appendix B. These solutions are presented in Figure (2a).

The two solutions have a definite physical meaning, since f_0' satisfies the equation which one would obtain from Equation (16a) if $\bar{W}^* = 0$. In other words, the solution f_0' illustrates the effect of the velocity gradient U_x^*, while f_1' is due to the divergence of the streamlines.

The displacement thickness now is:

$$\frac{\delta_1^+}{x} = \frac{1}{Re^{1/2}} \left[1.72 + \frac{B}{U_0} x \int_0^\infty (F' - f_0' - \frac{A}{B} f_1') \, d\eta \right] = \frac{1}{Re^{1/2}} \left[\underset{①}{1.72} - \underset{②}{.707 \frac{A}{U_0} x} - \underset{③}{4.05 \frac{B}{U_0} x} \right]$$

and the momentum thickness is similarily obtained as:

$$\frac{\delta_{11}^{++}}{x} = \frac{1}{Re^{1/2}} \left[\underset{①}{0.664} - \underset{②}{0.283 \frac{A}{U_0} x} - \underset{③}{1.03 \frac{B}{U_0} x} \right]$$

Designating the terms involved in computation of displacement and momentum thicknesses by ①, ②, and ③, we note that ① represents the effect of basic flow, ② the effect of acceleration in

the z direction,and ③ the effect of acceleration in the x direction.

We thus see that although this case is probably of not much practical significance, it demonstrates very clearly the effect on the basic flow u^o of accelerations in the z and x directions. Finally, it should be mentioned that these results are in qualitative agreement with those of Reference (16), when the parameter used by Howarth equals unity.

3) $W^* = A x^n \; ; \; U^* = \omega_2 = 0$

This is an example of rotational flow and represents a generalization of Case 1. The magnitude and direction of the external flow velocity is given by:

$$Q = U^o$$

$$\Theta = \frac{A}{U^o} x^n$$

The external flow streamlines are obtained from

$$z = \frac{1}{n+1} \frac{A}{U^o} x^{n+1} + \text{CONST.}$$

The external flow streamlines thus represent various parabolas and the flow due to each n may be imagined as caused by a cascade of infinitely thin blades. It should be noted that for values of $n < 0$, the velocities become infinite at the origin,and thus such regions must be excluded from our considerations.

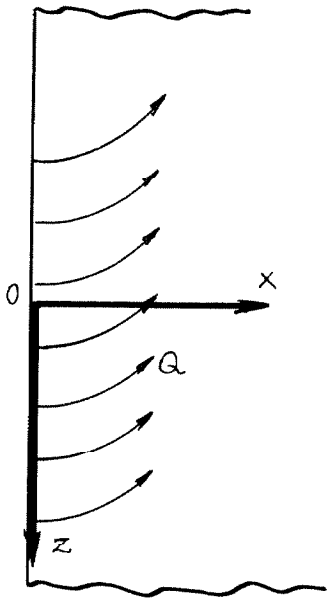

Equation (16b) becomes now for any particular value of n :

$$g_n''' + \frac{F}{2} g_n'' - n(F'g_n' - 1) = 0 \qquad (29)$$

with boundary conditions given by Equations (17). Equation (16a), just as in Case 1, need not be considered. It is perhaps not immediately clear that this is true. One, for instance, may surmise that in spite of the fact that $U^* = 0$, there exists some perturbation in the x direction due to the W flow. Imagine then that u is represented by

$$u = U^\circ F' + M(x,z)f'$$

instead of Equation (15). In such case Equation (16a) would become:

$$f''' + \frac{F}{2} f'' - \left(x \frac{M_x}{M} F'\right) f' + \left[F''\left(\frac{1}{2} + x \frac{M_x}{M}\right)\right] f = 0$$

with boundary conditions:

$$f(0) = f'(0) = f'(\infty) = 0$$

Since the equation is homogeneous, the solution which satisfies the boundary conditions is $f = 0$, and thus, no perturbation in the x direction exists.

The solution of Equation (29) for g when $n = 1$ may be obtained by setting:

$$g_1 = F - G(\eta)$$

where G must satisfy:

$$G''' + \frac{F}{2} G'' - F'G' - \left[1 - (F')^2\right] = 0 \qquad (30)$$

with boundary conditions:

$$G(0) = G'(0) = G'(\infty) = 0$$

The solution of Equation (30) for G' is given in Reference (13), where boundary layer for external flow having circular streamlines has been computed. For the convenience of the reader this solution is also shown in Figure (2b). Since for $n = 1$ the shape of the external flow streamlines is given by

$$z = \frac{A}{2U_0} x^2 + \text{CONST.}$$

which will nearly match the circles of radius $\frac{U^\circ}{A}$ for small values of x, it is not surprising that the boundary layer solutions correspond. This correspondence with Reference (13) is especially evident when the velocities q_1 (in the direction of external flow) and q_2 (normal to the direction of external flow) are considered:

$$q_1 = U^\circ F'$$

$$q_2 = W^*(g' - F') = Ax(F' + G' - F') = AxG'$$

These are the same as those given in Reference (13).

Equation (29) was also solved for $n = 2$ and $n = -1/2$ by relaxation. It should be mentioned that analytical relations between various solutions are difficult to obtain because of the nonhomogeneity of Equation (29), and because F and G are known only in terms of their tabulated values. The solutions for $n = 0, 1, 2, -1/2$ are shown in Figure (2b).

It may be seen from this figure that an increase in n from $n = 0$ to $n = 2$ corresponds to an increase in crosswise flow, $q_2 = W^*(g' - F')$ since the value of

$$g'_n - g'_0 = g'_n - F'$$

increases with n. On the other hand, a decrease in the value of n from $n = 0$ to $n = -1/2$ corresponds to a reversal of the direction of the crosswise flow, since the quantity $g' - F'$ becomes negative. This

behavior of three-dimensional boundary layer may be explained by considering the driving force of crosswise flow, which is the pressure gradient in the direction of z_2 coordinate. Consideration of this pressure gradient is equivalent in this case (velocity $Q \doteq$ constant) to consideration of the curvature of the external flow streamlines. Now for $m = 2$, this curvature is given by

$$c \doteq 2 \frac{A}{U^\circ} x$$

while for $m = -1/2$ the expression for curvature becomes:

$$c \doteq -\frac{1}{2} \frac{A}{U^\circ} x^{-3/2}$$

Thus it is apparent that the change in the direction of crosswise flow corresponds to the change in the direction of the crosswise pressure gradient.

The boundary layer thicknesses and maximum flow deflection for all these values of m are presented in Table I.

4) $W^* = Ax^m \; ; \; U^* = B x^m z^i \; ; \; \omega_2 = 0$

This may be rotational or irrotational flow. If the flow is irrotational, however, further restrictions on U^* must be made; that is, the coefficients must be so adjusted, that the relation

$$U^*_z = W^*_x$$

is satisfied. The external flow velocity is given by

$$Q = U^\circ \left(1 + \frac{B}{U^\circ} z^i x^m\right)$$

$$\theta = \frac{A}{U^\circ} x^m$$

TABLE I. SIGNIFICANT BOUNDARY LAYER QUANTITIES FOR FLOW: $U^* = B z^i x^m$, $W^* = A x^n$

n	$c\frac{U^\circ}{A}$	$\alpha\frac{U^\circ}{A}$	$\frac{\delta_2^+}{x}Re^{1/2}\frac{U^\circ}{A}$	$\frac{\delta_{21}^{++}}{x}Re^{1/2}\frac{U^\circ}{A}$	$\frac{\delta_{12}^{++}}{x}Re^{1/2}\frac{U^\circ}{A}$
0	0	0	0	0	0
1	1.0	$3.26x$	$1.59x$	$0.85x$	$0.74x$
2	$2x$	$4.18x^2$	$2.20x^2$	$1.14x^2$	$1.06x^2$
$-1/2$	$-\frac{1}{2}x^{-3/2}$	$-3.36x^{-1/2}$	$-2.71x^{-1/2}$	$-1.60x^{-1/2}$	$-1.11x^{-1/2}$
ANY VALUE					

m	$z^i]_{u_y)_{y=0}=0}$	$\frac{\delta_1^+}{x}Re^{1/2}-1.72$	$\frac{\delta_{11}^{++}}{x}Re^{1/2}-0.664$
ANY VALUE			
0	—	0	0
1	$-0.22\frac{U^\circ}{B}x^{-1}$	$-4.24\frac{B}{U^\circ}xz^i$	$-1.03\frac{B}{U^\circ}xz^i$
2	$-0.16\frac{U^\circ}{B}x^{-2}$	$-5.83\frac{B}{U^\circ}x^2z^i$	$-1.26\frac{B}{U^\circ}x^2z^i$
$-1/2$	$+0.44\frac{U^\circ}{B}x^{1/2}$	$+2.71\frac{B}{U^\circ}x^{-1/2}z^i$	$+0.50\frac{B}{U^\circ}x^{-1/2}z^i$

It should be noted that due to the linearization, no changes in the direction of the flow stemming from $U^*(x,z)$ are considered. Consequently, although the magnitude Q may now change along the streamline, all streamlines remain parallel and identical in shape to those considered in Case (3). We may expect, therefore, that the equation for W will remain unchanged, while the equation for u^* will reflect the effect of pressure gradients. Inspection of Equations (16) reveals that this indeed is the case. Equation (16a) becomes now:

$$f_m''' + \frac{F}{2} f_m'' - m F' f_m' + F''\left(\frac{1}{2} + m\right) f_m + m = 0 \qquad (31)$$

It should be noted that, as already previously pointed out, the presence of z^i in the expression for U^* has no effect whatsoever on the velocity profile f'. Physically, it is clear that this occurs because θ, the external flow direction, is not a function of z, and because the total turning of the external flow is of $O\left(\frac{W^*}{U_\infty}\right)$, so that along any particular streamline only very small variations of z occur.

The solution of Equation (31) was obtained numerically for $m = 1,\ 2,\ -1/2$. These solutions, together with the Blasius profile, are shown in Figure (2c). It is interesting to note that the behavior of the f' solutions in Figure (2c) and the g' solutions in Figure (2b) is essentially similar, indicating that apparently the effect of $F''\left(\frac{1}{2}+m\right) f_m$ term (by which the two Equations (29) and (30) differ) is mainly to increase the scale of the u^* profile. For $m = -1/2$ this term vanishes

and the two solutions are identical.

Since the flow in the x direction may now decelerate, there will in general exist lines along which the u velocity reverses its direction at $y = 0$. At such locations the boundary layer flow is in z direction only. To find the shape of such lines one computes first:

$$u_y)_{y=0} = U^\circ \sqrt{\frac{U^\circ}{\nu x}} \left[F''(0) + \frac{U^*}{U^\circ} f''(0)\right]$$

and this will be zero if

$$F''(0) = - \frac{U^*}{U^\circ} f''(0)$$

Since U^* is a function of x & z, the last equation gives the shape of the lines along which the reversal of u velocity takes place. These are:

$$z^i]_{u_y)_{y=0}=0} = - \frac{F''(0)}{f''(0)} \frac{U^\circ}{B} x^{-m}$$

In order to permit such estimates, the value of $z^i]_{u_y)_{y=0}=0}$ is included in Table I, where all other significant quantities for this case are listed.

5) $W^* = A x^m z^k$; $U^* = B x^m z^i$; $\omega_2 = 0$

To insure that this flow be possible and V remain still of $O(\delta)$, the components W^* and U^* were chosen so that they themselves satisfy continuity. (The situation, with respect to V, is then analogous to two-dimensional flow over flat plate). This may be accomplished by choosing:

$$m - 1 = n \qquad i = k - 1$$

$$B = -\frac{k}{m} A$$

For such case then:

$$W^* = A x^n z^k \; ; \quad U^* = -\frac{k}{n+1} A x^{n+1} z^{k-1}$$

and

$$Q = U^\circ \left[1 - \frac{k}{n+1} \frac{A}{U^\circ} z^{k-1} x^{n+1}\right]$$

$$\theta = \frac{A}{U^\circ} x^n z^k$$

The shape of the external flow streamlines is given by:

$$z \doteq (\text{CONST.})^{\frac{1}{1-k}} \left[1 + \frac{A}{U^\circ} \frac{1}{\text{CONST}} \frac{1}{n+1} x^{n+1}\right] \qquad k \neq 1$$

and

$$z \doteq \text{CONST.} \; e^{\left(\frac{A}{U^\circ} \frac{1}{n+1} x^{n+1}\right)} \qquad k = 1$$

It is clear then, that this case deals with both the direction θ and velocity Q varying with x and z. Equations (16) become:

$$f_n''' + \frac{F}{2} f_n'' - (n+1) F' f_n' + \left(n + \tfrac{3}{2}\right) F'' f_n - (n+1) F'' g_n + (n+1) = 0 \tag{32a}$$

$$g_n''' + \frac{F}{2} g_n'' + n\left(1 - F' g_n'\right) = 0 \tag{32b}$$

It should be noted that Equation (32b) remains identical with Equation (29), and Equation (32a) although changed from Equation (31), still is independent of the exponent of z. This occurs because along

each streamline there is only small variation with ξ . When $n=0$ Equations (32) become identical with Equations (25). Inspection of the shape of the streamlines in that case reveals that the streamlines are straight and diverging, so that the identical form of the equations is understandable.

The solution of Equation (32b) has been discussed in Case (3). To solve Equation (32a) it is more convenient (in order to avoid the integration of g'_n) to substitute:

$$f_n = \frac{1}{n+3/2}\left[\tfrac{1}{2} f_m + m(g_n + f_{2,n})\right]$$

where $m = n+1$, f_m satisfies Equation (31), and $f_{2,n}$ must satisfy:

$$f'''_{2,n} + \frac{F}{2} f''_{2,n} - mF' f'_{2,n} + (n+3/2) F'' f_{2,n} + (1 - g'_n F') = 0 \qquad (32c)$$

with boundary conditions:

$$f_{2,n}(0) = f'_{2,n}(0) = f'_{2,n}(\infty) = 0$$

The solution of Equation (32a) has been obtained numerically for $n = 1$, 2 , $-1/2$ and is shown in Figure (2d). It may be seen in this figure, that with n decreasing, the correction function $f'_{2,n}$ increases. Interpreted in terms of the u^* velocity profile, this means for $A\frac{k}{n+1} > 0$, that the velocity profile "spoils" more and more as n decreases. This behavior may easily be explained when the shape of

the streamlines of the external flow and the limiting deflection are considered.

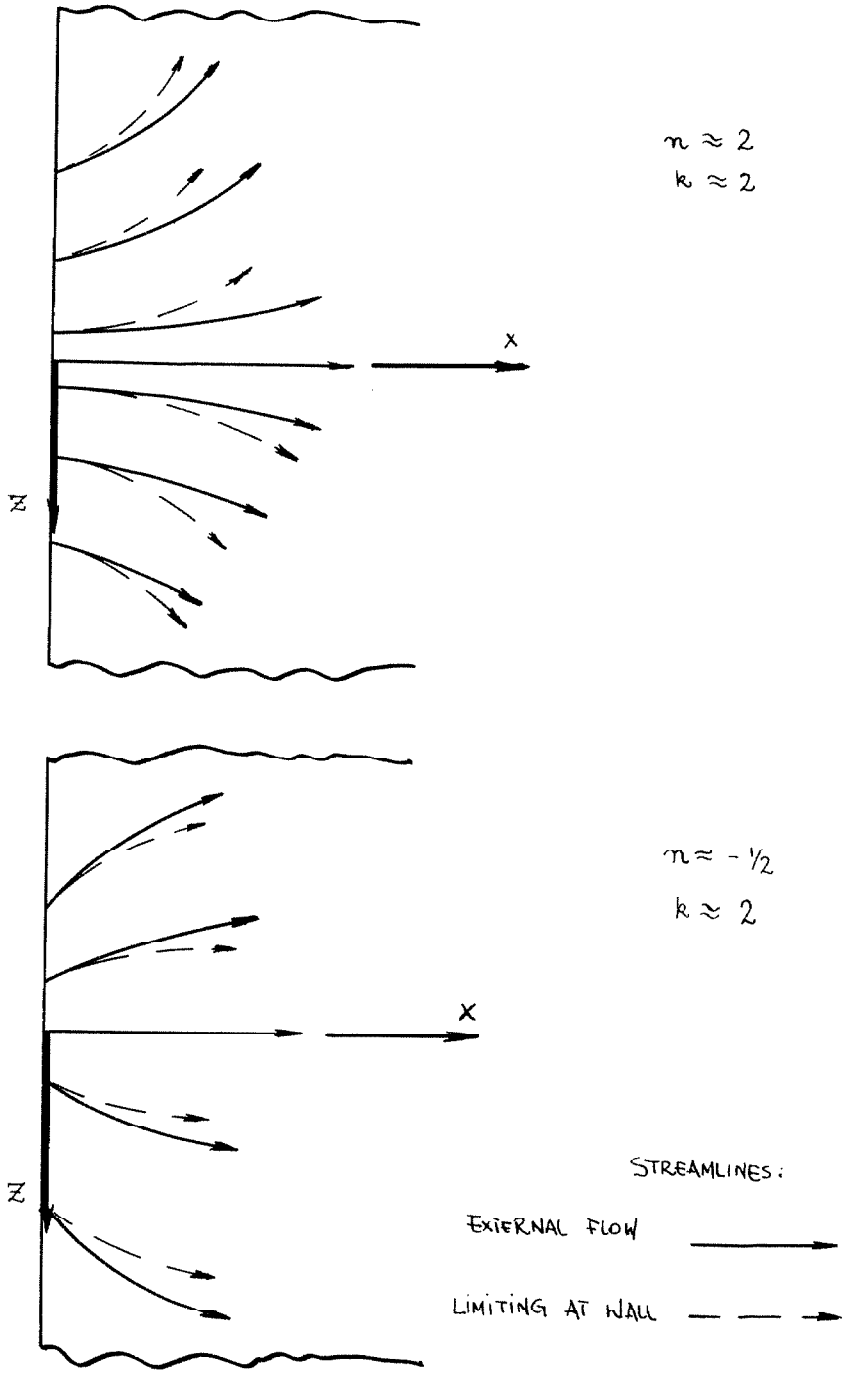

For $n > 1$, the streamlines of the external flow are concave, and thus the crosswise flow (indicated by the limiting deflection α) is such as to cause an outward flow of low momentum air. Consequently, the u^* velocity profile is less affected by the negative pressure gradient than in the case when such crosswise flow does not exist. This is especially apparent in Figure (3), where a comparison of the velocity profile for Cases (4) and (5) (when U^* is proportional to x^2) is made. On the other hand, for $n = -1/2$, the streamlines are convex, and the crosswise flow is now such as to cause an inward flow of low momentum air. This effect, combined with an unfavorable velocity gradient in the direction of the external flow, causes the large detrimental effect on the u^* velocity profile.

Since Equation (32b) is identical with Equation (29), the constants in the expressions for the momentum and displacement thicknesses δ_{12}^{++} δ_{21}^{++} and δ_2^+ remain identical to those of Case (3). To illustrate the magnitude of the remaining thicknesses, their size was computed for $n = 1$. The results of this computation are:

$$\frac{\delta_1^+}{x} Re^{1/2} = 1.72 + 1.90 \frac{A}{U^\circ} k z^{k-1} x^2$$

$$\frac{\delta_{11}^{++}}{x} Re^{1/2} = 0.664 + 0.257 \frac{A}{U^\circ} k z^{k-1} x^2$$

The location where u velocity reverses its direction may again be estimated from:

$$z^{k-1}\Big]_{u_y)_{y=0}=0} = \frac{F''(0)}{f''(0)} \frac{U^\circ}{kA} (n+1) x^{-(n+1)}$$

which gives for $n = 1$ $\quad z^{R-1}\Big]_{u_y/y=0} = 0.33 \frac{U^\circ}{kA} x^{-2.}$

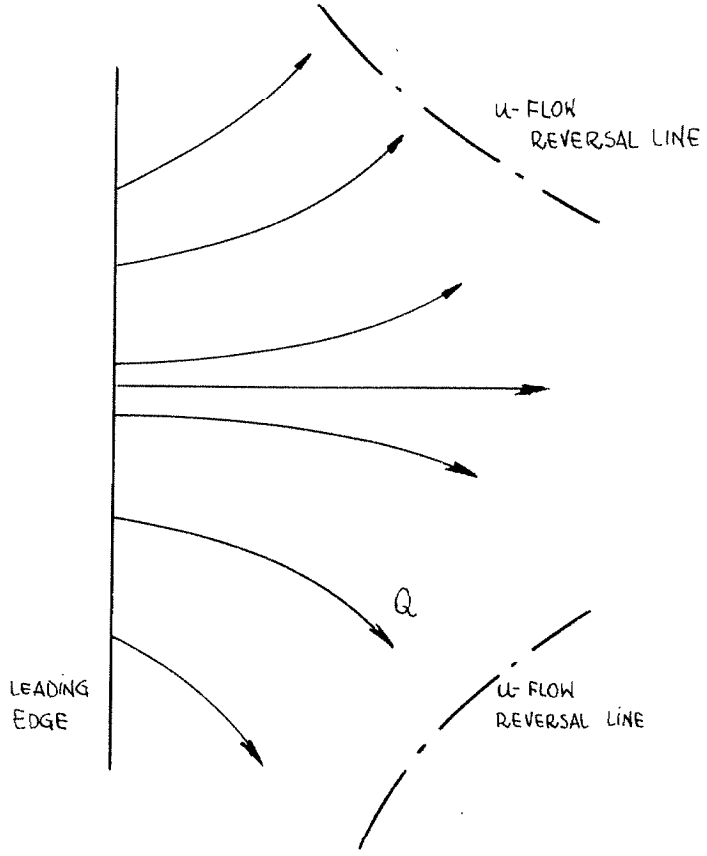

G. Effect of Angular Velocity

Case (1) is identical with that of a thin, hollow, semi-infinite, circular cylinder rotating with a constant angular velocity $\bar{\omega}$ about its axis, which is placed parallel to a stream moving with velocity U°, since for such case $\omega_2 = 0$, and $W = -a\omega$ = constant. Consequently, the result obtained for Case (1) is identical with that given by Howarth,[15] except for the fact that Howarth uses an absolute (non-rotating) system of coordinates.

Of more interest however is a case where ω_2 exists, that is, where the surface and the axis of rotation are not parallel. Consider, for example, external flow $W^* = Ax$, $U^* = 0$, $\omega_2 = 0$. Equation (16a) need not be considered, while Equation (16b) becomes

$$g''' + \frac{F}{2} g'' - F'g' + 1 - 2\frac{D}{A}(1 - F') = 0 \tag{33}$$

with boundary conditions:

$$g(0) = g'(0) = 0 \quad ; \quad g'(\infty) = 1.0$$

Solution of Equation (33) may be sought by setting

$$g = g_1 - 2\frac{D}{A} g_{1,\omega}$$

where g_1 satisfies Equation (29) with $n = 1$, and $g_{1,\omega}$ must satisfy:

$$g'''_{1,\omega} + \frac{F}{2} g''_{1,\omega} - F'g'_{1,\omega} + (1 - F') = 0 \tag{33a}$$

with boundary conditions:

$$g_{1,\omega}(0) = g'_{1,\omega}(0) = g'_{1,\omega}(\infty) = 0$$

The solution of Equation (33a) is presented in Figure (4). With this value of $g_{1,\omega}$:

$$g = F - G - 2\frac{D}{A} g_{1,\omega}$$

and the limiting deflection becomes:

$$\alpha = \frac{Ax}{U^\circ}\left[3.26 - 2\frac{D}{A}(2.05)\right]$$

When the external flow is potential:

$$A = 2\omega_z = 2D$$

so that

$$\alpha = 1.21\,\frac{Ax}{U^\circ} = 1.21\,\frac{2\omega_z x}{Q}$$

Fogarty [14] gives for an analogous case:

$$\alpha = \frac{2\omega_z x}{Q}$$

This difference must be laid to the fact that no attempt has been made in this investigation to achieve very high accuracy in the numerical solution of the various differential equations, and consequently, the value of $g''_{1,\omega}(0)$ as obtained from Figure (4) may be in slight error.

It may be seen from Figure (4), that the effect of negative ω_z is to increase the crossflow caused by $\bar{W}^* = Ax$ (providing $A > 0$).

On the other hand, had ω_z been positive, then the effect of angular rotation would have been to decrease the crossflow caused by $\bar{W}^* = Ax$. This fact may be of importance in certain types of turbomachinery where the hub shape is such as to give $D > 0$, because in such cases the crossflow may be decreased by simply increasing the angular velocity $\bar{\omega}$.

Similar qualitative considerations can be carried out in the case of the flow over compressor blades. Consider the situation indicated in the sketch below, and assume that on the suction surface the external flow is deflecting toward the tip of the blade, while on the pressure surface the flow deflects toward the root. Consideration of the coordinate system will show that A must be negative in both of these instances.

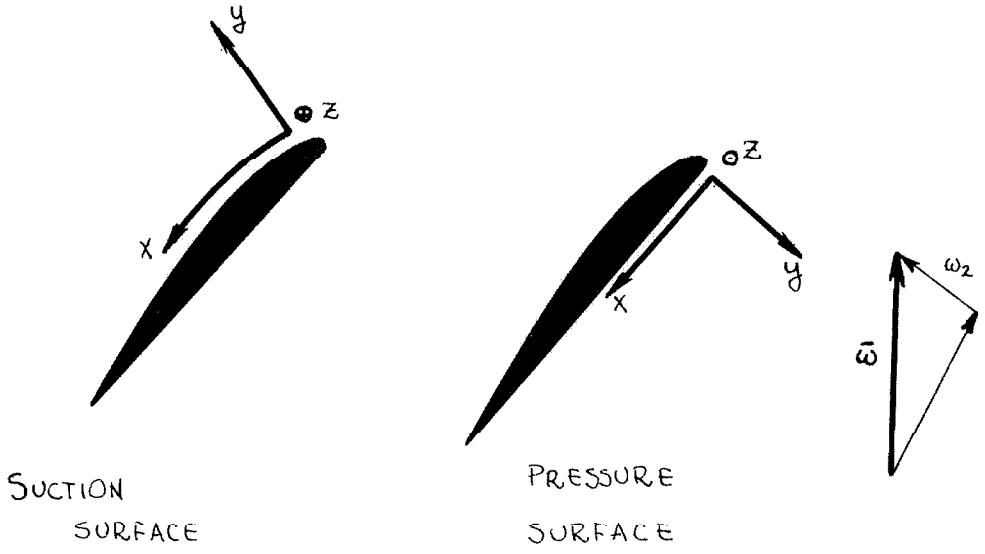

Since ω_z (and thus D) is positive on the suction surface and negative on the pressure surface, we see that angular rotation for this condition tends to increase the crossflow on the suction surface and decrease the crossflow on the pressure surface.

H. Effect of Compressibility

To estimate the effect of compressibility on three-dimensional boundary layer flow, the Equation system (1) and (2) must be replaced (considering an inertial system) by:

$$\frac{D\rho}{Dt} + \rho(\nabla\cdot\bar{q}) = 0 \tag{34a}$$

$$\rho\frac{D\bar{q}}{Dt} = -\nabla p + \mu\nabla^2\bar{q} + \frac{1}{3}\mu\nabla(\nabla\cdot\bar{q}) + 2\left[(\nabla\mu)\cdot\nabla\right]\bar{q} + (\nabla\mu)\times(\nabla\times\bar{q}) - \frac{2}{3}(\nabla\cdot\bar{q})(\nabla\mu) \tag{34b}$$

$$\rho\frac{DE}{Dt} + p(\nabla\cdot\bar{q}) = \Lambda + \nabla\cdot[(\kappa\nabla)T] \tag{34c}$$

$$\text{WITH} \quad \Lambda = \mu\left\{2\nabla\cdot[(\bar{q}\cdot\nabla)\bar{q}] + (\nabla\times\bar{q})^2 - 2\bar{q}\cdot\nabla(\nabla\cdot\bar{q}) - \frac{2}{3}(\nabla\cdot\bar{q})^2\right\}$$

and

$$p = \rho\mathcal{R}T \tag{34d}$$

If, now, all the quantities are considered relative to some standard quantities, the viscosity is assumed to vary linearly with the temperature, the Prandtl number is set equal to unity, and a condition of zero heat transfer at the plate surface is imposed, then, by application of the Howarth's transformation:

$$Y \equiv \left(\frac{\rho}{\rho^\circ}\right)^{-1/2}\int_0^y \frac{\rho}{\rho^\circ}\,dy$$

$$\bar{X} \equiv x$$

$$Z \equiv z$$

$$\psi \equiv \left(\frac{\rho}{\rho^\circ}\right)^{1/2}\bar{\psi}$$

$$\varphi \equiv \left(\frac{\rho}{\rho^\circ}\right)^{1/2}\bar{\varphi}$$

the Equation system (34) reduces to:

$$\bar{\psi}_Y \bar{\psi}_{XY} - (\bar{\psi}_X + \bar{\varphi}_Z)\bar{\psi}_{YY} + \bar{\varphi}_Y \bar{\psi}_{ZY} = -\frac{1}{\rho} p_X + \frac{1}{2}\left(\frac{p_X}{p}\bar{\psi} + \frac{p_Z}{p}\bar{\varphi}\right)\bar{\psi}_{YY} + \bar{\psi}_{YYY} \qquad (35a)$$

$$\bar{\psi}_Y \bar{\varphi}_{XY} - (\bar{\psi}_X + \bar{\varphi}_Z)\bar{\varphi}_{YY} + \bar{\varphi}_Y \bar{\varphi}_{ZY} = -\frac{1}{\rho} p_Z + \frac{1}{2}\left(\frac{p_X}{p}\bar{\psi} + \frac{p_Z}{p}\bar{\varphi}\right)\bar{\varphi}_{YY} + \bar{\varphi}_{YYY} \qquad (35b)$$

$$T + (\bar{\psi}_Y)^2 + (\bar{\varphi}_Y)^2 = \text{CONSTANT} \qquad (35c)$$

$$\frac{p}{p^\circ} = \rho \frac{T}{T^\circ} \qquad (35d)$$

Velocities in the boundary layer are here represented by:

$$u = \bar{\psi}_Y$$

$$w = \bar{\varphi}_Y$$

Definitions:

$$\bar{\eta} \equiv Y\sqrt{\frac{U^\circ}{X}}$$

$$\bar{\psi} \equiv \sqrt{X U^\circ}\left[\bar{F}(\bar{\eta}) + \frac{U^*}{U^\circ}\bar{f}(\bar{\eta})\right] \qquad (36)$$

$$\bar{\varphi} \equiv \sqrt{X U^\circ}\,\frac{W^*}{U^\circ}\,\bar{g}(\bar{\eta})$$

result in the zeroth order equation:

$$2\bar{F}''' + \bar{F}\bar{F}'' = 0 \qquad (37)$$

and after some manipulation in the first order equations

$$\bar{f}''' + \frac{\bar{F}}{2}\bar{f}'' - \left(\bar{\chi}\frac{U_{\bar{\chi}}^*}{U^*}\bar{F}'\right)\bar{f}' + \left[\bar{F}''\left(\frac{1}{2} + \bar{\chi}\frac{U_{\bar{\chi}}^*}{U^*}\right)\right]\bar{f} + \bar{\chi}\frac{W_{\bar{\chi}}^*}{U^*}\bar{F}''\bar{g} + \bar{\chi}\frac{U_{\bar{\chi}}^*}{U^*}\left[1 + \frac{\gamma-1}{2}M^2(1-\bar{F}'^2) - \frac{\gamma}{2}M^2\bar{F}\bar{F}''\right] = 0 \tag{38a}$$

$$\bar{g}''' + \frac{\bar{F}}{2}\bar{g}'' - \left(\bar{\chi}\frac{W_{\bar{\chi}}^*}{W^*}\bar{F}'\right)\bar{g}' + \bar{\chi}\frac{W_{\bar{\chi}}^*}{W^*}\left[1 + \frac{\gamma-1}{2}M^2(1-\bar{F}'^2)\right] = 0 \tag{38b}$$

It is thus seen that the relaxation of restrictions on compressibility of the fluid in three-dimensional boundary layer flow, causes, besides the characteristic "stretching" of the η coordinate, also the appearance of additional nonhomogeneous terms in Equations (38).

The effect of these additional terms may easily be evaluated if $W^* = Ax$ and $U^* = Bx$. For such cases

$$\begin{aligned} \bar{g} &= \bar{F} - \bar{G}\left(1 + \frac{\gamma-1}{2}M^2\right) \\ \bar{f} &= \bar{f}_0 - \bar{f}_1\left(\frac{\gamma}{2}M^2\right) + \bar{f}_{c,1}\left(\frac{\gamma-1}{2}M^2\right) \end{aligned} \tag{39}$$

where $\bar{f}_{c,1}$ satisfies

$$\bar{f}_{c,1}''' + \frac{\bar{F}}{2}\bar{f}_{c,1}'' - \bar{F}'\bar{f}_{c,1}' + \frac{3}{2}\bar{F}''\bar{f}_{c,1} + \left(1 - \bar{F}'^2\right) = 0 \tag{40}$$

with boundary conditions

$$\bar{f}_{c,1}(0) = \bar{f}_{c,1}'(0) = \bar{f}_{c,1}'(\infty) = 0$$

and $\bar{f}_0$, $\bar{f}_1$ satisfy Equations (27) and (28) respectively.

Similarily if $W^* = Az$ and $U^* = Bx$ then the solution of

Equations (38) is:

$$\bar{g} = \bar{F}$$

$$\bar{f} = \bar{f}_0 + \left(\frac{A}{B} - \frac{\gamma}{2}M^2\right)\bar{f}_1 + \frac{\gamma-1}{2}M^2\bar{f}_{c,1} \tag{41}$$

Solution of Equation (40) is shown in Figure (5a), and the velocity profiles $\bar{g}'$ and $\bar{f}'$ from Equations (39) at $M=1.5$ are shown in Figure (5b). It may be seen in this figure that compressibility has the overall effect of increasing the magnitude of the w^* and the u^* velocity.

I. Discussion of the Results and Remarks on Momentum-Integral Equations

Before proceeding with the discussion, it should be emphasized again, that the results of the present analysis are valid strictly only in the limit of vanishing pressure gradients of the external flow. The extent to which they apply, for small, but finite pressure gradients, depends on the relative magnitude of the effect here evaluated, rather than on the pressure gradient itself, and consequently, no definite statement as to the limit of the applicability of the results may be made.

Some idea, however, may be obtained comparing the results of Case (4) with $i=0$ to those for two-dimensional boundary layer. In particular, the separation point in such cases, and when $m=1$, is according to Reference (26) given by various methods as:

Inner and outer solution (Kármán and Millikan) $\qquad \frac{Bx}{U^o} = 0.102$

Expansion in series (Howarth) $\frac{Bx}{U^\circ} = 0.120$

Momentum equation (quartic expression for velocity) $\frac{Bx}{U^\circ} = 0.156$

The present method gives the value $\frac{Bx}{U^\circ} = 0.22$. It is thus seen that the present method tends to underestimate the position of the separation point by considerable amount. One may therefore expect that from a quantitative standpoint predictions of flow reversal position will be inaccurate.

At least part of this discrepancy may be caused by the fact that due to the large number of differential equations that had to be solved numerically, accuracy was sacrificed in favor of speed; that is, the number of points chosen for the relaxation procedure may have been not quite sufficient. Still, even with very accurate and tedious computational procedures, one may not expect a linearized solution to give an accurate representation of the phenomena everywhere in the flow field. Therefore, it is important to understand that the numerical results of this investigation represent at best quantitative trends only, and should not be interpreted as final values. This applies in particular to those results which involve the value of second derivative of velocity distribution functions at $y = 0$. For that reason too, the values of the appropriate friction coefficients were not listed, although they could have been easily obtained from the computed curves.

Keeping, however, the main object of this investigation in mind, which is to furnish information on the velocity distributions existing in three-dimensional boundary layer so that integral methods may be

applied, a number of questions arising in connection with application of such methods may now be answered.

In particular the choice of the coordinate system and the general character of the equations will be considered.

For the purpose of general treatment of three-dimensional boundary layer flow, the present results seem to indicate that a choice of an intrinsic coordinate system is preferable to a Cartesian coordinate system. This becomes apparent when the expressions for the velocities in the intrinsic coordinate system are considered:

$$q_1 = U^{\circ} F' + U^{*} f'$$

$$q_2 = W^{*}(g' - F') \tag{42}$$

As may be seen from these expressions, the crossflow velocity is small, even for relatively large W^{*}. This, then, suggests a possible simplification of the resulting equations when such are written in an intrinsic coordinate system. Furthermore, when curvature of the external flow streamlines is zero, Cases (1), (2), and (5) indicate that crossflow will also tend to vanish, and the equations along the s_1 coordinate will behave like two-dimensional ones. Finally, the intrinsic coordinate system has the advantage of giving a more significant physical picture of boundary layer flow, inasmuch as it inherently makes clear how the movement of the fluid in the boundary layer differs from that of the external flow.

The form of the momentum-integral equations in an intrinsic coordinate system has been given in Reference (23) and is:

$$\frac{\partial \delta_{11}^{++}}{\partial s_1} + \frac{\partial \delta_{12}^{++}}{\partial s_2} + \frac{1}{Q}\frac{\partial Q}{\partial s_1}\left(2\delta_{11}^{++} + \delta_1^{+}\right) - 4\frac{\omega_2}{Q}\delta_{12}^{++} - \frac{\tau_{0,1}}{\rho Q^2} = 0 \tag{43a}$$

$$\frac{\partial \delta_{22}^{++}}{\partial s_2} + \frac{\partial \delta_{21}^{++}}{\partial s_1} + \frac{2}{Q}\frac{\partial Q}{\partial s_1}\left(\delta_2^{+} - \delta_{12}^{++}\right) + \frac{1}{Q}\frac{\partial Q}{\partial s_2}\left(\delta_{22}^{++} - \delta_{11}^{++} - \delta_1^{+}\right) - \frac{2\omega_2}{Q}\left(\delta_{11}^{++} + \delta_{12}^{++}\right) + \frac{\tau_{0,2}}{\rho Q^2} = 0 \tag{43b}$$

We note that the three-dimensional momentum-integral equations consist of two equations with five unknowns. Since these were derived from a determinate system of Equations (1) and (2), additional relations must exist between the various momentum and displacement thicknesses, and these could be found if the velocities q_1 and q_2 were known. The conventional procedure, at this point, is to assume the velocities q_1 and q_2 as a two parameter family, and use the ensuing differential equations to solve for these two parameters. We thus assume that

$$q_1 = q_1(P_1, P_2)$$

$$q_2 = q_2(P_1, P_2)$$

so that Equations (42) become:

$$\left(\frac{\partial \delta_{11}^{++}}{\partial P_1}\right)\frac{\partial P_1}{\partial s_1} + \left(\frac{\partial \delta_{12}^{++}}{\partial P_1}\right)\frac{\partial P_1}{\partial s_2} + \left(\frac{\partial \delta_{11}^{++}}{\partial P_2}\right)\frac{\partial P_2}{\partial s_1} + \left(\frac{\partial \delta_{12}^{++}}{\partial P_2}\right)\frac{\partial P_2}{\partial s_2} + H_1 = 0 \tag{44a}$$

$$\left(\frac{\partial \delta_{21}^{++}}{\partial P_1}\right)\frac{\partial P_1}{\partial s_1} + \left(\frac{\partial \delta_{22}^{++}}{\partial P_1}\right)\frac{\partial P_1}{\partial s_2} + \left(\frac{\partial \delta_{21}^{++}}{\partial P_2}\right)\frac{\partial P_2}{\partial s_1} + \left(\frac{\partial \delta_{22}^{++}}{\partial P_2}\right)\frac{\partial P_2}{\partial s_2} + H_2 = 0 \tag{44b}$$

where H_1 and H_2 are functions of P_1, P_2, ω_2, Q but contain no derivatives of either of the parameters P_1 and P_2.

We thus see that in terms of these parameters the momentum-integral equations become two quasilinear partial differential equations, which may be elliptic, parabolic, or hyperbolic, depending on the nature of the coefficients. More specifically, the nature of these equations depends on the quantity $\mathcal{D}$ which is defined as:

$$\mathcal{D} \equiv \begin{vmatrix} \frac{\partial \delta_{11}^{++}}{\partial P_1} & \frac{\partial \delta_{21}^{++}}{\partial P_1} \\ \frac{\partial \delta_{11}^{++}}{\partial P_2} & \frac{\partial \delta_{21}^{++}}{\partial P_2} \end{vmatrix} \begin{vmatrix} \frac{\partial \delta_{12}^{++}}{\partial P_1} & \frac{\partial \delta_{12}^{++}}{\partial P_1} \\ \frac{\partial \delta_{12}^{++}}{\partial P_2} & \frac{\partial \delta_{22}^{++}}{\partial P_2} \end{vmatrix} - \frac{1}{4} \left[\begin{vmatrix} \frac{\partial \delta_{11}^{++}}{\partial P_1} & \frac{\partial \delta_{21}^{++}}{\partial P_1} \\ \frac{\partial \delta_{12}^{++}}{\partial P_2} & \frac{\partial \delta_{22}^{++}}{\partial P_2} \end{vmatrix} + \begin{vmatrix} \frac{\partial \delta_{12}^{++}}{\partial P_1} & \frac{\partial \delta_{22}^{++}}{\partial P_1} \\ \frac{\partial \delta_{11}^{++}}{\partial P_2} & \frac{\partial \delta_{21}^{++}}{\partial P_2} \end{vmatrix} \right]^2$$

The System (44) then is:

elliptic for $\mathcal{D} > 0$

parabolic for $\mathcal{D} = 0$

hyperbolic for $\mathcal{D} < 0$

The evaluation of $\mathcal{D}$ hinges on the specific choice of the parameters P_1, P_2. To consider this question a bit further, we note that inasmuch as q_2 is small, the momentum thickness δ_{22}^{++} is of second order as compared to δ_{11}^{++} and may be neglected in Equations (44). For such small crossflow case the quantity $\mathcal{D}$ becomes:

$$\mathcal{J} \doteq -\frac{1}{4}\left[\begin{vmatrix} \frac{\partial \delta_{12}^{++}}{\partial P_1} & \frac{\partial \delta_{21}^{++}}{\partial P_1} \\ \frac{\partial \delta_{12}^{++}}{\partial P_2} & \frac{\partial \delta_{21}^{++}}{\partial P_2} \end{vmatrix}\right]^2 \tag{45a}$$

or since $\delta_{12}^{++} = \delta_2^{+} - \delta_{12}^{++}$

$$\mathcal{J} \doteq -\frac{1}{4}\left[\begin{vmatrix} \frac{\partial \delta_{12}^{++}}{\partial P_1} & \frac{\partial \delta_2^{+}}{\partial P_1} \\ \frac{\partial \delta_{12}^{++}}{\partial P_2} & \frac{\partial \delta_2^{+}}{\partial P_2} \end{vmatrix}\right]^2 \tag{45b}$$

It is thus obvious from Equations (45) that for small crossflow the simplified form of Equations (44) cannot be elliptic.

When the simplified equations are hyperbolic, the slope of the characteristics in the physical plane (s_1, s_2) is given by:

$$\left.\frac{ds_2}{ds_1}\right]_+ = \frac{\begin{vmatrix} \frac{\partial \delta_{12}^{++}}{\partial P_1} & \frac{\partial \delta_{21}^{++}}{\partial P_1} \\ \frac{\partial \delta_{12}^{++}}{\partial P_2} & \frac{\partial \delta_{21}^{++}}{\partial P_2} \end{vmatrix}}{\begin{vmatrix} \frac{\partial \delta_{11}^{++}}{\partial P_1} & \frac{\partial \delta_{21}^{++}}{\partial P_1} \\ \frac{\partial \delta_{11}^{++}}{\partial P_2} & \frac{\partial \delta_{21}^{++}}{\partial P_2} \end{vmatrix}} \tag{46a}$$

and

$$\left.\frac{ds_2}{ds_1}\right]_- = 0 \tag{46b}$$

so that one of the characteristics is a streamline of the external flow. Inspection of Equation (46a) and Equation (45a) shows that when the equations are parabolic the other characteristic becomes also the streamline of the external flow.

The simplified equations will become parabolic when

$$\begin{vmatrix} \frac{\partial \delta_{12}^{++}}{\partial P_1} & \frac{\partial \delta_2^{+}}{\partial P_1} \\ \frac{\partial \delta_{12}^{++}}{\partial P_2} & \frac{\partial \delta_2^{+}}{\partial P_2} \end{vmatrix} = 0$$

This will occur when $\delta_{12}^{++} = \delta_2^{+} = 0$, (when there is no crossflow at all) and when $\delta_{12}^{++} = \mathcal{F}\, \delta_2^{+}$, where $\mathcal{F}$ is not an implicit function of the parameters P_1 and P_2. Consequently if a simple "form factor" relation exists between the thicknesses δ_{12}^{++} & δ_2^{+}, the equations will be parabolic. Now, for small crossflow, the expressions for δ_2^{+} and δ_{12}^{++} are (Cf. Appendix A):

$$\frac{\delta_2^{+}}{x} = \frac{1}{Re^{1/2}} \frac{W^*}{U^\circ} \int_0^\infty (g' - F')\, d\eta$$

$$\frac{\delta_{12}^{++}}{x} = \frac{1}{Re^{1/2}} \frac{W^*}{U^\circ} \left[\int_0^\infty (1-F')g'\, d\eta - \int_0^\infty F'(1-F')\, d\eta \right]$$

and these can differ at most by a constant, since g' & F' are functions of η only. This fact is further explicitly shown in Table I for the various cases studied. From these expressions it follows then that: 1) for small crossflow the momentum-integral equations are parabolic with the

single characteristic lying along the streamline of the external flow and 2) the correct choice of the parameters P_1 and P_2 must be such that it will result in parabolic equations when the crossflow is small.

It appears, then, that a proper procedure in integrating the three-dimensional boundary layer momentum-integral equations is to integrate these along the streamline of the external flow (along the s_1 coordinate), which may always be done as long as the initial conditions are specified along the s_2 coordinate.

III. ANALYSIS OF THREE-DIMENSIONAL BOUNDARY LAYER FLOW ON A SHARPLY CURVED SURFACE

A. Preliminary Remarks

The analysis of Part II,although useful in studying boundary layer flow whenever that flow takes place on surfaces which are plane or only slightly curved, is inapplicable if that flow occurs close to "bounding walls" as may be the case in corners between the blades and the casing of a compressor. Since the experimental evidence points strongly to these regions as regions of high total pressure loss (see for instance Reference (27)),it is desirable and of interest to study such configurations.

As mentioned in the introduction, in spite of its importance,the problem of corner boundary layer flow has been treated (to the best knowledge of the author) in only two investigations (References (20) and (21)). Actually the problem consists of two separate parts; first one, due to the interaction of the boundary layer flowing on the two intersecting walls,and the second one due to the rapid change in surface curvature. In References (20 and (21), the corners treated are sharp, and thus no distinction can be made between the two different phases of the problem.

In practice,however, the corners are rarely sharp and usually some sort of fillet exists between the two intersecting walls. This fact immediately suggests that the two walls be treated as one continuous surface with very large curvature. If the radius of this curvature is

of order of magnitude of boundary layer thickness, or larger (a restriction which is almost always met in practice), the interaction effect of the two separate boundary layers is completely removed and it is expected that a simplification of equations will result.

This, then, is the model which will be treated in Part III of this investigation. The effect of angular velocity or compressibility on corner flow will not be considered.

B. Derivation of Boundary Layer Equations

For the purpose of this analysis it is convenient to use an orthogonal, curvilinear coordinate system illustrated in Figure (6). The transformation from the Cartesian system x, y, z to the curvilinear system $\bar{x}, \bar{y}, \bar{z}$ is given by:

$$\begin{aligned} x &= \bar{x} \\ y &= \bar{y}_1 + \bar{y}\cos\beta \qquad ; \ \bar{y}_1 = \text{CONST.} - \int_0^{\bar{z}} \sin\beta \, d\bar{z} \\ z &= \int_0^{\bar{z}} \cos\beta \, d\bar{z} \quad + \bar{y}\sin\beta \end{aligned} \tag{47}$$

Restricting the analysis to $c = c(\bar{z}) = \frac{d\beta}{d\bar{z}}$, the length stretching factors become:

$$h_1 = 1 \quad ; \quad h_2 = 1 \quad ; \quad h_3 = 1 + c\bar{y} \tag{48}$$

It should be pointed out that in this coordinate system the $\bar{z}$ axis plays a role of a reference line and will be used to describe the shape of the wall over which the fluid is flowing. Coordinate $\bar{y}$ will then

measure the distance perpendicular to this wall, while the $\bar{x}$ axis is pointed in the direction of the main flow, so that $\bar{x} = \bar{y} = 0$ represent the leading edge of the configuration.

By use of Equations (48) and standard transformation formulae, the Navier-Stokes equations of motion (1) and the equation of continuity (2) are transformed to: (velocities u, v, w are taken here in the $\bar{x}$, $\bar{y}$, $\bar{z}$ directions respectively)

$$u\frac{\partial u}{\partial \bar{x}} + v\frac{\partial u}{\partial \bar{y}} + \frac{w}{1+c\bar{y}}\frac{\partial u}{\partial \bar{z}} = -\frac{1}{\rho}\frac{\partial p}{\partial \bar{x}} + \nu\left[\frac{\partial^2 u}{\partial \bar{y}^2} + \frac{\partial^2 u}{\partial \bar{x}^2} + \frac{1}{(1+c\bar{y})^2}\frac{\partial^2 u}{\partial \bar{z}^2} + \frac{c}{1+c\bar{y}}\frac{\partial u}{\partial \bar{y}} - \frac{\bar{y}}{(1+c\bar{y})^3}\frac{\partial u}{\partial \bar{z}}\frac{dc}{d\bar{z}}\right]$$

$$u\frac{\partial v}{\partial \bar{x}} + v\frac{\partial v}{\partial \bar{y}} + \frac{w}{1+c\bar{y}}\frac{\partial v}{\partial \bar{z}} - \frac{cw^2}{1+c\bar{y}} = -\frac{1}{\rho}\frac{\partial p}{\partial \bar{y}} + \nu\left[\frac{\partial^2 v}{\partial \bar{x}^2} + \frac{\partial^2 v}{\partial \bar{y}^2} + \frac{1}{(1+c\bar{y})^2}\frac{\partial^2 v}{\partial \bar{z}^2} - \frac{2c}{(1+c\bar{y})^2}\frac{\partial w}{\partial \bar{z}} - \frac{c^2 v}{(1+c\bar{y})^2} + \frac{c}{1+c\bar{y}}\frac{\partial v}{\partial \bar{y}}\right.$$

$$\left. + \left(\frac{c\bar{y}}{1+c\bar{y}} - 1\right)\frac{w}{(1+c\bar{y})^2}\frac{dc}{d\bar{z}} - \frac{\bar{y}}{1+c\bar{y}}\frac{\partial v}{\partial \bar{z}}\frac{dc}{d\bar{z}}\right] \tag{49}$$

$$u\frac{\partial w}{\partial \bar{x}} + v\frac{\partial w}{\partial \bar{y}} + \frac{w}{1+c\bar{y}}\frac{\partial w}{\partial \bar{z}} + \frac{cvw}{1+c\bar{y}} = -\frac{1}{\rho}\frac{1}{1+c\bar{y}}\frac{\partial p}{\partial \bar{z}} + \nu\left[\frac{\partial^2 w}{\partial \bar{x}^2} + \frac{\partial^2 w}{\partial \bar{y}^2} + \frac{1}{(1+c\bar{y})^2}\frac{\partial^2 w}{\partial \bar{z}^2} - \frac{\bar{y}}{(1+c\bar{y})^3}\frac{\partial w}{\partial \bar{z}}\frac{dc}{d\bar{z}}\right.$$

$$\left. + \frac{2c}{(1+c\bar{y})^2}\frac{\partial v}{\partial \bar{z}} + \frac{v}{(1+c\bar{y})^2}\left(1 - \frac{c\bar{y}}{1+c\bar{y}}\right)\frac{dc}{d\bar{z}} + \frac{c}{1+c\bar{y}}\frac{\partial w}{\partial \bar{y}} - \frac{wc^2}{(1+c\bar{y})^2}\right]$$

and

$$(1+c\bar{y})\frac{\partial u}{\partial \bar{x}} + vc + (1+c\bar{y})\frac{\partial v}{\partial \bar{y}} + \frac{\partial w}{\partial \bar{z}} = 0 \tag{50}$$

Applying boundary layer approximations, that is, considering v and $\bar{y}$ of $O(\delta)$, c of $O(\frac{1}{\delta})$, and neglecting all terms of order δ or

smaller, Equations (49) are simplified to

$$u\frac{\partial u}{\partial \bar{x}} + v\frac{\partial u}{\partial \bar{y}} + \frac{w}{1+c\bar{y}}\frac{\partial u}{\partial \bar{z}} = -\frac{1}{\rho}\frac{\partial p}{\partial \bar{x}} + \nu\left[\frac{\partial^2 u}{\partial \bar{y}^2} + \frac{c}{1+c\bar{y}}\frac{\partial u}{\partial \bar{y}}\right]$$

$$-\frac{cw^2}{1+c\bar{y}} = -\frac{1}{\rho}\frac{\partial p}{\partial \bar{y}} \qquad (51)$$

$$u\frac{\partial w}{\partial \bar{x}} + v\frac{\partial w}{\partial \bar{y}} + \frac{w}{1+c\bar{y}}\frac{\partial w}{\partial \bar{z}} + \frac{cvw}{1+c\bar{y}} = -\frac{1}{\rho}\frac{1}{1+c\bar{y}}\frac{\partial p}{\partial \bar{z}} + \nu\left[\frac{\partial^2 w}{\partial \bar{y}^2} + \frac{c}{1+c\bar{y}}\frac{\partial w}{\partial \bar{y}} - \frac{wc^2}{(1+c\bar{y})^2}\right]$$

It is interesting to note, that even if c were considered of $O\left(\frac{1}{\delta^2}\right)$ or larger, no additional terms from Equations (49) would have to be retained in Equations (51).

Equations (50) and (51) are the boundary layer equations of motion for flow over a sharply, laterally curved surface. They differ from the usual three-dimensional boundary layer equations, such as derived for instance in References (1) and (2), by the presence of additional viscous terms, depending on curvature of the wall.

C. Perturbed Boundary Layer Flow Equations

It is clear from the form of the Equations (50) and (51) that if $W = \frac{\partial p}{\partial \bar{z}} = 0$; then $w=0$ will satisfy the third momentum equation as well as the boundary conditions, and thus constitutes the solution for this particular case. This fact suggests that we seek solutions by small perturbation procedure analogous to the one used previously, because

such solutions will then match the solutions of Part II in regions where curvature goes to zero.

To obtain the perturbed boundary layer flow equations we consider a velocity and pressure system given by Equations (9) and (10). Substitution of these quantities into Equations (50) and (51) yields the zeroth order equations (basic flow):

$$u^\circ \frac{\partial u^\circ}{\partial \bar{x}} + v^\circ \frac{\partial u^\circ}{\partial \bar{y}} = \nu\left(\frac{\partial^2 u^\circ}{\partial \bar{y}^2} + \frac{c}{1+c\bar{y}} \frac{\partial u^\circ}{\partial \bar{y}}\right)$$

$$\frac{\partial u^\circ}{\partial \bar{x}} + \frac{\partial v^\circ}{\partial \bar{y}} + \frac{v^\circ c}{1+c\bar{y}} = 0 \qquad (52)$$

and the first order equations:

$$u^\circ \frac{\partial u^*}{\partial \bar{x}} + u^* \frac{\partial u^\circ}{\partial \bar{x}} + v^\circ \frac{\partial u^*}{\partial \bar{y}} + v^* \frac{\partial u^\circ}{\partial \bar{y}} + \frac{w^*}{1+c\bar{y}} \frac{\partial u^\circ}{\partial \bar{z}} = -\frac{1}{\rho} \frac{\partial p^*}{\partial \bar{x}} + \nu\left(\frac{\partial^2 u^*}{\partial \bar{y}^2} + \frac{c}{1+c\bar{y}} \frac{\partial u^*}{\partial \bar{y}}\right)$$

$$u^\circ \frac{\partial w^*}{\partial \bar{x}} + v^\circ \frac{\partial w^*}{\partial \bar{y}} + \frac{c v^\circ w^*}{1+c\bar{y}} = -\frac{1}{\rho} \frac{\partial p}{\partial \bar{z}} \frac{1}{1+c\bar{y}} + \nu\left(\frac{\partial^2 w^*}{\partial \bar{y}^2} + \frac{c}{1+c\bar{y}} \frac{\partial w^*}{\partial \bar{y}} - \frac{w^* c^2}{(1+c\bar{y})^2}\right)$$

$$\frac{\partial p^*}{\partial \bar{y}} = O(w^*)^2 \qquad (53)$$

$$\frac{\partial u^*}{\partial \bar{x}} + \frac{\partial v^*}{\partial \bar{y}} + \frac{1}{1+c\bar{y}} \frac{\partial w^*}{\partial \bar{z}} + \frac{v^* c}{1+c\bar{y}} = 0$$

D. Solution of the Basic Flow Equations

The system of Equations (52) may be reduced to a single partial differential equation by defining a stream function Ω :

$$u^* \equiv \frac{1}{1+c\bar{y}} \frac{\partial \Omega}{\partial \bar{y}}$$
$$v^* \equiv \frac{1}{1+c\bar{y}} \frac{\partial \Omega}{\partial \bar{x}} \tag{54}$$

Equation of continuity is then identically satisfied, while the momentum equation becomes:

$$\Omega_{\bar{y}}\Omega_{\bar{y}\bar{x}} - \Omega_{\bar{x}}\Omega_{\bar{y}\bar{y}} - \nu\Omega_{\bar{y}\bar{y}\bar{y}} + \left[\bar{y}\Omega_{\bar{y}}\Omega_{\bar{y}\bar{x}} - \bar{y}\Omega_{\bar{x}}\Omega_{\bar{y}\bar{y}} + \Omega_{\bar{x}}\Omega_{\bar{y}} + \nu(\Omega_{\bar{y}\bar{y}\bar{y}} - 2\bar{y}\Omega_{\bar{y}\bar{y}\bar{y}})\right]c + \nu c^2(\bar{y}\Omega_{\bar{y}\bar{y}} - \Omega_{\bar{y}} - \bar{y}^2\Omega_{\bar{y}\bar{y}\bar{y}}) = 0 \tag{55}$$

To obtain solution of Equation (55) we set: $\xi = c\sqrt{\frac{\nu\bar{x}}{U^*}}$, $\eta = \bar{y}\sqrt{\frac{U^*}{\nu\bar{x}}}$ (56)

$$\Omega = \sqrt{U^*\nu\bar{x}}\left[F(\eta) + \xi k(\eta) + \xi^2 k_1(\eta) + \cdots\right]$$

It is evident from the differential equations (52) and (53) that $\bar{y} = -\frac{1}{c}$ is a singularity of the equation. An examination of the coordinate transformation, from the original Cartesian system to the present curvilinear system, shows the necessity of restricting $\bar{y} < -\frac{1}{c}$ for a unique correspondence. This condition makes the maximum permissible value of ξ to be

$$\xi_{MAX} = \frac{1}{\eta_\delta} \tag{57}$$

Consequently, it is sufficient to consider only the first term in the expansion of the stream funcion. Substituting, therefore, Equation (56) into

(55), neglecting all higher powers of ξ than the first, and equating each of the coefficients of ξ to zero, we obtain the zeroth in ξ equation:

$$2F''' + FF'' = 0 \tag{58}$$

and the first in ξ equation:

$$2k''' + 2Fk'' - (F')^2 + (\eta F - 2)F'' + F'(F'\eta - F) = 0 \tag{59}$$

The boundary conditions on Equations (58) and (59) may be determined if the expressions for velocities are considered. These are:

$$u^\circ = \frac{U^\circ}{1+\xi\eta}(F' + \xi k')$$

$$v^\circ = -\frac{1}{2}\frac{1}{1+\xi\eta}\sqrt{\frac{U^\circ \nu}{\bar{x}}}\left[(F - F'\eta) + \xi(2k - k'\eta)\right] \tag{60}$$

so that the boundary conditions on Equations (58) and (59) become:

$$F(0) = F'(0) = k(0) = k'(0) = 0$$

$$F'(\infty) = 1.0 \qquad k'(\infty) = \eta$$

Obviously then, $F(\eta)$ is just the usual Blasius function. Equation (59) was solved for k' numerically. This solution is shown in Figure (7a). It may be seen in this figure that $k' \approx \eta$ and therefore a fair approximation for u° velocity of the basic flow is

$$u^\circ = U^\circ \frac{F' + \xi\eta}{1 + \xi\eta} \tag{62}$$

This approximation has been used subsequently.

E. Discussion of the Solution For Basic Flow

Equations (52) were solved by expanding the expression for stream function in terms of the curvature parameter ξ . It is interesting to note that a different approach might have been undertaken if c were not required to go into $c = 0$. Setting:

$$y = \left(\frac{1}{c} + \bar{y}\right)$$

Transforms Equations (52) into:

$$u^\circ \frac{\partial u^\circ}{\partial \bar{x}} + v^\circ \frac{\partial u^\circ}{\partial \bar{y}} = \frac{\nu}{y} \frac{\partial}{\partial y}\left(y \frac{\partial u^\circ}{\partial y}\right)$$

$$\frac{\partial u^\circ}{\partial \bar{x}} + \frac{\partial v^\circ}{\partial y} + \frac{v}{y} = 0 \qquad (52a)$$

which are identical with the equations for an axially symmetric jet. (Reference (26), pp. 147).

Introducing a stream function:

$$\Omega = \nu \bar{x}\, d(\eta)$$

defined by

$$u^\circ \equiv \frac{1}{y} \frac{\partial \Omega}{\partial y}$$

$$v^\circ \equiv -\frac{1}{y} \frac{\partial \Omega}{\partial \bar{x}}$$

$$\eta \equiv \frac{1}{2} \frac{y^2 v^\circ}{\nu \bar{x}}$$

transforms Equations (52a) into:

$$2\eta d''' + d d'' + 2 d'' = 0 \qquad (52b)$$

with boundary conditions different from those of a jet, namely:

at $\eta = \eta_0 = \frac{1}{2}\frac{U^\circ}{c^2\sqrt{x}}$; $d = d' = 0$

at $\eta \to \infty$; $d' = 1.0$

Note, now, that as $C \to \infty$ (that is the corner becomes very sharp), $\eta_0 \to 0$.

The boundary conditions indicate that function d may be expanded about $\eta_0 = 0$:

$$d = \frac{d''(\eta_0)}{2!}\eta^2 + \frac{d'''(\eta_0)}{3!}\eta^3 + \cdots$$

Substituting this expansion into the differential Equation (52b) and taking the limit as $\eta \to \eta_0 \to 0$, we obtain the result that

$$d''(0) = 0 \tag{63}$$

or that for very large curvatures the velocity has a separation profile. In Figure (8) is shown velocity profile taken from Reference (20) along a 45° line. It may be seen from this figure that this velocity profile exhibits, indeed, the indications of separated flow, and thus seems to confirm the result (63). The existence of such separated or very nearly separated profiles for very large curvatures of the wall and the identical form of Equations (52a) with those for a symmetrical jet, might perhaps shed some light on the phenomenon of transverse contamination. These considerations are, however, beyond the scope of this investigation.

In any case, in view of the discussion of the validity of the perturbation procedure in boundary layer flow, result (63) indicates that

Equations (52a) are inadmissible for such handling of the problem.

Since the coordinate transformation (47) is right handed, the curvature parameter ξ will always be:

$\xi > 0$ for convex wall ($\bar{z}$ bends away from $\bar{y}$)

$\xi < 0$ for concave wall ($\bar{z}$ bends toward $\bar{y}$)

The Equation (62) for the u° velocity indicates thus that the effect of a concave wall is detrimental to the boundary layer flow, while a convex wall tends to improve the u° velocity profile.

F. Solution of the First Order Equations

In order to solve the perturbation equations it is first necessary to express the variation of pressure in terms of the external flow. By making use of the Eulerian equations, as previously explained, one obtains:

$$-\frac{1}{\rho}\frac{\partial p^*}{\partial \bar{x}} = U^\circ \frac{\partial U^*}{\partial \bar{x}}$$

$$-\frac{1}{\rho}\frac{1}{1+c\bar{y}}\frac{\partial p^*}{\partial \bar{z}} = U^\circ \frac{\partial W^*}{\partial \bar{x}} + \frac{c}{1+c\bar{y}} W^* \left(\lim_{y\to\delta} v^\circ\right) \qquad (64)$$

It should be noted that now, use must be made of the assumption that V is correctly represented by the $\lim_{y\to\delta} v$.

Introducing the components of the vector potential, now defined as

$$
\begin{aligned}
u^*(1+c\bar{y}) &\equiv \frac{\partial \Psi}{\partial \bar{y}} \\
w^* &\equiv \frac{\partial \varphi}{\partial \bar{y}} \\
v^*(1+c\bar{y}) &\equiv -\left(\frac{\partial \Psi}{\partial \bar{x}} + \frac{\partial \varphi}{\partial \bar{z}}\right)
\end{aligned}
\tag{65}
$$

the equation of continuity is again identically satisfied, while the momentum equations become:

$$
\begin{aligned}
&u^o \Psi_{\bar{y}\bar{x}} + u^o_{\bar{x}} \Psi_{\bar{y}} + v^o\left(\Psi_{\bar{y}\bar{y}} - \frac{c}{1+c\bar{y}} \Psi_{\bar{y}}\right) - u^o_{\bar{y}}\left(\Psi_{\bar{x}} + \varphi_{\bar{z}}\right) + u^o_{\bar{z}} \varphi_{\bar{y}} \\
&\qquad = (1+c\bar{y}) U^o U^*_{\bar{x}} + \nu\left[\frac{c^2}{(1+c\bar{y})^2} \Psi_{\bar{y}} - \frac{c}{1+c\bar{y}} \Psi_{\bar{y}\bar{y}} + \Psi_{\bar{y}\bar{y}\bar{y}}\right]
\end{aligned}
\tag{66}
$$

$$
u^o \varphi_{\bar{y}\bar{x}} + v^o \varphi_{\bar{y}\bar{y}} + \frac{c v^o}{1+c\bar{y}} \varphi_{\bar{y}} = U^o W^*_{\bar{x}} + \nu\left[\varphi_{\bar{y}\bar{y}\bar{y}} + \frac{c}{1+c\bar{y}} \varphi_{\bar{y}\bar{y}} - \frac{c^2}{(1+c\bar{y})^2} \varphi_{\bar{y}}\right] + \frac{c W^*}{1+c\bar{y}} \lim_{\eta \to \infty} v^o
$$

It may be noted that again, as in the flow over a plane wall, the second momentum equation (and thus the w^* velocity) is completely independent of the first (or the u^* velocity), and is affected only by the basic flow and the external flow, both of which are known.

Since we demand from the solutions that these go smoothly into the solutions for three-dimensional boundary layer when $c \to 0$, the vector potential components are now expanded similarily to Equations (57).

$$\psi(\bar{x},\eta,\bar{z}) = \frac{U^*}{U^\circ}\sqrt{\nu\bar{x}U^\circ}\left[f(\eta) + \xi\, l(\eta) + \xi^2 l_1(\eta) + \cdots\right]$$

$$\varphi(\bar{x},\eta,\bar{z}) = \frac{W^*}{U^\circ}\sqrt{\nu\bar{x}U^\circ}\left[g(\eta) + \xi\, t(\eta) + \xi^2 t_1(\eta) + \cdots\right] \tag{67}$$

Introducing Equations (67) and (57) into Equations (66), results in the zeroth in ξ equations:

$$f''' + \frac{F}{2}f'' - \left(\bar{x}\frac{U^*_{\bar{x}}}{U^*}F'\right)f' + \left[\left(\frac{1}{2} + \bar{x}\frac{U^*_{\bar{x}}}{U^*}\right)F''\right]f + \bar{x}\frac{W^*_{\bar{z}}}{U^*}F''g + \bar{x}\frac{U^*_{\bar{x}}}{U^*} = 0$$

$$g''' + \frac{F}{2}g'' - \left(\bar{x}\frac{W^*_{\bar{x}}}{W^*}F'\right)g' + \bar{x}\frac{W^*_{\bar{x}}}{W^*} = 0 \tag{68}$$

and the first order in ξ equations:

$$l''' + \frac{F}{2}l'' - \left[\left(\frac{1}{2} + \bar{x}\frac{U^*_{\bar{x}}}{U^*}\right)F'\right]l' + \left[\left(1 + \bar{x}\frac{U^*_{\bar{x}}}{U^*}\right)F''\right]l - L(\bar{x},\eta,\bar{z}) = 0$$

$$t''' + \frac{F}{2}t'' - \left[\left(\frac{1}{2} + \bar{x}\frac{W^*_{\bar{x}}}{W^*}\right)F'\right]t' - T(\bar{x},\eta,\bar{z}) = 0 \tag{69}$$

with the nonhomogeneous parts defined as:

$$\begin{aligned} L(\bar{x},\eta,\bar{z}) \equiv {} & -3\eta\bar{x}\frac{U^*_{\bar{x}}}{U^*} - 2\eta f''' - \left(k + \frac{F}{2}\eta - 1\right)f'' + \left[\bar{x}\frac{U^*_{\bar{x}}}{U^*}(F'\eta + k') + \frac{1}{2}(k' + F') - F'\eta\right]f' \\ & - \left(\bar{x}\frac{U^*_{\bar{x}}}{U^*} + \frac{1}{2}\right)(F''\eta + k'' - F')f - \bar{x}\frac{W^*_{\bar{z}}}{U^*}(F''\eta + k'' - F')g \\ & + \bar{x}\frac{W^*}{U^*}\frac{d\log c}{d\bar{z}}(k' - F'\eta)g' - \bar{x}\left(\frac{W^*_{\bar{z}}}{U^*} + \frac{W^*}{U^*}\frac{d\log c}{d\bar{z}}\right)F''t \end{aligned} \tag{69a}$$

$$\begin{aligned} T(\bar{x},\eta,\bar{z}) \equiv {} & -\eta g''' - \left(k + \frac{F}{2}\eta + 1\right)g'' + \left[\bar{x}\frac{W^*_{\bar{x}}}{W^*}(F'\eta + k') + \frac{1}{2}(F'\eta - F)\right]g' \\ & - 2\bar{x}\eta\frac{W^*_{\bar{x}}}{W^*} - \frac{1}{2}\lim_{\eta\to\infty}(F'\eta - F) \end{aligned}$$

Equations (68) as might have been expected are identical with Equations (16) when $\omega_2 = 0$.

Since the expressions for the velocities are now:

$$u^* = \frac{U^*}{1+\xi\eta}(f' + \xi l')$$

$$v^* = -\frac{1}{1+\xi\eta}\sqrt{\frac{\nu\bar{x}}{U^\circ}}\left\{U^*_{\bar{x}}(f+\xi l) + \frac{U^*}{2\bar{x}}\left[f + 2\xi l - \eta(f'+\xi l')\right] + \left[W^*_{\bar{z}}(g+\xi t) + W^*\frac{d\log c}{d\bar{z}}\xi t\right]\right\} \qquad (70)$$

$$w^* = W^*(g' + \xi t')$$

the boundary conditions on Equations (69) become:

$$f(0) = f'(0) = l(0) = l'(0) = g(0) = g'(0) = t(0) = t'(0) = 0$$

$$f'(\infty) = g'(\infty) = 1.0 \qquad (71)$$

$$l'(\infty) = \eta$$

$$t'(\infty) = 0$$

Inspection of the boundary conditions shows that functions f & g are identical with those obtained for the flow over a plane wall.

To change Equations (69) into total differential equations, proper form of expressions for $U^*(\bar{x},\bar{z})$ and $W^*(x,\bar{z})$ must be chosen. This investigation will be restricted to cases where $U^*(\bar{x},\bar{z}) = 0$ and $W^* = W^*(\bar{x})$. For such cases, inspection of Equations (69) and (70) shows that $l = 0$ is not a solution of Equation (69) and thus the velocity u^* is improperly normalized when $U^* = 0$. Since, however, U^* was considered an arbitrary function of $\bar{x}$ and $\bar{z}$, we may replace it

in Equations (67) (with the exception of the term originating in $\frac{\partial p^*}{\partial \bar{x}}$) by some other function $M(\bar{x}, \bar{z})$, which is not zero when $U^* = 0$. In this case the equation for f becomes:

$$f''' + \frac{F}{2} f'' - \bar{x} \frac{M_{\bar{x}}}{M} F' f' + \left(\frac{1}{2} - \bar{x} \frac{M_{\bar{x}}}{M} \right) F'' f = 0 \tag{68a}$$

and that for ℓ :

$$\ell''' + \frac{F}{2} \ell'' - \left(\frac{1}{2} + \bar{x} \frac{M_{\bar{x}}}{M} \right) F' \ell' + \left(1 + \bar{x} \frac{M_{\bar{x}}}{M} \right) F'' \ell - L = 0$$

with (69b)

$$L = 2\eta f''' - \left(k + \frac{F}{2} \eta - 1 \right) f'' + \left[\bar{x} \frac{M_{\bar{x}}}{M} (F'\eta + k') + \frac{1}{2}(k' + F') - F'\eta \right] f'$$
$$- \left(\bar{x} \frac{M_{\bar{x}}}{M} + \frac{1}{2} \right) (F''\eta + k'' - F') f + \bar{x} \frac{W^*}{M} \frac{d \log c}{d\bar{z}} (k' - F'\eta) g - \bar{x} \frac{W^*}{M} \frac{d \log c}{d\bar{z}} F'' t$$

with boundary conditions

$$f(0) = f'(0) = \ell(0) = \ell'(0) = f'(\infty) = \ell'(\infty) = 0 \tag{71a}$$

These boundary conditions indicate that $f = 0$ is a solution of Equation (68a) and only Equation (69b) will have to be considered in this case.

Inspection of Equation (69b) indicates that a convenient choice of function M appears to be:

$$M(\bar{x}, \bar{z}) = \bar{x} \frac{d \log c}{d\bar{z}} W^* \tag{72}$$

so that with this choice of M and $W^* = W^*(\bar{x})$, Equations (69b) become:

$$l''' + \frac{F}{2} l'' - \left[\left(\frac{3}{2} + \bar{x}\frac{W_{\bar{x}}^*}{W^*}\right)F'\right]l' + \left(2 + \bar{x}\frac{W_{\bar{x}}^*}{W^*}\right)F''l - L = 0$$

$$L = (k' - F'\eta)g' - F''t \tag{69c}$$

For $W^* = A\bar{x}^n$ and $U^* = 0$ Equations (69) become thus

$$l''' + \frac{F}{2} l'' - \left[\left(\frac{3}{2} + n\right)\right]F'l' + (2+n)F''l + F''t - (k' - F'\eta)g' = 0 \tag{73a}$$

$$t''' + \frac{F}{2}t'' - \left[\left(\frac{1}{2} + n\right)\right]F't' - \eta g''' + \left(k + \frac{F}{2}\eta + 1\right)g'' - \left[n(F'\eta + k') + \frac{1}{2}(F'\eta - F)\right]g'$$

$$+ 2n\eta + \frac{1}{2}\lim_{\eta \to \infty}(F'\eta - F) = 0 \tag{73b}$$

Equations (73) were solved numerically for $n = 0$ and $n = 1$. These solutions are shown in Figures (7b) and (7c).

G. An Example of a Flow in a Corner

To illustrate the manner in which the derived results are applied to an actual boundary layer flow over a sharply curved wall, such flow has been computed assuming the wall shape to be hyperbolic.

For such a wall

$$2zy = \sigma = \text{constant}$$

and

$$z^2 - y^2 = \chi$$

so that the curvature becomes

$$c = \pm \frac{\sigma}{(\chi^2+\sigma^2)^{3/4}}$$

and

$$\frac{d\log c}{d\bar{z}} = -3\,\frac{\chi}{(\chi^2+\sigma^2)^{3/4}}$$

Since χ and σ are known for each value of z and y, both the curvature and its logarithmic derivative may easily be computed. It remains, however, to establish the scale of η as compared to that of z and y. This may be done by considering the condition of no interaction:

$$c_{MAX}\, y_\delta = 1 = \xi_{MAX}\, \eta_\delta$$

Since

$$c_{MAX} = \sigma^{-1/2}$$

and

$$\xi_{MAX} = 0.125 \quad (\text{ASSUMING } \eta_\delta = 8)$$

so that the maximum value of $\bar{x}$, for which the assumptions made here apply, is given by

$$\bar{x}_{MAX} = 0.125\, \sigma^{1/2}\, Re^{1/2}$$

The present computations were carried out for $\bar{x}_{MAX}\, c_{MAX} = 10$ and $Re = 62500$. Two cases were computed with $W^* = A\, x^n$, $U^* = 0$ and $n = 0$ and $n = 1$. The results of these computations are shown in Figures (9a) to (9d) where q_{12} and the directional deviation $\theta - \vartheta$ are plotted. It should be noted, that in order to afford a direct comparison, the magnitude of the velocity W^* is the same in both cases, which means that the constant A is different in the two cases.

Physically, such an external flow may be thought of as a vortex

of constant strength for $n=0$ and a vortex of an increasing strength for $n=1$. Examination of Figure (9a) shows that for $n=0$ an accumulation of low momentum air occurs on the "upstream" wall of the corner. This is confirmed by Figure (9b), where the directional deviations indicate crossflow from the "downstream" wall onto the "upstream" wall. The indications, therefore, are that by causing the large curving of the external flow, the corner establishes a crosswise pressure gradient and thus causes an accumulation of low momentum air on the "upstream" wall. Away from the corner where the streamlines of the external flow become straight again, the boundary layer flow becomes identical with that described in Case (1) of Part II.

When $n=1$, however, examination of Figures (c) and (9d) reveals that now the large accumulation of the low momentum air occurs on the "downstream" wall with corresponding large deflections in that region. This, apparently, is due to the fact that in this case the external flow posseses a crosswise pressure gradient before it reaches the corner, and this pressure gradient not only opposes the one established by the corner, but also causes complete stall of the u flow on the "downstream" wall, so that almost all the flow (as evidenced by large deflection) that takes place in that region is the $\bar{z}$ direction.

H. Discussion of Results and Qualitative Comparison with Experiment

The results of the present analysis furnish some light on the behavior of boundary layers in cascades. We imagine a blade passage

as represented schematically below with $\bar{z}$ axis suitably bent to the cross-sectional shape of the passage walls (P), (C), and (S).

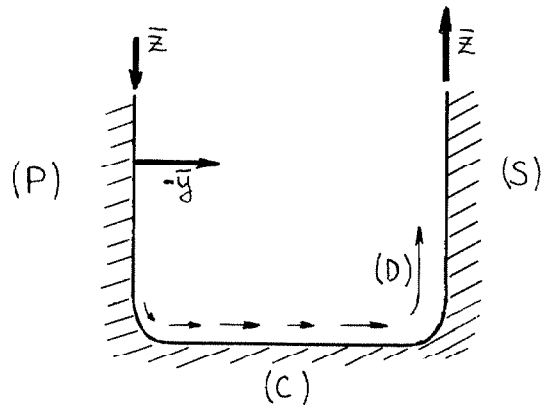

$W = A\bar{x}$

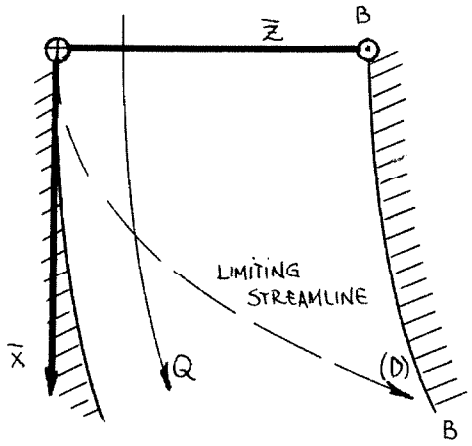

The shape of the passage in the $\bar{x}$ direction may be represented by a parabolic variation of W^* velocity (say $W^* = A\bar{x}$). Results of corner flow investigation indicate that we may expect larger than usual cross-wise flows along the line B-B. In particular, concentrating our attention on the limiting streamline which starts at the (P) wall of

this passage, the results of Case (3) in Part II indicate that the direction of this limiting streamline on wall (C) would be given by:

$$\alpha(\bar{x}) = 3.26 \frac{A}{U_\infty} \bar{x}$$

Assuming about 22° degrees of turning at the outlet from the passage, and that the total length of the passage along the S_1 coordinate $\approx$ chord, we may inquire at what spacing of walls (P) and (S) the limiting streamline would reach wall (S) at the trailing edge. A simple computation yields

$$\text{Solidity} = \frac{\text{Chord}}{\text{Spacing}} \doteq 1.8$$

Finally, upon reaching the second corner, the limiting streamline would be sharply swept up on wall (S) at point (D), due to the very large deflections along the line B-B. Although such a picture of boundary layer behavior furnishes at best only a very approximate and rough idea of flow in cascades, where undoubtedly neither the passage shape nor the external flow can be represented so simply, still, it is felt that this picture retains most of the important characteristics. To ascertain this belief and to obtain at least some qualitative comparison with experiment, References (28) and (29) concerned with visualization of such flows were studied. The examination of the data of these references shows similarily shaped limiting streamlines on wall (C) and large swept flow (D). The limiting streamline is shown to reach the trailing edge of the other blade at solidity 1.5. Consequently, it is felt that at least some of the results of the present analysis have a qualitative experimental confirmation.

REFERENCES

1. Howarth, L., "The Boundary Layer in Three-Dimensional Flow - Part I. Derivation of the Equations for Flow Along a General Curved Surface", Philosophical Mag., Vol. XLII, pp. 239-243, (March 1951).

2. Hayes, Wallace D., "The Three-Dimensional Boundary Layer", NAVORD Rep. 1313, NOTS 384, U. S. Naval Ordnance Test Station (Inyokern), (May 9, 1951).

3. Moore, Franklin K., "Three-Dimensional Compressible Laminar Boundary Layer Flow", NACA TN 2279, (1951).

4. Burgers, J. M. "Some Considerations on the Development of Boundary Layers in the Case of Flows Having a Rotational Component", Nederl, Akad. van Wetenschappen, Vol. XLIV, Nos. 1-5, pp. 12-25, (1941).

5. Tetervin, Neal, "Boundary-Layer Momentum Equations for Three-Dimensional Flow", NACA TN 1479, (1947).

6. Prandtl, L., "On Boundary Layers in Three-Dimensional Flow", Reps. and Trans. No. 64, British M.A.P., (May 1, 1946).

7. Sears, W. R., "The Boundary Layer of Yawed Cylinders", Journal of Aeronautical Sciences, Vol. 15, No. 1, pp. 49-52, (Jan. 1948).

8. Wild, J. M., "The Boundary Layer of Yawed Infinite Wings", Journal of Aeronautical Sciences, Vol. 16, No. 1, pp. 41-45, (Jan. 1949).

9. Young, A. D. and Booth, T. B., "The Profile Drag of Yawed Wings of Infinite Span", Coll. Aero., Canfield, Rep. No. 38.

10. Altman, J. M. and Hayter, N. F., "A Comparison of the Turbulent Boundary-Layer Growth on an Unswept and a Swept Wing", NACA TN 2500.

11. Bödewart, U. T., "Die Drehströmung über festem Grunde", ZAMM, 20, 241, (1940).

12. von Kármán, Th., "On Laminar and Turbulent Friction", NACA TM 1092, (1946).

13. Mager, A. and Hansen, A. G., "Laminar Boundary Layer Over Flat Plate in a Flow Having Circular Streamlines", NACA TN 2658, (1952).

14. Fogarty, L. E., "The Laminar Boundary Layer on a Rotating Blade", Journal of Aeronautical Sciences, Vol. 18, No. 4, pp. 247-252, (April 1951).

15. Howarth, L., "Note on the Boundary Layer on a Rotating Sphere", Philosophical Magazine, Ser. 7, Vol. XLII, pp. 1308-1315, (Nov. 1951).

16. Howarth, L. "The Boundary Layer in Three Dimensional Flow. Part II, The Flow Near a Stagnation Point", Philosophical Magazine, Ser. 7, Vol. XLII, pp. 1433-1440, (Dec. 1951).

17. Moore, F. K., "Laminar Boundary Layer on a Circular Cone in Supersonic Flow at a Small Angle of Attack", NACA TN 2521, (1951).

18. Moore, F. K., "Displacement Effect of a Three-Dimensional Boundary Layer", NACA TN 2722, (1952).

19. Moore, F. K., "Laminar Boundary Layer on a Cone in Supersonic Flow at Large Angle of Attack", NACA TN 2844, (1952).

20. Carrier, G. F., "The Boundary Layer in a Corner", Quart. of Appl. Math., Vol. IV, No. 4, pp. 367-370, (Jan. 1947).

21. Loitsianskii, L. G. and Bolshakov, V. P., "On Motion of Fluid in Boundary Layer Near Line of Intersection of Two Plates", NACA TM 1308, (1951).

22. Timman, R., "A Calculation Method for Three-Dimensional Laminar Boundary Layers", National Luchtvaartlab. Amsterdam, Rep. F.66 , (1951).

23. Mager, A., "Generalization of Boundary-Layer Momentum-Integral Equations to Three-Dimensional Flows Including Those of Rotating System", NACA TR 1067, (1952).

24. Gruschwitz, E., "Turbulente Reibungsschichten mit Sekundärströmung", Ingenieur-Archiv, Bd. VI, pp. 355-365, (1935).

25. Kuethe, A. M., McKee, P. B. and Curry, W. H., "Measurements in the Boundary Layer of a Yawed Wing", NACA TN 1946, (1949).

26. Goldstein, S. (ed), "Modern Developments in Fluid Dynamics" Vol. I, Clarendon Press, (Oxford), (1938).

27. Bowen, J. T., Sabersky, R. H., Rannie, W. D., "Theoretical and Experimental Investigations of Axial Flow Compressors", Mech. Eng. Laboratory, C.I.T. (Navy contract N6-ORI-102 Task order IV), (Jan. 1949).

28. Herzig, H. Z., Hansen, A. G., Costello, G. R., "Visualization of Secondary-Flow Phenomena in Blade Row", NACA RM E52 F19, (Aug. 1952).

29. Hansen, A. G., Costello, G. R. and Herzig, H. Z., "Effect of Geometry on Secondary Flows in Blade Rows", NACA RM E52 H26, (Oct. 1952).

APPENDIX A

Expressions for Various Boundary Layer Quantities

a) Flow Over a Plane Surface

Velocity along the s_1 coordinate:

$$q_1 = u\cos\theta + w\sin\theta$$

$$\theta \approx \frac{W^*}{U^\circ} + O\left(\frac{W^*}{U^\circ}\right)^2$$

$$\cos\theta \approx 1.0 \qquad \sin\theta \approx \frac{W^*}{U^\circ}$$

$$q_1 \doteq \left(U^\circ F' + U^* f'\right) + O\left(\frac{W^*}{U^\circ}\right)^2$$

Velocity along the s_2 coordinate:

$$q_2 = w\cos\theta - u\sin\theta \approx W^* g' - \frac{W^*}{U^\circ}\left(U^\circ F' - U^* f'\right) \approx W^*\left(g' - F'\right)$$

Velocity of the external flow:

$$Q = \left[\left(U^\circ + U^*\right)^2 + W^{*2}\right]^{1/2} \approx U^\circ\left(1 + \frac{U^*}{U^\circ}\right)$$

Direction of the external flow:

$$\theta = \arctan\frac{W^*}{U^\circ + U^*} \approx \frac{W^*}{U^\circ}$$

Direction of boundary layer flow:

$$\vartheta(\eta) = \arctan\frac{W^* g'}{U^\circ F' + U^* f'} \approx \frac{W^* g'}{U^\circ F'}$$

Crossflow deflection:

$$\vartheta - \theta = \frac{W^* g'}{U^\circ F'} - \frac{W^*}{U^\circ} = \frac{W^*}{U^\circ}\left(\frac{g'}{F'} - 1\right)$$

Limiting deflection:

$$\alpha(x,0,z) = \frac{W^*}{U^\circ}\left[\frac{g''(0)}{F''(0)} - 1\right]$$

Displacement thicknesses:

$$\frac{\delta_1^+}{x} = \frac{1}{Q Re^{1/2}} \int_0^\infty (Q - q_1)\, d\eta \approx \frac{1}{Re^{1/2}}\left[\int_0^\infty (1-F')\, d\eta + \frac{U^*}{U^\circ}\int_0^\infty (F'-f')\, d\eta\right]$$

$$\frac{\delta_2^+}{x} = \frac{1}{Q Re^{1/2}} \int_0^\infty q_2\, d\eta \approx \frac{1}{Re^{1/2}} \frac{W^*}{U^\circ}\int_0^\infty (g'-F')\, d\eta$$

Momentum thicknesses:

$$\frac{\delta_{11}^{++}}{x} = \frac{1}{Re^{1/2}Q^2} \int_0^\infty (Q-q_1) q_1\, d\eta \approx \frac{1}{Re^{1/2}}\left[\int_0^\infty F'(1-F')\, d\eta + 2\frac{U^*}{U^\circ}\int_0^\infty \left[F'(F'-f'-1/2)+1/2 f'\right] d\eta\right]$$

$$\frac{\delta_{22}^{++}}{x} = \frac{1}{Re^{1/2}Q^2} \int_0^\infty q_2^2\, d\eta \approx O\left(\frac{W^*}{U^\circ}\right)^2$$

$$\frac{\delta_{12}^{++}}{x} = \frac{1}{Re^{1/2}Q^2} \int_0^\infty (Q-q_1) q_2\, d\eta \approx \frac{W^*}{U^\circ}\frac{1}{Re^{1/2}}\left[\int_0^\infty (1-F') g'\, d\eta - \int_0^\infty F'(1-F')\, d\eta\right]$$

$$\frac{\delta_{21}^{++}}{x} = \frac{1}{Re^{1/2}Q^2} \int_0^\infty q_1 q_2\, d\eta = \frac{\delta_2^+}{x} - \frac{\delta_{12}^{++}}{x} \approx \frac{W^*}{U^\circ}\frac{1}{Re^{1/2}}\left[\int_0^\infty F'(g'-F')\, d\eta\right]$$

b) Flow Over a Sharply Curved Surface: $U^* = 0$; $W^* = Ax^n$

Velocity along the ζ_1 coordinate:

$$q_1 \approx U^\circ F' + \xi\left[U^\circ \eta (1-F') + \bar{x}\,\frac{d\log c}{d\bar{z}}\, W^* l'\right]$$

Velocity along the s_2 coordinate:

$$q_2 \approx W^* \left\{ g' - F' + \xi \left[(1-F')\eta - t' \right] \right\}$$

Displacement thicknesses:

$$\frac{\delta_1^+}{\bar{x}} Re^{1/2} \approx \int_0^\infty (1-F')d\eta - \xi \left[\int_0^\infty \eta(1-F')d\eta + \bar{x} \frac{d\log c}{d\bar{z}} \frac{W^*}{U^\circ} \int_0^\infty t' d\eta \right]$$

$$\frac{\delta_2^+}{\bar{x}} Re^{1/2} \approx \frac{W^*}{U^\circ} \left\{ \int_0^\infty (g' - F')d\eta + \xi \left[\int_0^\infty (1-F')d\eta - \int_0^\infty t' d\eta \right] \right\}$$

Momentum thicknesses:

$$\frac{\delta_{11}}{\bar{x}} Re^{1/2} \approx \int_0^\infty (F'-1)F' d\eta + \xi \left[\int_0^\infty (1-F')^2 \eta d\eta - \int_0^\infty F'(1-F')\eta d\eta - \frac{W^*}{U^\circ} \bar{x} \frac{d\log c}{d\bar{z}} \int_0^\infty F' t' d\eta \right]$$

$$\frac{\delta_{22}^{++}}{\bar{x}} Re^{1/2} \approx O\left(\frac{W^*}{U^\circ}\right)^2$$

$$\frac{\delta_{12}^{++}}{\bar{x}} Re^{1/2} \approx \frac{W^*}{U^\circ} \left\{ \int_0^\infty g'(1-F')d\eta - \int_0^\infty F'(1-F')d\eta - \xi \left[\int_0^\infty g'(1-F')\eta d\eta - \int_0^\infty F'(1-F')\eta d\eta \right.\right.$$
$$\left.\left. + \int_0^\infty (1-F')\eta d\eta - \int_0^\infty t'(1-F')d\eta \right] \right\}$$

$$\frac{\delta_{21}^{++}}{\bar{x}} Re^{1/2} \approx \frac{W^*}{U^\circ} \left\{ \int_0^\infty (g' - F')F' d\eta + \xi \left[\int_0^\infty g'(1-F')\eta d\eta - \int_0^\infty t' F' d\eta \right] \right\}$$

APPENDIX B

Numerical Procedure Used in the Solution of the Differential Equations

To illustrate in detail the numerical procedure followed, let us consider Equation (29):

$$g''' + \frac{F}{2} g'' - n(F'g' - 1) = 0 \qquad (29)$$

with boundary conditions:

$$g(0) = g'(0) = 0 \quad ; \quad g'(\infty) = 1.0$$

Because of the two point boundary conditions it is convenient to solve Equation (29) by use of the relaxation procedure. We note that Equation (29) is of second order in g' :

$$\frac{d^2(g')}{d\eta^2} + \frac{F}{2} \frac{d(g')}{d\eta} - n(F'g' - 1) = 0 \qquad (29A)$$

At a specific value of $\eta = \eta_o$, Equation (29A) may be approximated by an algebraic expression:

$$\frac{1}{h^2}(g'_1 + g'_{-1} - 2g'_o) + \frac{F}{4h}(g'_1 - g'_{-1}) - n(F'_o g'_o - 1) = 0 \qquad (29B)$$

which utilizes the values of g'_1 at $\eta = \eta_o + h$ and g'_{-1} at $\eta = \eta_o - h$. Examination of Equation (29) and function F' reveals that $g' = 1.0$ will

satisfy that equation for all $\eta > 6.0$. Consequently, the boundary condition at infinity may be replaced by an equivalent boundary condition say at $\eta = 8$:

$$g'(8) = 1.0$$

Dividing now the interval $0 \leq \eta \leq 8$ into r parts of size h, we get, together with the two boundary conditions at $\eta = 0$ and $\eta = 8$, $r+1$ algebraic equations for the determination of the $r+1$ values of g'. These must be solved simultaneously and it is convenient to do so by relaxation. In this method the initial values of g' are first guessed at. These will in general not satisfy Equation (29B), giving at each value of η a definite residue. By systematically modifying (relaxing) the initially assumed values of g', so that <u>all</u> the residues are reduced to zero, the simultaneous solution of the $r+1$ equations is obtained. But this solution is equivalent to an approximate solution of the differential Equation (29). The degree of the approximation clearly depends on the size of the interval h. In this investigation $h = 1.0$ was used for most of the differential equations so solved. In certain cases, however, where greater detail was deemed necessary, the size of h was locally decreased. It should also be mentioned that for most of the cases solved, the residues were considered sufficiently small to cease further relaxing when they all were less than $|0.005|$.

When the differential equations were of higher order, say for instance:

$$f''' + \frac{F}{2} f'' - m F' f' + F''\left(\frac{1}{2} + m\right) f + m = 0 \tag{31}$$

it was found convenient, to solve instead, a system of two simultaneous equations:

$$\frac{d^2}{d\eta^2}(f') + \frac{F}{2}\frac{d}{d\eta}(f') - m F' f' + F''\left(\frac{1}{2} + m\right) f + m = 0 \tag{31A}$$

$$\int_0^{\eta} f' \, d\eta = f \tag{31B}$$

Here the solution of Equation (31A) for f' was first obtained by relaxation. The function $F''\left(\frac{1}{2} + m\right) f$ in this initial step, could either be guessed at, or simply set equal to zero. Next, with the so obtained values of f', Equation (31B) was solved for f using Simpson's rule. These values of f were used in the new solution of Equation (31A) and the process was repeated until no further changes in f' were obtained. For most of the so solved equations, the convergence was very rapid, and usually only four to five cycles were needed to give the final solution.

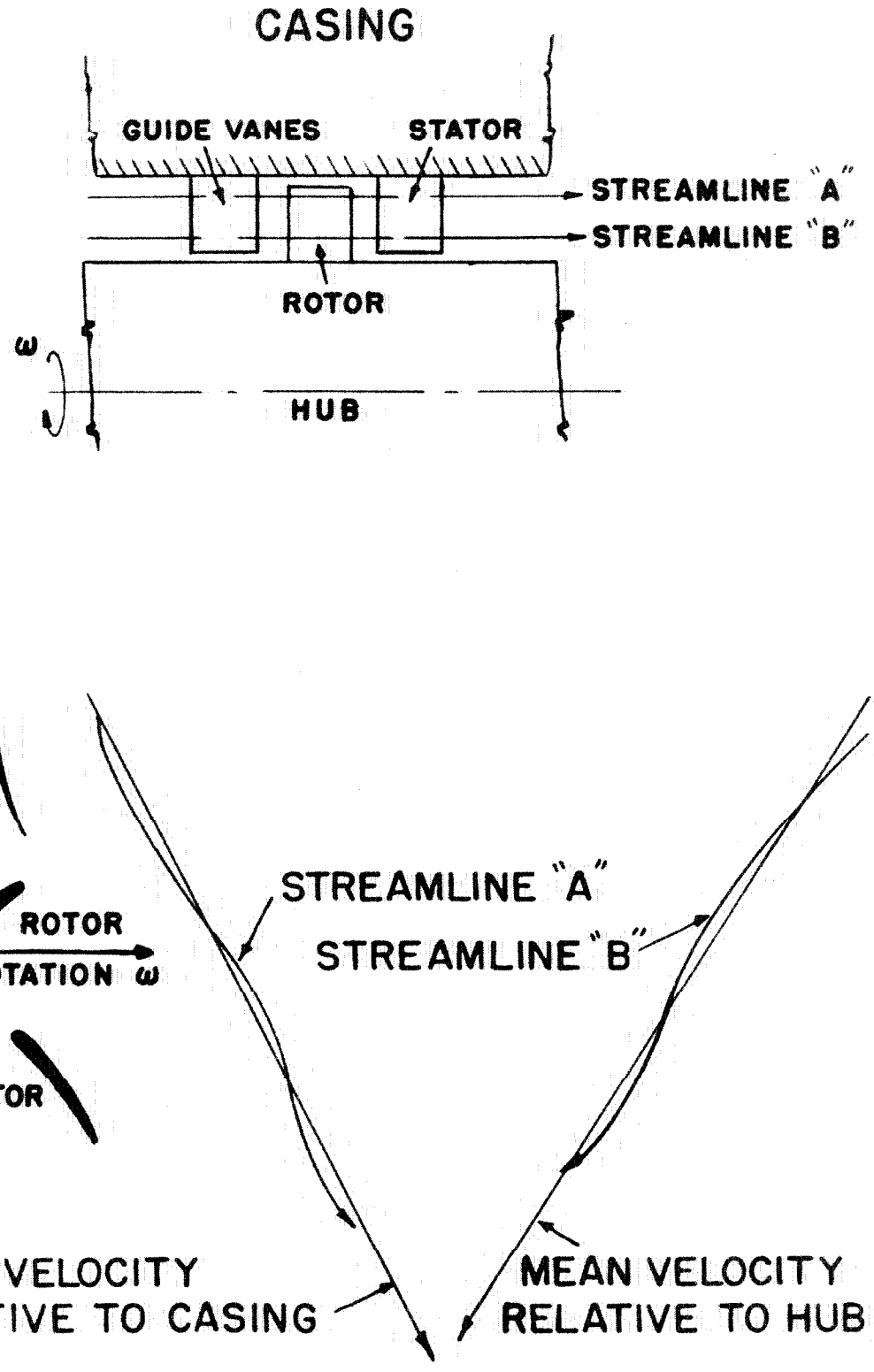

FIGURE 1.- SCHEMATIC REPRESENTATION OF EXTERNAL FLOW IN AN AXIAL COMPRESSOR.

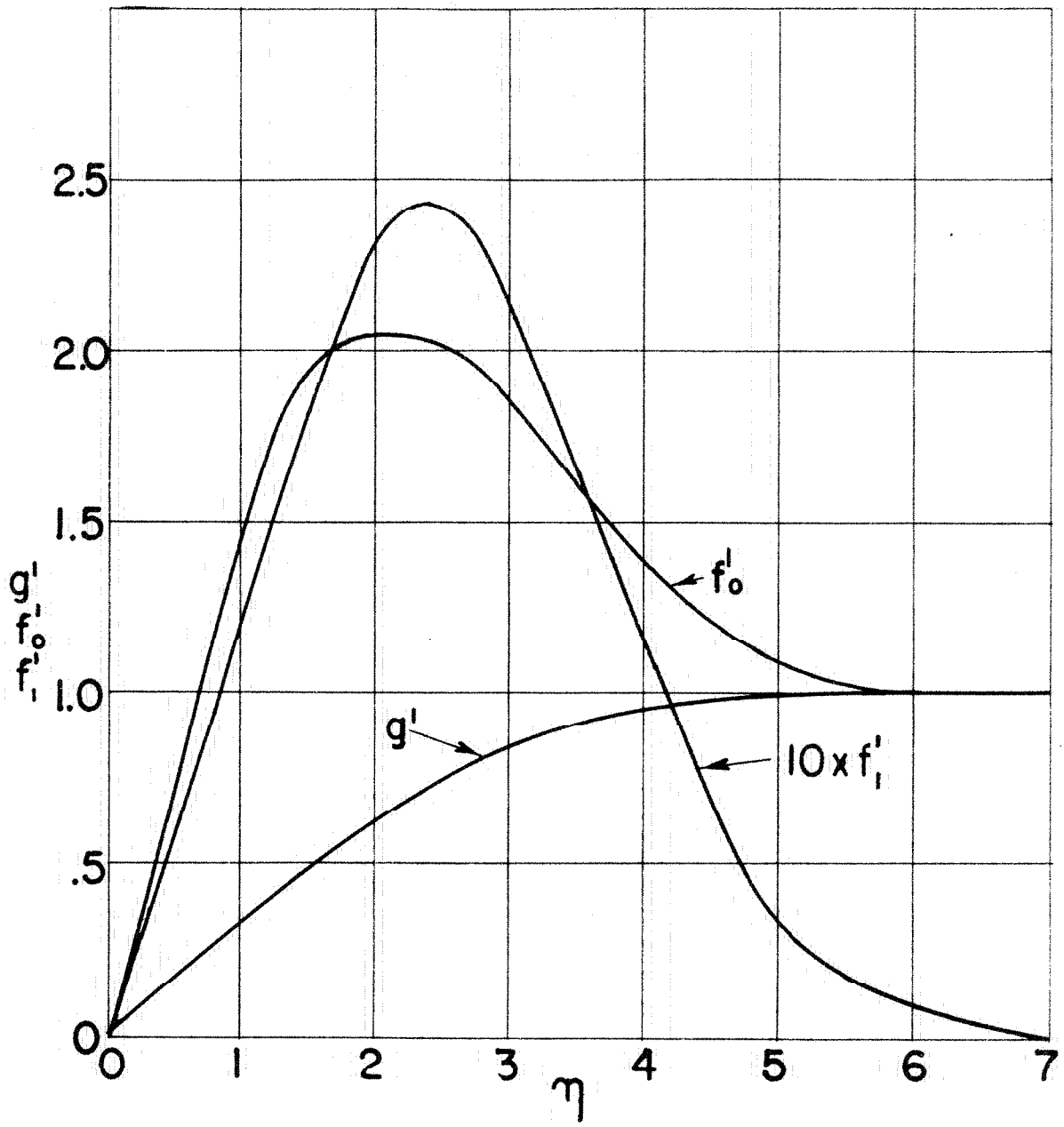

FIGURE 2.-

BOUNDARY LAYER PERTURBATION VELOCITY PROFILES

a) EXTERNAL FLOW : $W^* = Az$; $U^* = Bx$

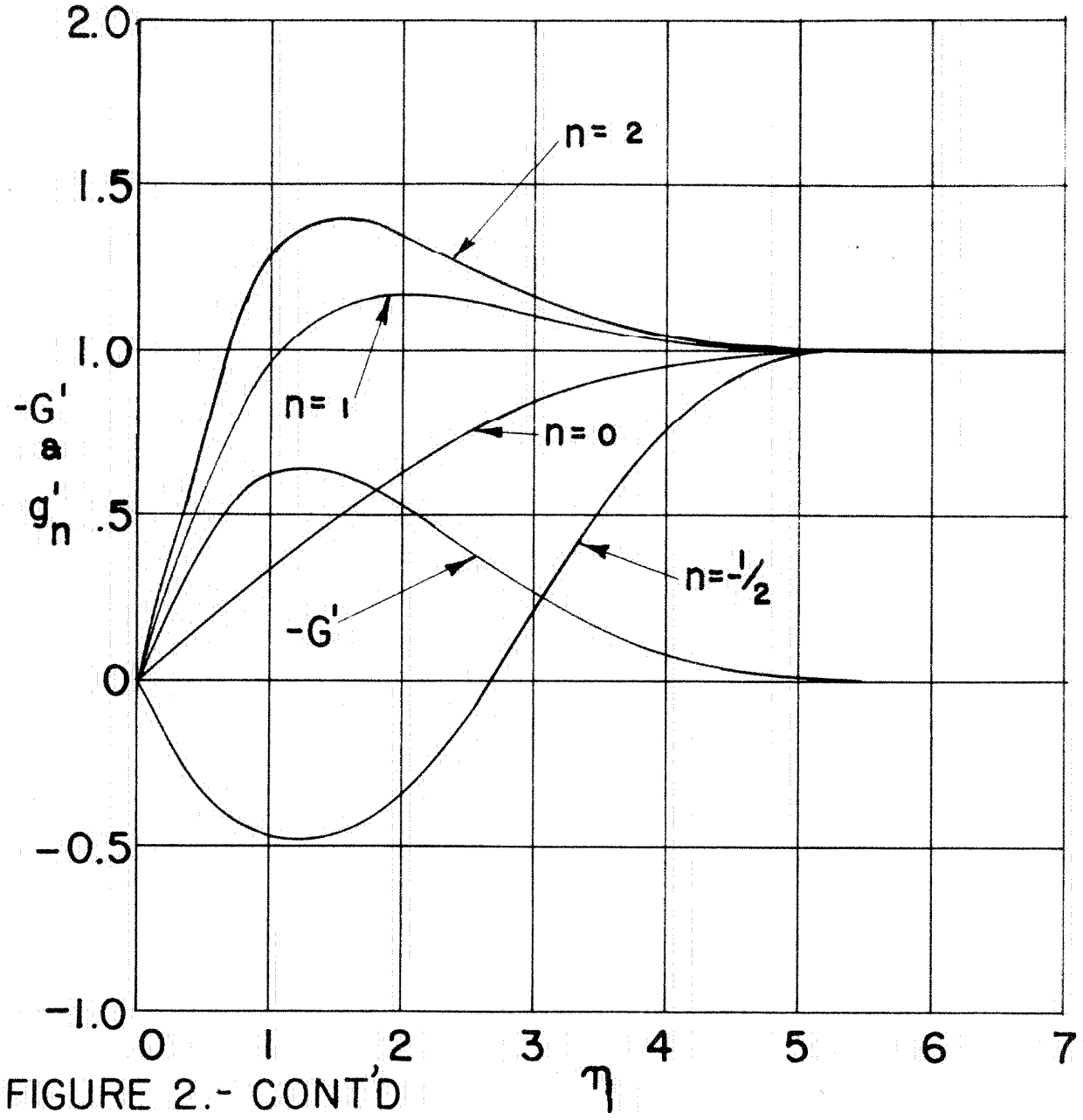

FIGURE 2.- CONT'D

b.) EXTERNAL FLOW : $W^* = Ax^n$; $U^* = 0$

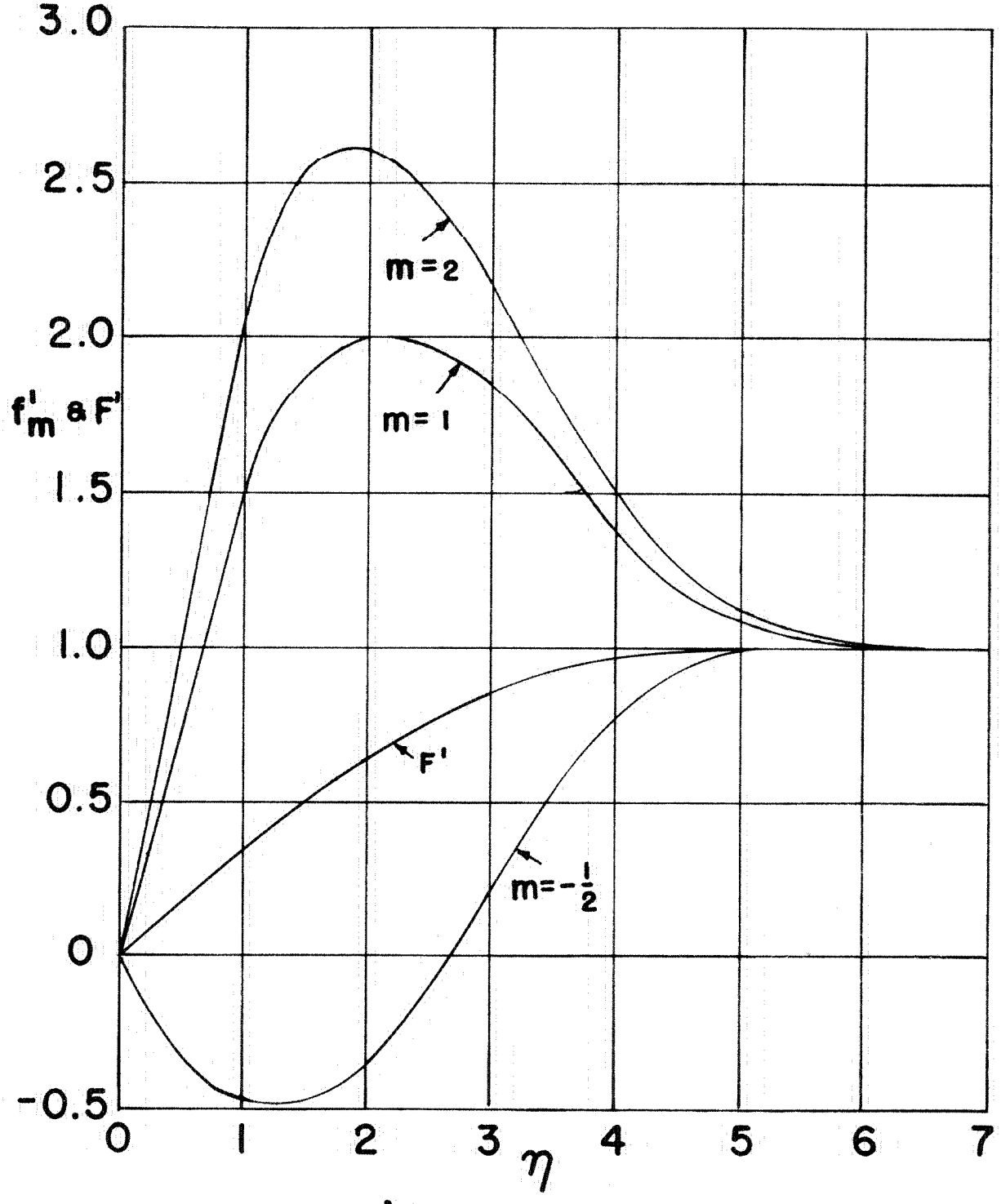

FIGURE 2.- CONT'D

c) EXTERNAL FLOW: $W^* = Ax^n$; $U^* = Bx^m z^l$

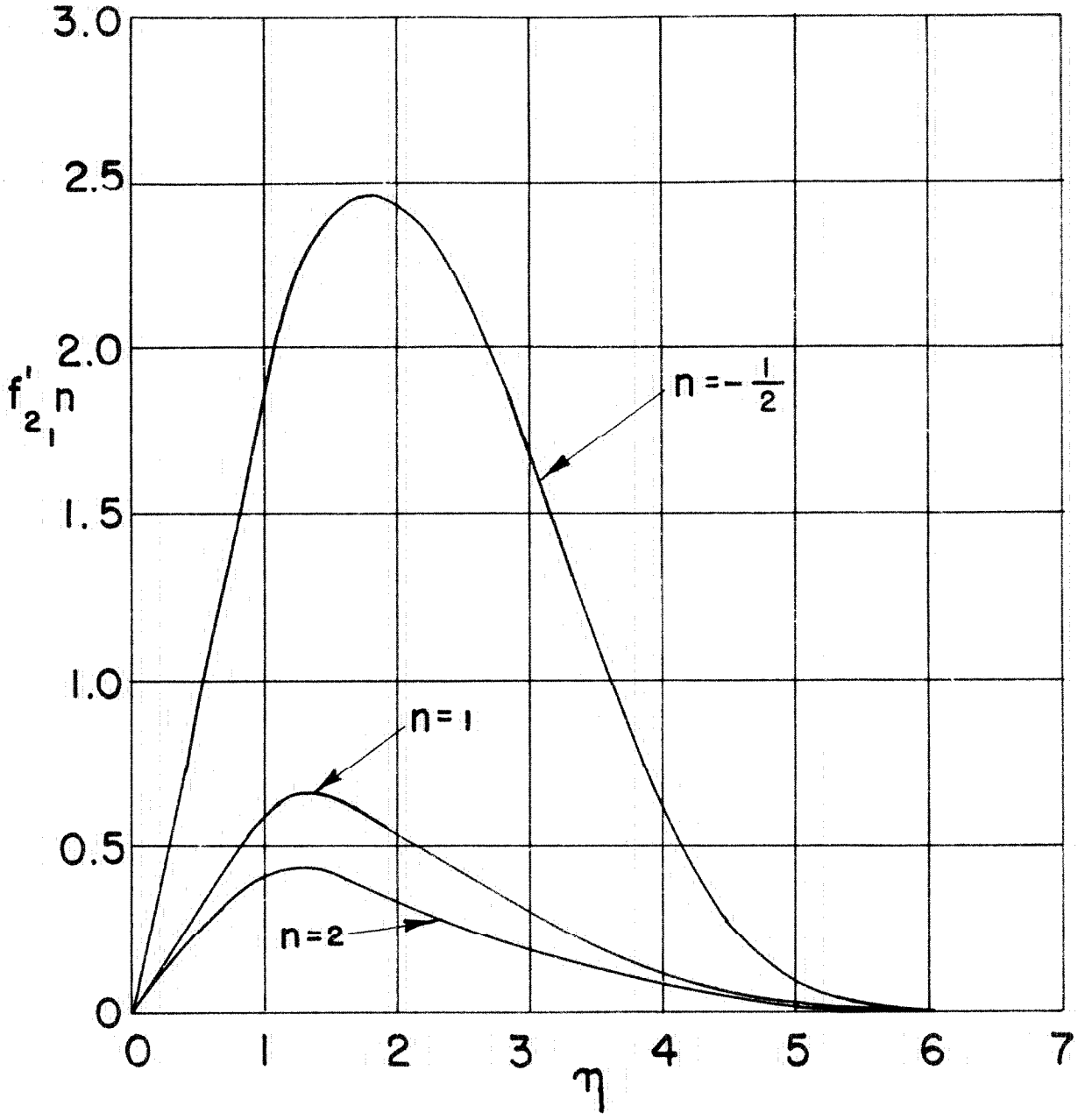

FIGURE 2.- CONT'D

d.) EXTERNAL FLOW :

$$W^* = Ax^n z^k \; ; \; U^* = -\frac{k}{n+1} Az^{k-1} x^{n+1}$$

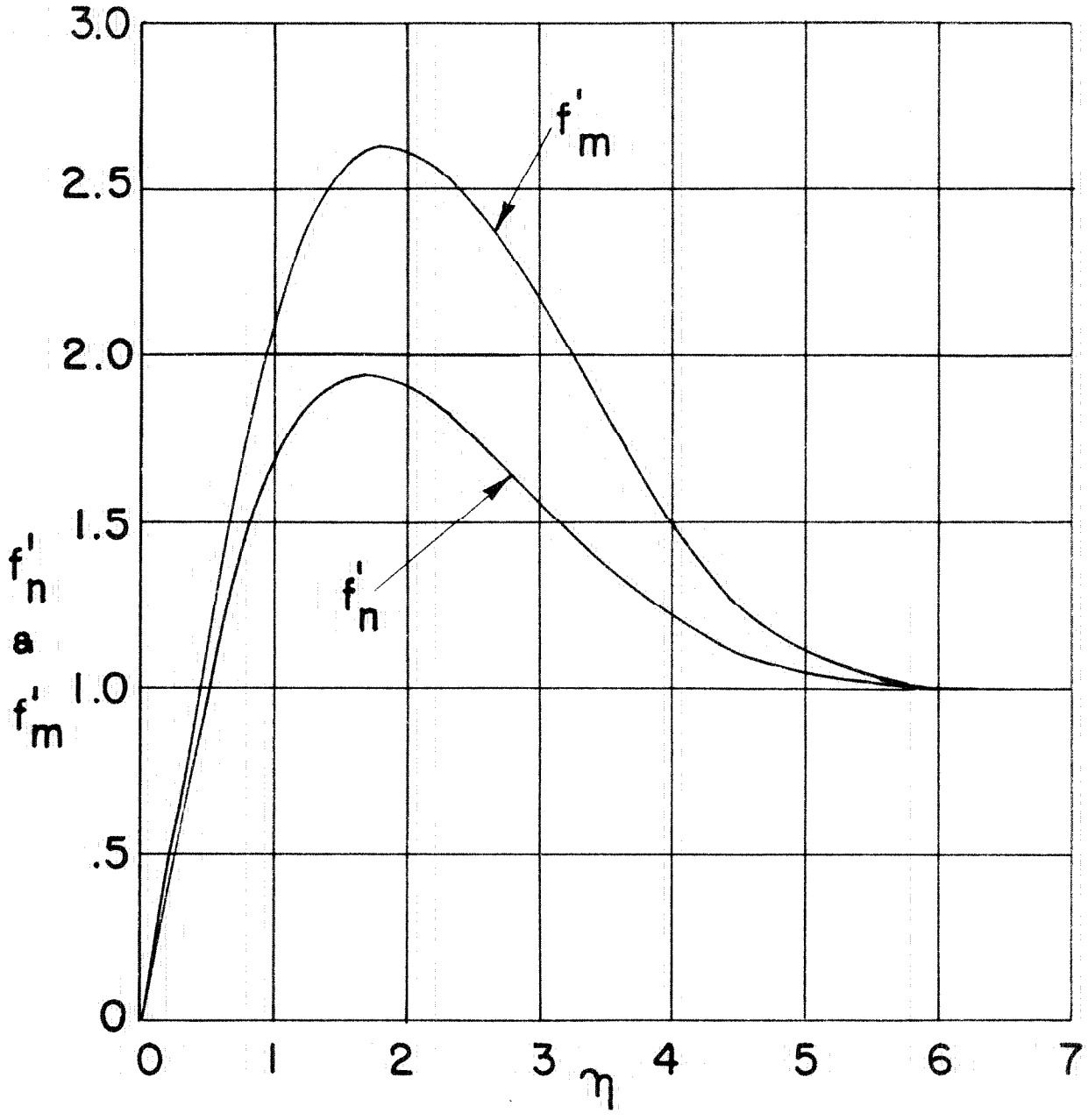

FIGURE 3.- COMPARISON OF THE u^* VELOCITY PROFILES FOR EXTERNAL FLOWS $W^* = Ax^n$; $U^* = Bz^i x^2$ AND $W^* = Axz^k$; $U^* = -\frac{k}{2} Az^{k-1} x^2$

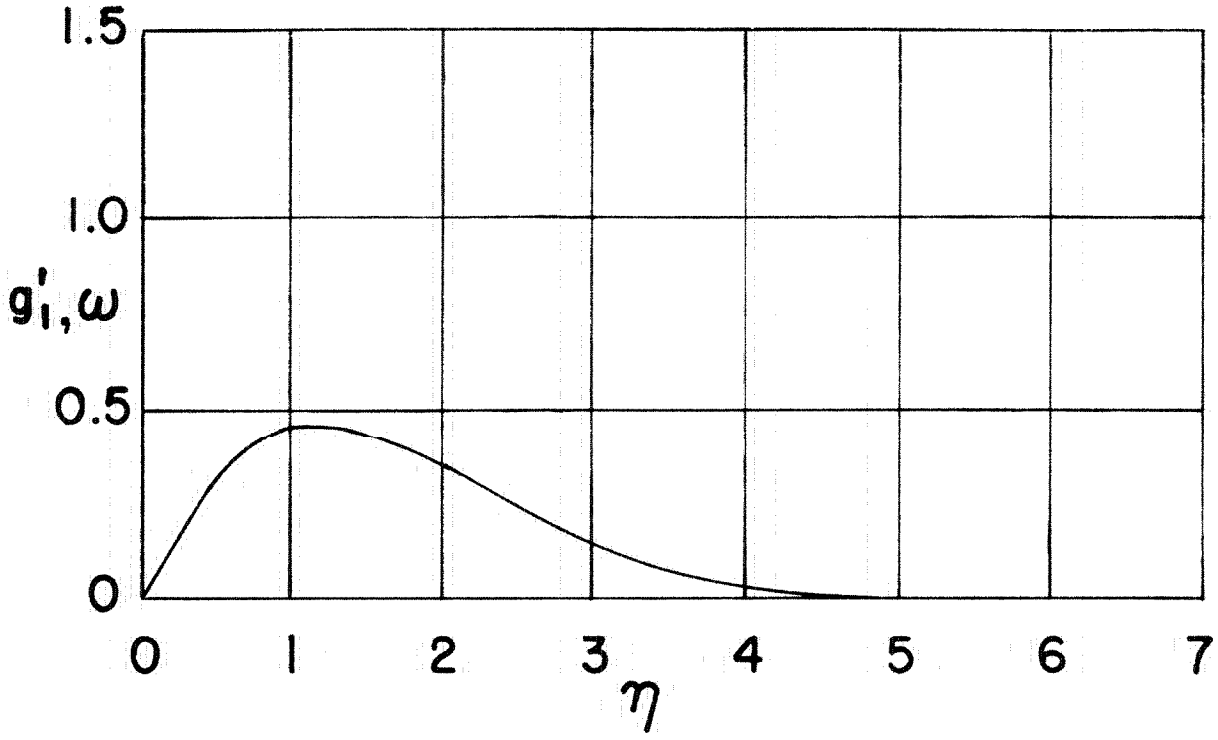

FIGURE 4.- EFFECT OF ANGULAR VELOCITY

$\omega_2 = D$

EXTERNAL FLOW : $W^* = Ax$; $U^* = 0$

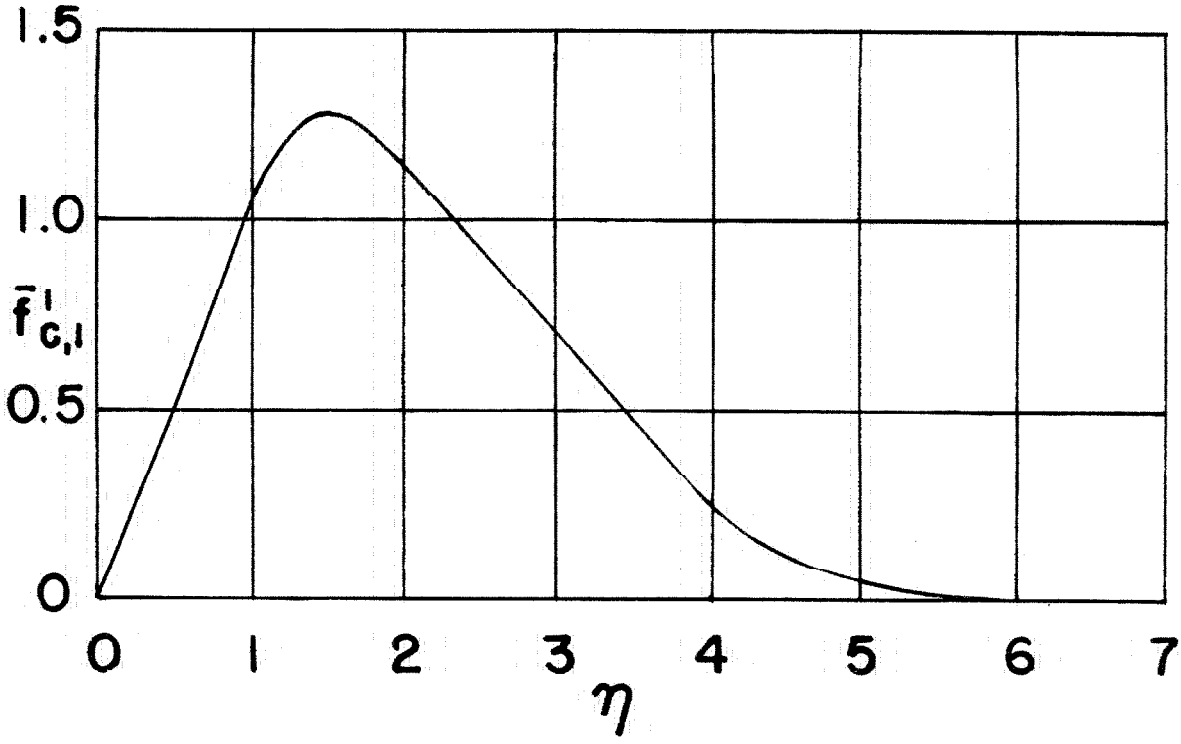

FIGURE 5.- EFFECT OF COMPRESSIBILITY

a) FUNCTION $\bar{f}'_{c,1}$

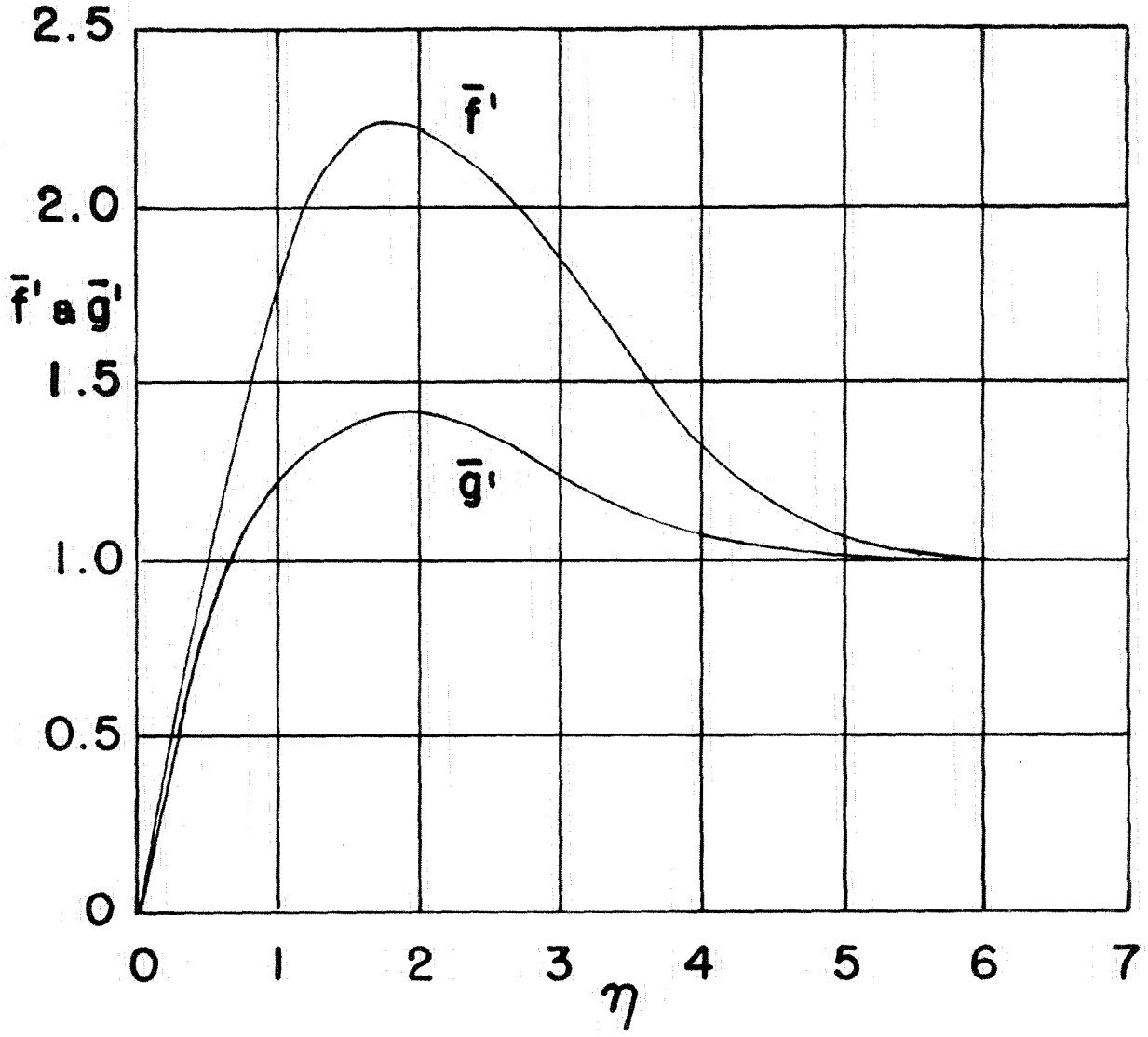

FIGURE 5.- CONT'D

b) PERTURBATION VELOCITY PROFILES FOR EXTERNAL FLOW $W^* = Ax$; $U^* = Bx$ AT M=1.5

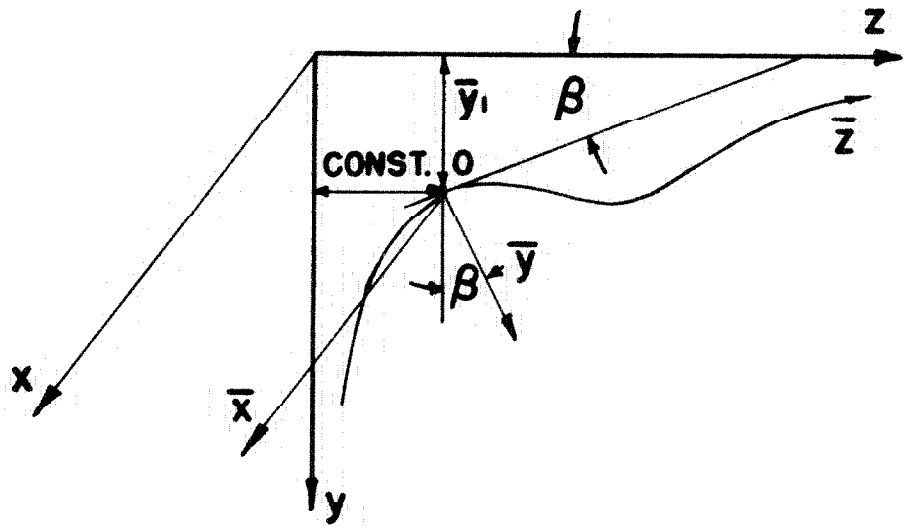

FIGURE 6.—CURVILINEAR COORDINATE SYSTEM

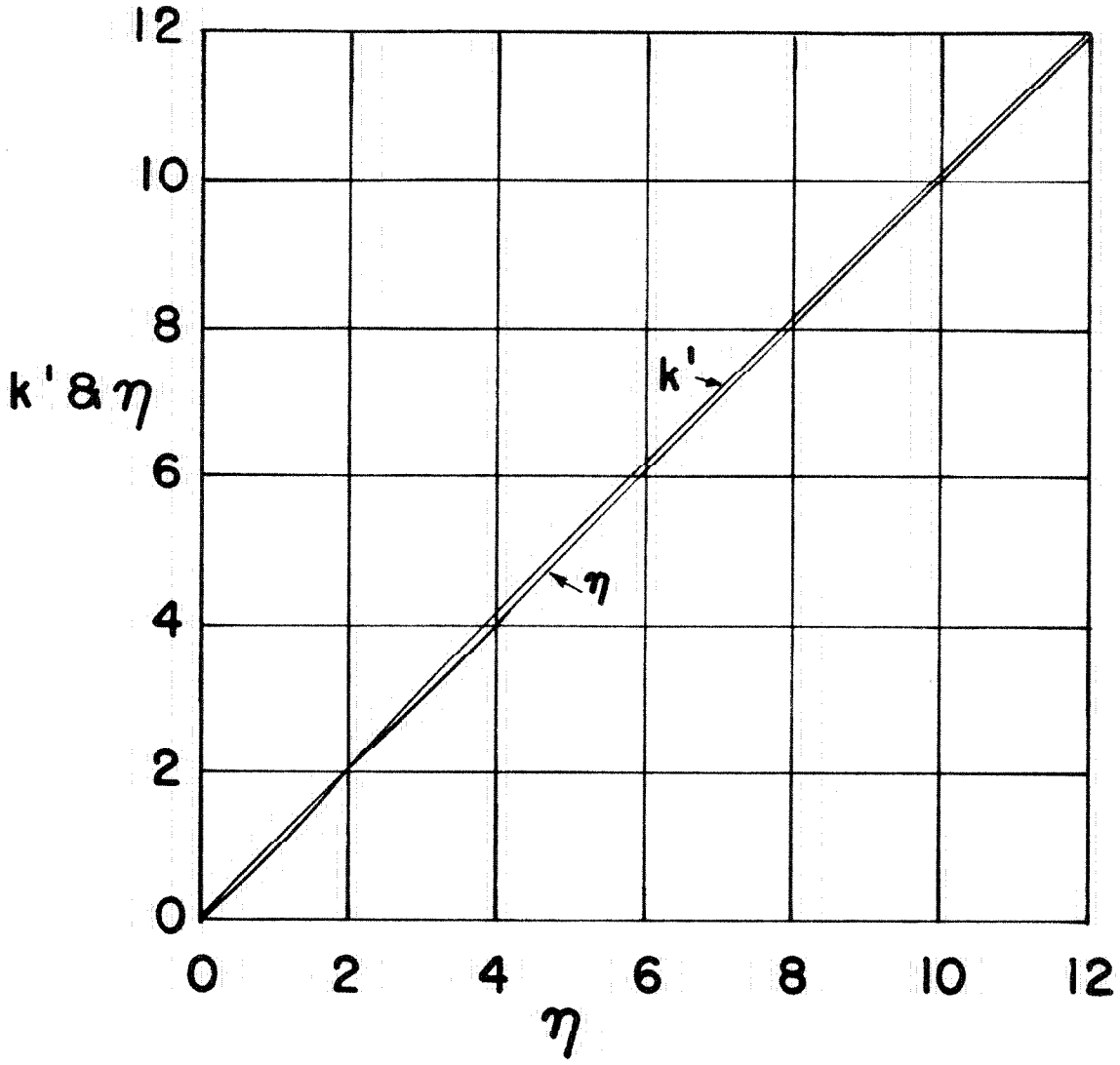

FIGURE 7.- EFFECT OF LARGE LATERAL WALL CURVATURE

a) MODIFICATION TO BASIC FLOW

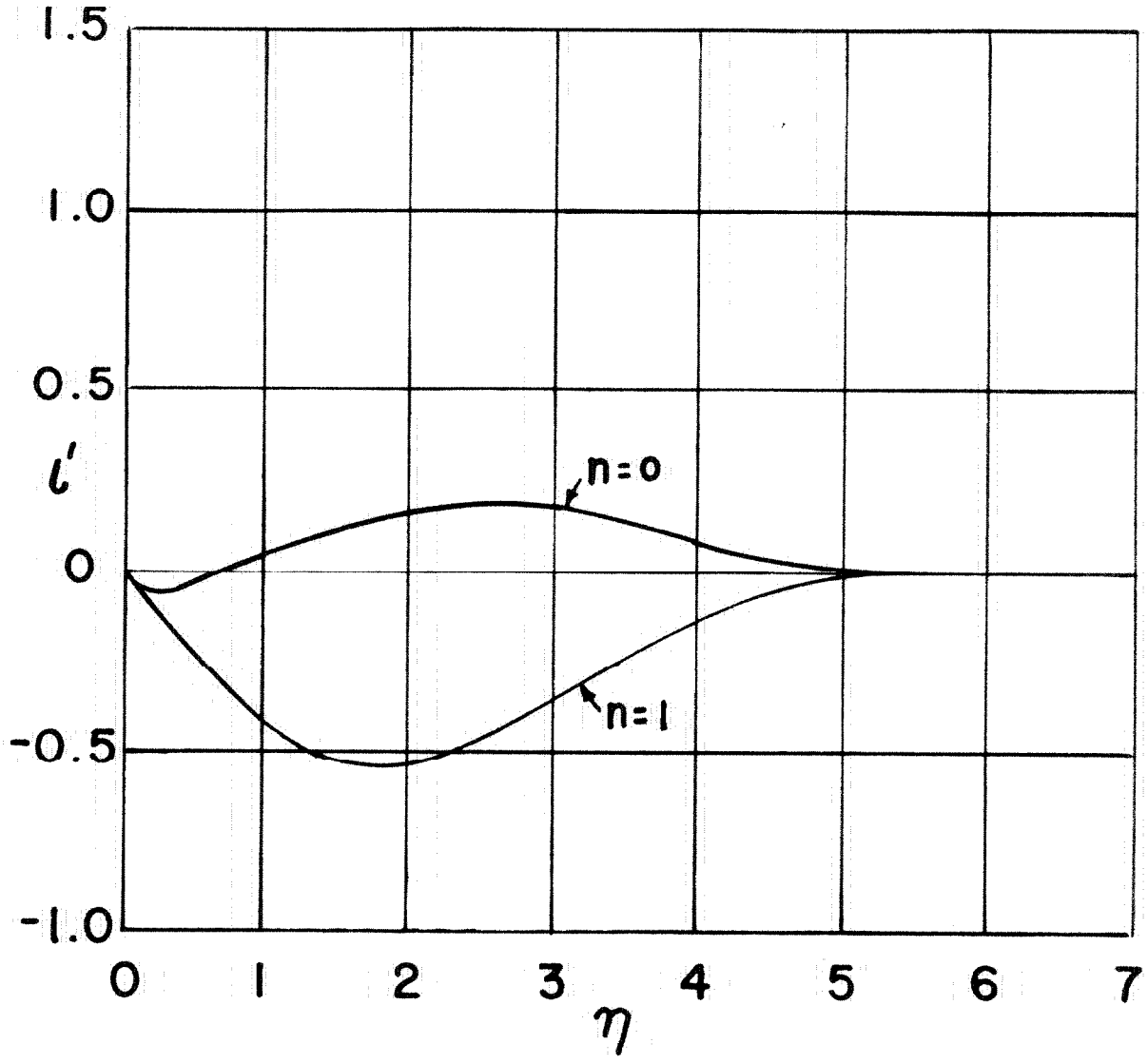

FIGURE 7.- CONT'D

b) EXTERNAL FLOW: $W^* = Ax^n$; $U^* = 0$

MODIFICATIONS TO u^* FLOW

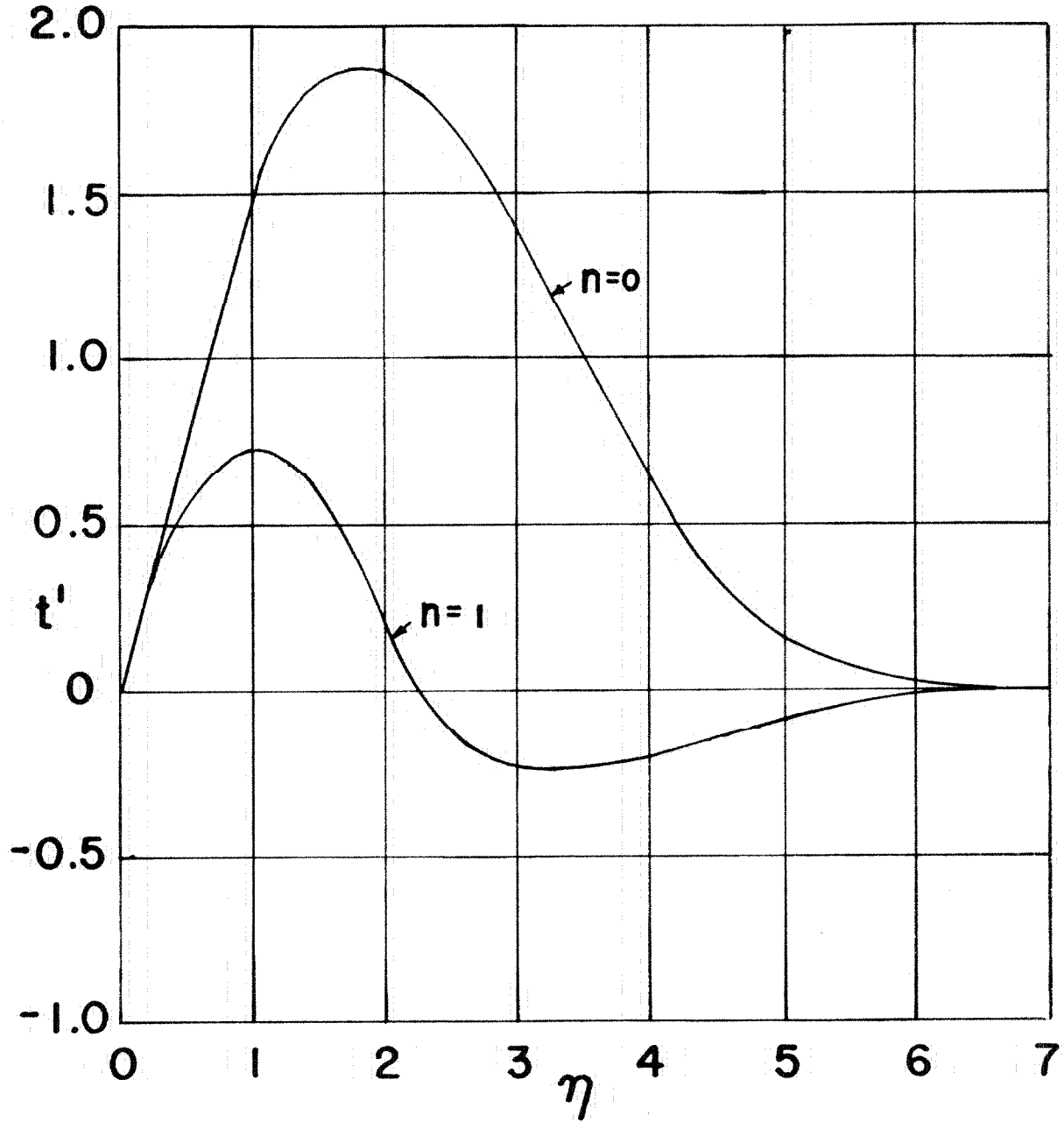

FIGURE 7.- CONT'D

c) EXTERNAL FLOW: $W^* = Ax^n$; $U^* = 0$

MODIFICATION TO w^* FLOW

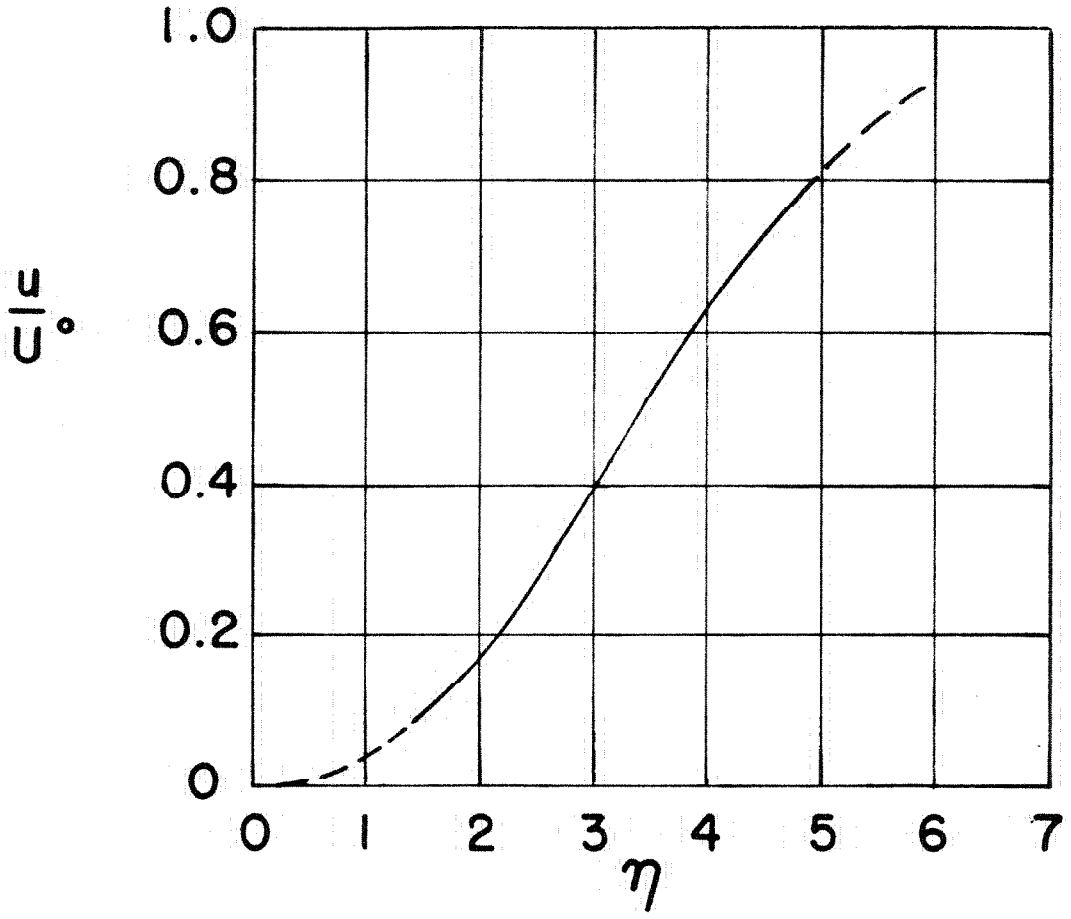

FIGURE 8.- VELOCITY PROFILE ALONG A 45° LINE IN A RIGHT CORNER.
EXTERNAL FLOW: U° = CONST.
(DATA FROM REFERENCE 20)

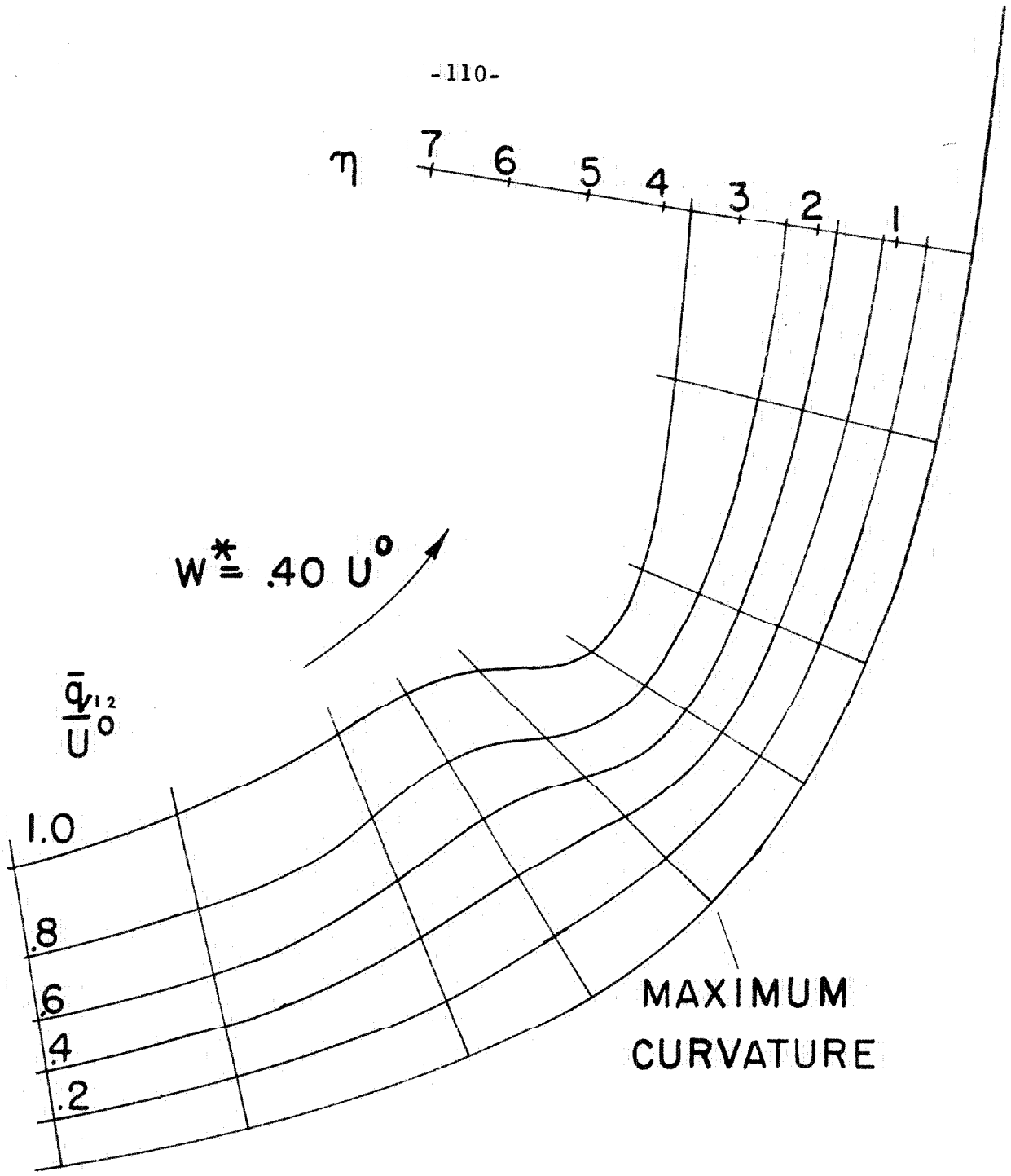

FIGURE 9.- FLOW OVER A HYPERBOLICALLY SHAPED WALL

a) EXTERNAL FLOW : $U^* = 0$; $W^* = A$ CONSTANT q_{12} PROFILES

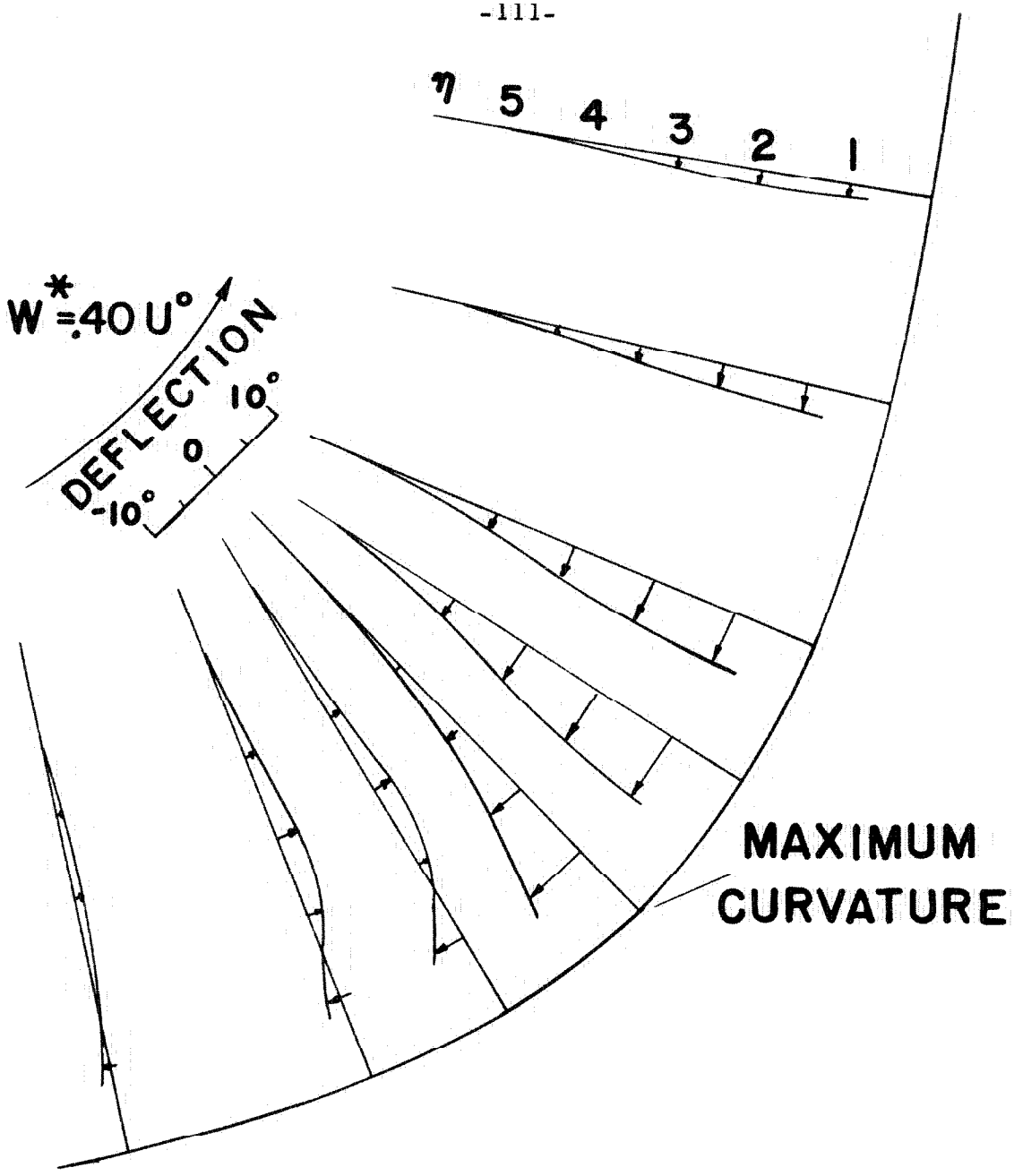

FIGURE 9.- CONT'D

b) EXTERNAL FLOW: $U^* = 0$; $W^* = A$

DEFLECTION $\theta - \vartheta(\eta)$

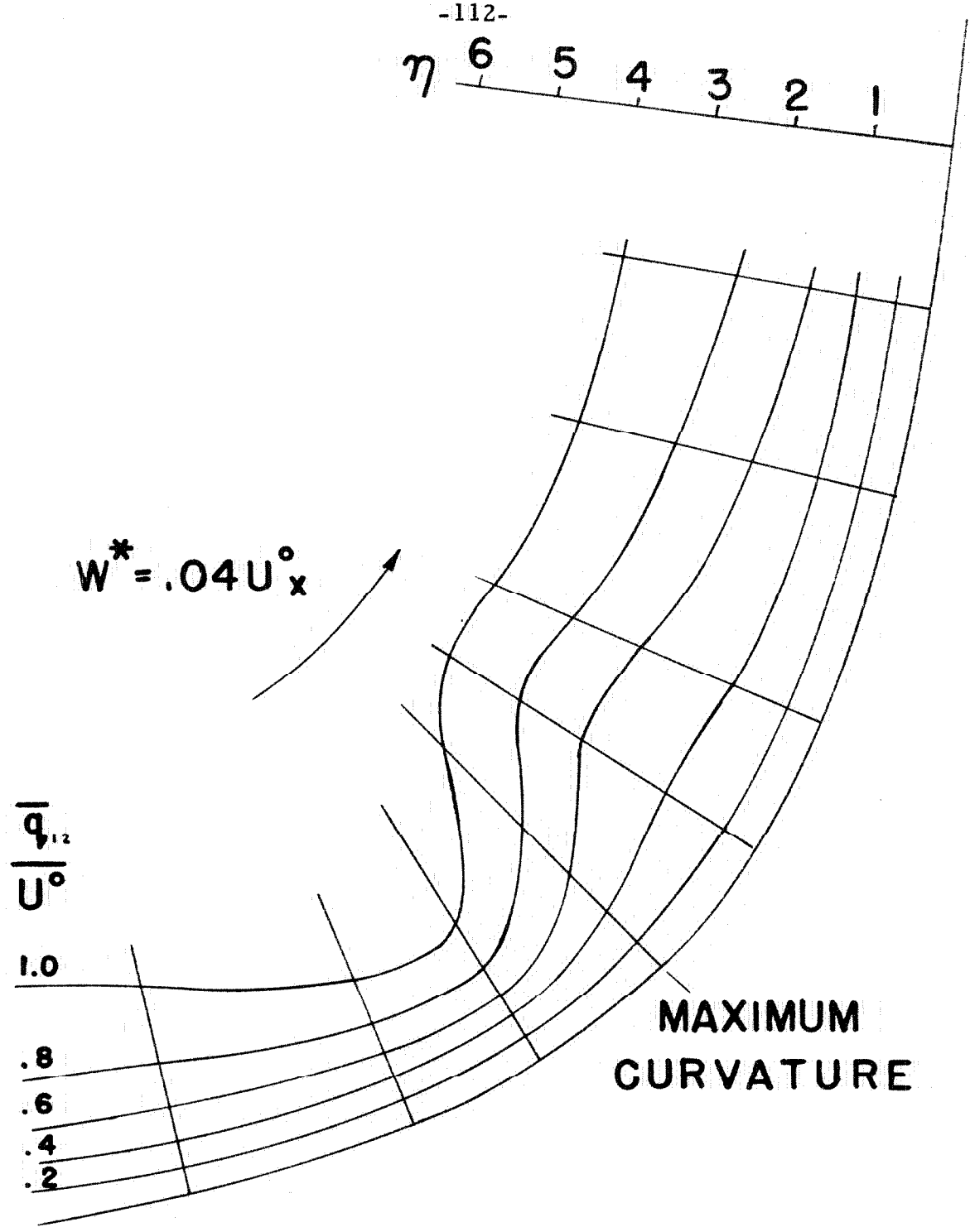

FIGURE 9. - CONT'D

c) EXTERNAL FLOW: $U^* = 0$; $W^* = Ax$

CONSTANT q_{12} PROFILES

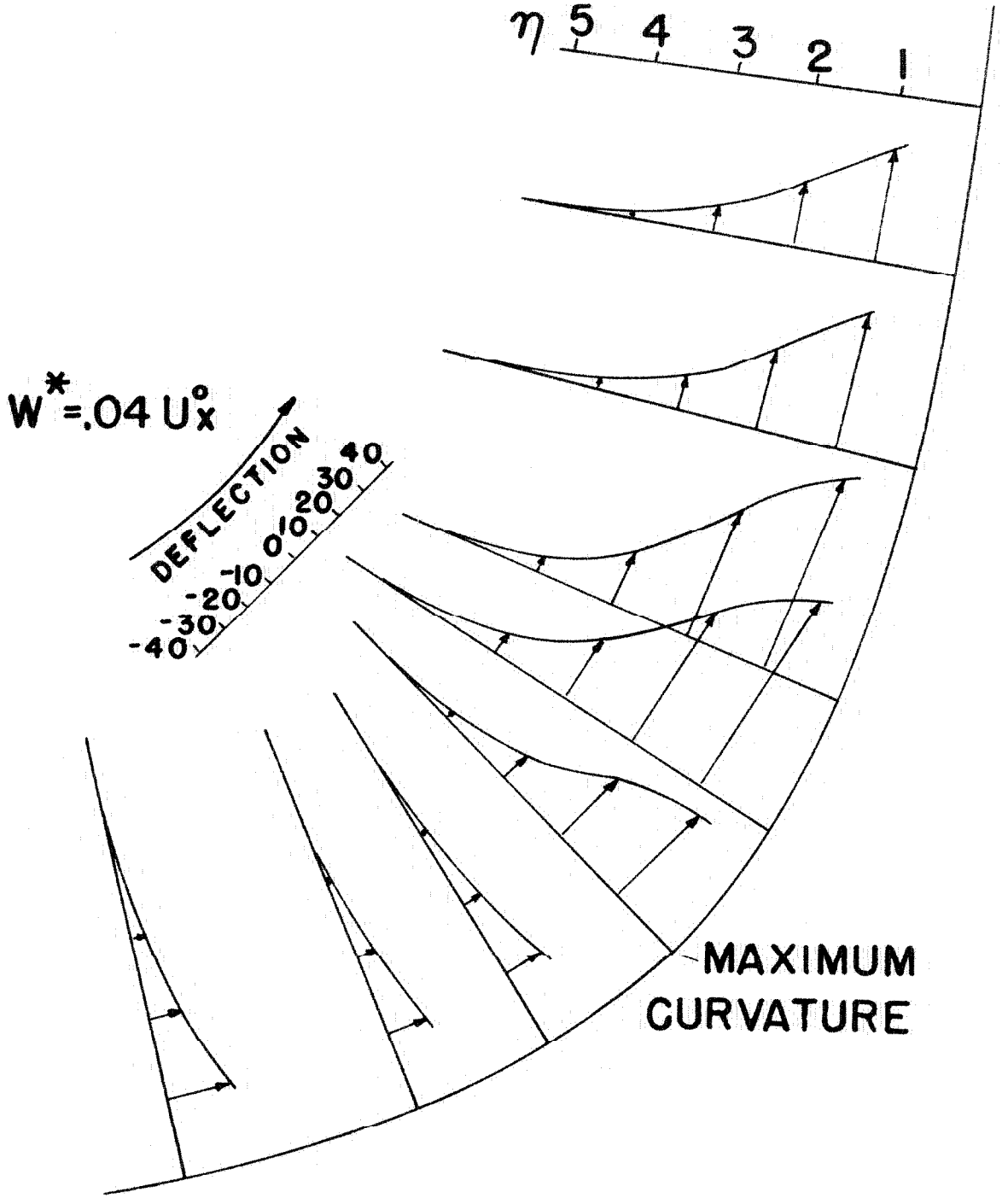

FIGURE 9.- CONT'D

d) EXTERNAL FLOW: $U^* = 0$; $W^* = Ax$

DEFLECTION $\theta - \vartheta(\eta)$